THE ROLE OF SURFACE SUSCEPTIBILITY IN THE THEORY OF ADSORPTION

ARPITA DATTA

DEPARTMENT OF MATHEMATICS

A thesis submitted for the degree of Doctor of Philosophy of the University of London and the Diploma of Imperial College.

1977

TO

BABI

" Where the mind is without fear
and the head is held high ;
Where knowledge is free ;
Where the world has not been broken up
into fragments by narrow domestic walls ;
Where words come out from the depth of truth ;
Where tireless striving stretches
its arm towards perfection
Where the clear stream of reason has not lost its way
into the dreary desert sand of dead habit ;
Where the mind is led forward by thee
into ever-widening thought and action -
Into that heaven of freedom, my Father,
let us all awake. "

R. TAGORE.

ACKNOWLEDGEMENTS

I would like to express my sincere gratitude to Dr. D. M. Newns for his patient supervision throughout the course of this work and my stay at Imperial College. His encouragement and enthusiasm have been much appreciated.

Many thanks are due to the members of the staff and students in the Mathematical Physics group for their help and friendship over the last three years. Special thanks must go to Dr. R. Jacobs and Dr. J. P. Muscat for many helpful discussions and to Miss J. Pindelska, our librarian, for her super-efficiency in producing the right book at the right time out of nowhere.

Last but by no means least, I am deeply grateful to my mother for her limitless patience and understanding which enabled me to complete this work.

TABLE OF CONTENTS

THE ROLE OF SURFACE SUSCEPTIBILITY IN THE THEORY OF ADSORPTION

Arpita Datta

ABSTRACT

In this thesis we are interested in making a study of the atom-surface interactions using a linear response theory formalism. We approach this problem two different angles.

1. The first deals with a dynamic problem using a semi-classical infinite square barrier model, SCISBM, and involves the excitations of the core level adatom with the metal substrate when subjected to X-ray photoemission (XPS). The calculations concern intrinsic satellites of the system, a quantity that has been experimentally observed through use of XPS, and also involve the physical concepts of relaxation shifts, line shapes and infra-red divergence.

2. The second half of the thesis is concerned with the same physical system but now approached from a magnetic point of view. The object of interest is a localised static surface spin susceptibility formed by the application of a localised magnetic field in three dimensions for itinerant paramagnets. This quantity is of importance in some theories of chemisorption and catalysis and we use the exact three-dimenional expressions for the non-interacting electron susceptibility to calculated the localised surface magnetization. We apply our results to a calculation of binding energy of an adatom with the metal substrate. The infinite square barrier model (ISBM) is used.

Our calculations are based on the RPA or time-dependant Hartree approximation.

CHAPTER I

INTRODUCTION

Generally speaking, progress in understanding the behaviour at surfaces in Physics has lagged far behind that in understanding the bulk properties of matter. The reason for this is partly due to theoretical difficulties. A metal bounded by its surface loses the simplifications due to translational invariance afforded by bulk crystalline solids. Furthermore, it is a region of strong inhomogenity since the electron density reduces from its bulk value to zero in a distance roughly comparable to atomic dimensions. Another hindrance to the rapid development of surface science was the lack of reliable experimental data on the properties of surfaces. But with the advance in ultra-high-vacuum technology during the fifties and the development of new experimental surface techniques which have enabled reasonably accurate reproducible measurements, interest revived. This advance combined with advances made in manybody theory gave the boost resulting in the recent boom of development in surface physics.

Quantum theory lies of course at the very core of attempts to analyse and interprete the properties of both bulk and surface matter. According to some, there is little doubt amongst scientists (if not

philosophers) that the workings and properties of ordinary matter can ultimately be reduced to electrodynamics and quantum theory

Ideally, the information one seeks includes the geometry and electronic structure of clean and adsorbate covered surfaces and it also proves useful in understanding some general properties associated with the surface, preferably in the form of measurable physical quantities e.g.

1. the work function ϕ defined as the minimum work required to remove an electron from the metal at $0^{o}K$ i.e. the energy difference between an electron at the Fermi level and the vacuum level. Typical values for ϕ of metals are 2-3ev for alkalies or 4-5ev for transition metals.
2. the binding energy ΔE of an atom to the surface, defined as the work required to remove an atom from the surface. This is an important concept as it is crucial in determining chemisorbed as opposed to physisorbed systems ($\Delta E \geqslant 0.5$ ev in the former case whereas $\Delta E \leqslant 0.3$ ev in the latter case). Ideally, one would like to determine the binding energy as a function of site absorption and the distance between the surface and adatom.

Response functions play a key role in understanding the properties of many-body systems. This is of course quite natural due to the very method whereby experiments

are performed e.g. in a typical experimental set up we apply a perturbation to the system under investigation and measure the resulting response. The correlation or linear response of the surface to some applied external perturbation is often referred to as the generalized susceptibility of the system. This is the underlying theme throughout this thesis in which the geometry of the situation involves an atom adsorbed on the substrate metallic surface. This response of the metal surface to some perturbing potential is of fundamental importance to the weaker interaction of physical adsorption (which is predominantly Van-der-Waal forces) as well as treatments of the complex problem of covalent chemisorption. Due to the inherent complexities in the problem of adsorbate systems and chemical reactions on metal surfaces, simplified assumptions are necessary.

Newns (1970) and Beck and Celli (1970) independantly, although in the same year, derive an expression for the linear response of a metal to an external charge distribution using the random phase approximation (RPA) or time-dependant Hartree approximation, using a self-consistent approach. The infinite square barrier model was considered. Both are essentially equivalent.

Peukert (1971) considers interacting electrons confined to a slab of finite thickness and uses a Green's function technique (Kadanoff - Baym, 1962, formalism - also used by Zaremba, 1974, in his thesis which examines the magnetic

susceptibility for a bounded Fermi system).

One model which has been widely used to calculate various properties of metal surfaces is the so - called 'jellium' or uniform planar background model, in which the ion cores are spread out into a uniform distribution of charge. In 1969, Lang made self - consistent calculations for the electron density which instead of abruptly stopping at the termination of the positive background, spread out beyond this point into vacuum, forming a transition region of atomic dimension localised about the background boundary. Lang and Kohn (1970) use a fully self - consistent calculation to obtain numerical results for various density distribution, potentials and surface energies for differing metallic densities, r_s. While giving reasonable results for low density metals, results upon higher density metals ($r_s \leq 4$) eg. aluminium, differ significantly with experiment. Thus the jellium model seems inadequate for low values of r_s and improvements are possible by replacing the jellium by a pseudopotential model of ions.

There exist excellent recent reviews on the chemisorption theory eg. Grimley , (1975) ; Gomer, (1975) ; Muscat and Newns (1977). Ying, Smith and Kohn (1975) first invoked the density functional theory (introduced by Hohenberg, Kohn and Sham, 1964 and 1965) to obtain the linear response of a planar jellium surface to a point charge

and they applied the theory to the chemisorption of hydrogen on tungsten. The actual electronic density was found self - consistently by minimising the energy functional and solving the resulting equation with the Poisson equation. The only parameter involved in the calculation was r_s. The work function was found to be in good agreement with experiment, but the distance of the image was too large compared with previous theory.

In 1975, Lang and Williams use a more sophisticated theory and apply a self - consistent wave - mechanical formulation of the density functional theory to Ying et al's model by going beyond linear response theory. Dipole moments and binding energies for the adsorption of hydrogen, lithium and oxygen on an $r_s = 2$ substrate yielded encouraging agreement with experiment on transition metals.

However, certain natural objections arise to this idealised jellium approach in that it is too simplistic to realistically represent the electronic structure of a transition metal, by neglecting the different roles played by the s-p and d- bands. But it does satisfy the momentary need to explain the existence of vast amount of data needing interpretation.

Another consequence of the atom-jellium model is the restriction imposed by adatom penetration. Very electronegative adatoms e.g. oxygen on aluminium,

which do in fact tend to penetrate the metal surface, cannot be included in this theory. In 1976, Ying et al conducted an ultra-violet photoemission study of oxygen adsorbed on clean polycrystalline aluminium and measured the energy of the oxygen 2p-resonance and the dipole moment of the adatom, given by the change in work function. In the former, experimental measurements were more than three times larger and no change in work function was measured, whereas a significant dipole moment had been predicted by theory (Lang et al, 1975). So the process of absorption, a likelihood in practise is neglected in the atom-jellium model in favour of pure adsorption alone.

A concept relatively new to chemisorption theory is the induced covalent band theory ICBT, which was initially formulated by Schrieffer and Gomer in 1971.

This was to treat systems in which the intra-atomic Coulomb interaction, U, on the adsorbate is large compared with the interaction strength between the adsorbate and metallic substrate, and so the charge fluctuations are so small that only neutral adsorbate states need be considered to lowest order. The exchange interaction, J, between the adatom and solid induces a spin density in the vicinity of the adsorption site and this induced spin cloud couples to the adatom spin through J to form a bond. Their qualitative argument is as follows :

The energy required to create a spin S on a metal surface

atom is

$$\Delta E = (\mu_B S)^2 / 2\chi_{loc}$$

where μ_B = Bohr magneton.

and χ_{loc} is the local spin susceptibility of the surface substrate atom.

If a full spin $S = \frac{1}{2}$ is induced on the metal surface atom, a bond with the adsorbate can be formed, lowering the energy by an amount Wm. However, if no spin were present i.e. S =0, the adsorbate would experience an exchange interaction Wr with the surface. Through a process of linear interpolation, the net energy change may be written as a function of S, thus :

$$\Delta E(S) = (\mu_B S)^2 / 2\chi_{loc} - 2S(W_m + W_r) + W_r$$

which satisfies the above requirements. Minimizing the above equation with respect to S, gives

$$\Delta E = -\frac{2(W_m + W_r)^2}{\mu_B^2}\chi_{loc} + W_r$$

where the term $\frac{Wm + Wr}{\mu_B}$ may be interpreted as the lowering of energy due to the solid spin responding to the exchange interaction, J.

Paulson and Schrieffer (1975) study a quantitative formulation of this theory and consider hydrogen on a tight-binding s-band solid. They calculate the binding energy for different metal band-widths for both the

weak and strong interaction limits and obtain physically reasonable results, showing binding curve minima for reasonable value of band lengths.

Surface Plasmon

Now, surface plasmon excitation is of interest to us and plays a tremendously important role in connecting the interaction between a fast charged particle and a metal surface. We begin by introducing the concept of surface plasmon in the following way :

Consider a classical interface between a medium of dielectric constant $\varepsilon(\omega)$ in the plane $z < 0$ and vacuum at $z > 0$. The surface is therefore at $z = 0$. (See Fig. 1.1). Now, in both the mediums, the potential ϕ should satisfy Laplace's equation viz.

$$\nabla^2 \phi = 0 \qquad \ldots\ldots\ldots\ldots (1.1)$$

If $\underline{Q}$ is a two-dimensional Fourier wave vector, then a solution of (1.1) is given by

$$\phi = e^{i\underline{Q}.\underline{x} - Q|z|} \qquad \ldots.(1.2)$$

which is continuous at the surface $z = 0$.

If $\underline{E}$ is the electric field and $\underline{D}$ the displacement then from any standard book on Electrodynamics e.g. Jackson, 1962,

$$\left.\begin{aligned} \underline{E} &= \nabla\phi \\ \underline{D} &= \varepsilon \underline{E} \end{aligned}\right\} \qquad \begin{aligned} &\ldots.(1.3A) \\ &\ldots.(1.3B) \end{aligned}$$

where ε is the dielectric constant proportional to

the electric susceptibility of the medium. From consideration of continuity of $\underline{D}$ at the surface, we have

$$\varepsilon(\omega) + 1 = 0 \quad \ldots (1.4)$$

But the classical expression for $\varepsilon(\omega)$ is given by

$$\varepsilon(\omega) = 1 - \frac{\omega_p^2}{\omega^2} \quad \ldots (1.5A)$$

where $\omega_p^2 = (4\pi ne^2)/m$, the plasma frequency...(1.5B)

n is the number of electrons / unit volume.

Substitute (1.5A) in (1.4) yields

$$\omega_s = \omega_p/\sqrt{2} \quad \ldots (1.6).$$

which is defined as the surface plasmon frequency

This expression (1.6) for ω_s is in reasonably good agreement with experimental calculations for free electron-like materials e.g. Kloos and Raether, 1973, obtain values of 7.1 ev and 10.6ev for magnesium and aluminium respectively, while the theory predicts values of 7.72eV and 11.2eV respectively. However for non-free electron like material e.g. transition metals, equation (1.5A) cannot be used for classical dielectric function.

In 1957 , Ritchie was the first to theoretically observe the importance of surface plasmon oscillation in thin films using a dielectric treatment which he shows is essentially equivalent to first order perturbation theory. Their existence was first experimentally confimed by Powell and Swan (1960) who made measurements of the electron-energy-loss spectra of the free-electron-like

metals, aluminium and magnesium.

Objective

Adatom resonances play a uniquely important part in efforts to understand chemisorption and physisorption because they lead to readily identifiable structure in the measured excitation spectra. One relatively new method for studying electron-loss structure associated with electrons travelling through solids is X-ray photoemission (XPS). Here the X-ray beam penetrates thousands of angstroms and photoemission occurs. Of more theoretical interest, XPS provides a possibility of observing intrinsic as well as extrinsic plasmon structure. Recent interest in the possibility of observing intrinsic surface plasmon satellites in free electron like metals by XPS (Bradshaw et al, 1976) has inspired part of our present work which is concerned with the excitation of the core state of an adsorbed atom on the metal surface. The dynamics of the resulting hole preparation and decay and the form of the excitation spectrum of the density fluctuation determine the intensities and positions of intrinsic satellites (Harris, 1975) and give rise to the so-called extra-atomic relaxation effects (Gadzuk, 1975) which incorporate relaxation shifts, line shapes and shake-up spectra.

In the following chapters of this thesis we give further details with the relevant references and so we conclude this introduction here to avoid repetition.

A rough outline of this work may be made as follows :

A) <u>The dynamic problem</u>

In Chapter II, we define the surface response function R for our semi-classical infinite square barrier model (SCISBM) and express some of its properties through the spectral function S, which is found to obey certain general sum rules. We graphically illustrate this S-function, separating out the contributions due to the electron-hole and surface plasmon excitations.

In Chapter III, we apply the results of Chapter II to calculate the intrinsic satellite spectrum N of the core level of the adatom, separate out contributions due to transient and adiabatic responses and determine the magnitude of the relaxation shifts. Graphs for N are given, with a discussion on intrinsic and extrinsic effects. Further intrinsic N are computed using data from relevant papers. Our results are compared with available experimental data.

This completes the first half of the thesis.

B) <u>The static problem</u>

The second half of this thesis deals with the static spin susceptibility and magnetization of

surface enhanced itinerant electrons in three dimensions. The arguments promoted by Schrieffer and Gomer in 1971 for the ICBT (given earlier on) were the first to emphasise on the role played by the local spin susceptibility in the theory of chemisorption and provide our motivation for the latter half work in this thesis. Chapter IV serves as a self-contained introduction to this topic, while Chapter V includes the results and discussions of our infinite square barrier model (ISBM) which is used in contrast to the previous SCISBM.

FIG (1.1)

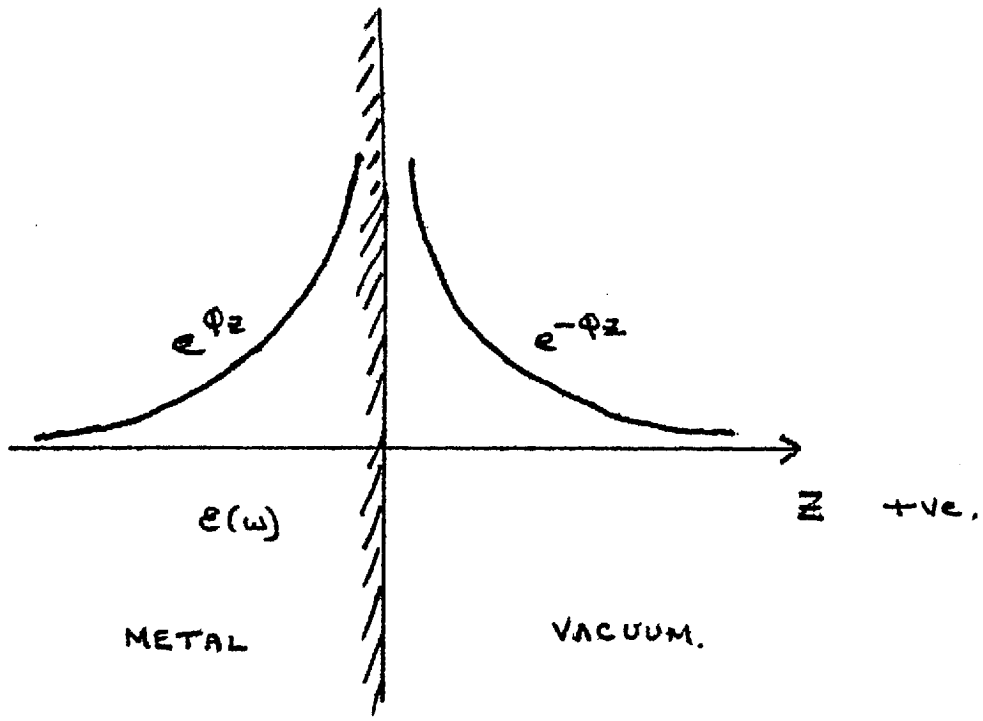

CHAPTER II

FORMULATION OF THE PROBLEM

Our main interest lies in the numerical calculation of the intrinsic satellite spectrum $N_+(\omega)$ of an adsorbed atom on a metal surface. As discussed in the previous chapter, this is related to the probability of creating an excitation of energy $\hbar\omega$ in an electron gas when a charge localised on the atom is suddenly switched on due to core hole creation by photoemission. It is therefore of importance to study the response function of the surface. What comes in (assuming the atom lies outside the surface) is the density-density response function when both the source and the probe lie outside the surface. This response function has a spectral density $S_g(\omega)$ which is the main topic discussed in this chapter.

The model of the surface of the electron gas used here is a microscopic one since it is desired to take into account effects such as finite screening length, surface plasmon dispersion and damping and electron hole excitations. The random phase approximation (RPA) is used.

As specified previously, the next two chapters of this thesis is related to the semi-classical infinite square barrier model (SCISBM) for the dynamic case in which our frequency ω is finite. The SCISBM is a

special case of the infinite square barrier model (ISBM), the latter being used in Chapters IV and V for static calculations involving the magnetization problem. It is therefore relevant to discuss the ISBM at this stage.

PROPERTIES OF THE ISB MODEL.

A large proportion of the work on the theory of metal surfaces has made use of the infinite barrier model which was first introduced by Bardeen in 1936. As the name suggests, this model assumes that the electrons are confined to the surface by an infinitely high potential barrier given by

$$V(z) = \begin{cases} 0 & \ldots \quad z < 0 \\ \infty & \ldots \quad z > 0 \end{cases}$$

assuming a Cartesian co-ordinate frame (x,y,z) associated with the physical system such that the metal lies in the region $z < 0$ and the metal surface is in the x-y plane, z=o. The z-axis is thus perpendicular to the surface of the metal, while the metal itself is a semi-infinite system. Using Schrodinger's equation of motion viz.

$$H\psi = E\psi$$

where H is the Hamiltonian of the system,

E is the total energy of the system

and ψ is the basic quantum - mechanical wave function,

We can write ψ for a given momentum quantum number

$\underline{q} = (\underline{\rho}, q_z)$ as :

$$\psi_q = \psi_x \psi_y \psi_z$$

$$\propto e^{i\underline{q}.\underline{x}} \sin q_z z \quad \ldots \quad z < 0 \text{ (inside the metal)}$$

$$0 \quad \ldots \quad z > 0 \text{ (outside the metal)}$$

where $\underline{X} = (x,y)$. The electron density is given as a function of z by

$$\rho(z) = \sum_{q<k_F} \psi_q^* \psi_q$$

$$\propto \iiint \sin^2(z q_z)\, dq$$

where the triple integral is carried out in momentum space over a sphere of radius k_F, the Fermi momentum. This integration is easily performed by converting to spherical polar co-ordinates, whereby we obtain (see Gradshtein and Ryshik), Bardeen's (1936) expression

$$\rho(z) = \frac{k_F^3}{(3\pi)^2}\left\{1 + \frac{3\cos(2k_F z)}{(2k_F z)^2} - \frac{3\sin(2k_F z)}{(2k_F z)^3}\right\} \Theta(-z) \quad \ldots\ldots (2.1)$$

where the first term is just the electron density inside the metal, while the last two oscillatory terms are the Bessel Function $J_{3/2}(2k_F z)$ or the spherical Bessel Function $j_1(2k_F z)$ and $\Theta(z)$ is the ordinary Heaviside unit step function given by

$$\Theta(z) = 1 \quad \ldots \quad z > 0$$

$$0 \quad \ldots \quad z < 0$$

The very simplicity of the infinite barrier model provides sufficient reason for its popularity. Many quantities can

be expressed in terms of simple functions, so allowing detailed analysis of the statistical behaviour of electrons in the surface region. A simple model has many virtues provided its limitations are borne in mind when studying a subject as complex as the inhomogeneous electron gas. It is clear from the form of our wave function $\psi_q(\underline{r})$ and the electron density $\rho(z)$, that the placing of an infinite barrier potential is equivalent to assuming that all the electronic states are specularly reflected at the boundary and that the probability of finding an electron within the positive z half-space is zero. A finite potential barrier would be clearly more realistic as it allows for quantum tunnelling effects into the vacuum. The IBM confines electrons too strongly and cannot account for questions concerning the evanescent tails of metal wave functions.

Another criticism, made by Lang (1973), is that the only characteristic length which appears is the Fermi wavelength $\propto k_F^{-1}$. But for high values of metallic densities (or low r_s), in the self-consistent calculations the Fermi-Thomas screening length $k_{FT} = \sqrt{\frac{4k_F}{\pi}}$ is expected to play an important role. Lang's self-consistent calculations for the electron density for r_s equals 5.0 using a planar uniform background model compares well with the IBM case except for the tail of the profiles. Both densities display a pronounced oscillatory behaviour arising from quantum interference effects at the boundary and extend far into the bulk. For $r_s = 2.0$

on the other hand the oscillations in the self-consistent profile are diminished in amplitude and it resembles the monotonic Fermi-Thomas profile more closely. Lang's calculations were based upon the wave mechanical formulation of the density functional theory and employed a local approximation for the surface exchange correlation potential. Although this approximation is not beyond criticism, his density profiles are probably the most reliable ones available at present.

In the SCISBM the electron density is :

$$\rho(z) = \frac{k_F^3}{(3\pi)^2} \Theta(-z) \quad . \; . \; . \quad (2.2)$$

i.e. constant and equal to the bulk value within the metal and zero outside. This approximation to the IBM by smoothing out of the Friedel-type oscillations will be under consideration in our calculations in this chapter and the next. This is more of a mathematical model chosen for convenience rather than a physical model chosen for realism, although it does in fact give reasonable dynamical properties. But we must keep in mind that this model does violate Heisenberg's uncertainty principle in quantum mechanics from which we expect the density to die down gradually to zero in a distance of the order of atomic dimensions viz. $\hbar/p_F$.

The electron densities given by (2.1) and (2.2) are drawn in Fig. (2.1) and compared with Lang's self-consistent density profiles.

DERIVATION OF AN EXPRESSION FOR THE LINEAR RESPONSE IN THE SCISBM.

To begin with, we wish to calculate the linear response of the system to a perturbing potential $V(\underline{r},t)$ in the Hamiltonian. Assume the existence of an external time-dependant potential e.g. an external charge at a distance d from the surface of the semi-infinite metal, say at the point (0,0,d) in the Cartesian framework system. We also assume translational invariance in the $\underline{X} = (x,y)$ plane. Let $U(\underline{r},t)$ be the source potential due to the external charge distribution and $\phi(\underline{r},t)$ the potential in the metal due to the charge density. Then the self-consistency reads

$$V(\underline{r},t) = U(\underline{r},t) + \phi(\underline{r},t) \quad \ldots (2.3)$$

while the RPA gives the response $\delta\rho$ by

$$\delta\rho(\underline{r},t) = \int_0^t dt' \int d\underline{r}' \, R(\underline{r},t,\underline{r}',t') V(\underline{r}',t') \ldots (2.4)$$

where the response function R is defined by (Kubo, 1957):

$$R(\underline{r},t,\underline{r}',t') = i\langle\phi_0|[\rho(\underline{r}',t'),\rho(\underline{r},t)]|\phi_0\rangle\Theta(t-t') \quad (2.5)$$

where $|\phi_0\rangle$ is the time-independant Heisenberg ground state of the unperturbed system,

and $\rho(\underline{r},t)$ is a density operator which may be defined in terms of creation and destruction operators corresponding to the one particle wave functions of the unperturbed system.

We assume a summation over spin indices in (2.5) coming from the density operators and that the perturbation is switched on at time t = 0. Atomic units are used throughout. Define the Fourier Transform of a function g(t) as

$$g(\omega) = \int_0^\infty e^{i\omega t}\, g(t)\, dt \quad \ldots \quad (2.6)$$

Using (2.6) in (2.3) and (2.4) gives us

$$V(\underline{r}, \omega) = U(\underline{r}, \omega) + \phi(\underline{r}, \omega) \quad \ldots \quad (2.7)$$

$$\delta\rho(\underline{r}, \omega) = \int d\underline{r}'\, R(\underline{r}, \underline{r}', \omega)\, V(\underline{r}', \omega) \quad \ldots \quad (2.8)$$

Now define the Fourier Cosine Transform of a function f($\underline{r}$) as

$$f_{\underline{q}} = \int d\underline{r}\, e^{i\underline{q}.\underline{x}} \cos(q_z z) f(\underline{r}) \quad \ldots \quad (2.9)$$

and use in (2.7), (2.8) to give

$$V(\underline{q}, \omega) = U(\underline{q}, \omega) + \phi(\underline{q}, \omega) \quad \ldots \quad (2.10)$$

$$\delta\rho(\underline{q}, \omega) = \int dq_z'\, R_{\underline{q} q_z q_z'}(\omega)\, V_{\underline{q} q_z'}(\omega) \quad \ldots \quad (2.11)$$

where

$$R_{\underline{q} q_z q_z'}(\omega) = \int d^2(x-x')\, dz\, dz'\, e^{i\underline{q}.(\underline{x}-\underline{x}')} \cos(z q_z) \cos(z' q_z')\, R(\underline{r}, \underline{r}', \omega) \quad \ldots \quad (2.12)$$

Equation (2.12) incorporates into it the translational invariance in the x-y plane.

Consider the operator $\tilde{O} = e^{i\underline{q}.\underline{x}} \cos(q_z z)\, \nabla^2 \quad \ldots \quad (2.13)$

Apply $\tilde{O}$ to the left hand-side of the scalars in equation (2.7) and integrate over a volume v of the electron gas. Utilise Green's theorem (as stated in Appendix A2) to obtain

$$\int_v \tilde{O} V \, d\underline{r} = \int_v V \nabla^2 \left(e^{i\underline{q}.\underline{x}} \cos(q_z z)\right) d\underline{r} + \int_S e^{i\underline{q}.\underline{x}} \cos(q_z z) \underline{\nabla} V . d\underline{S}$$
$$- \int_S V \underline{\nabla} \left(e^{i\underline{q}.\underline{x}} \cos(q_z z)\right) . d\underline{S} \quad \ldots (2.1$$

where $d\underline{S} = (0,0,\hat{k})dxdy$ is the unit vector in the positive z-direction that is, normal to the surface. Consequently the only non-zero term arising from the dot product $\underline{\nabla} V . d\underline{S}$ is $\frac{\partial V}{\partial z}$ Now,

$$\nabla^2 \left(e^{i\underline{q}.\underline{x}} \cos(q_z z)\right) = -(q^2 + q_z^2) e^{i\underline{q}.\underline{x}} \cos(q_z z) = -|q|^2 e^{i\underline{q}.\underline{x}} \cos(q_z z)$$

The second surface integral is zero at z = 0. We have from (2.14) the result

$$\nabla^2 V = -|q|^2 V_q + V_q'(0) \quad \ldots \quad (2.15)$$

As we assume the source charge distribution lies outside the electron gas, we have from Poisson's equation that

$$4\pi \delta\rho_q = -|q|^2 V_q + V_q'(0) \quad \ldots \quad (2.16)$$

Now in the region $0 < z < d$ we have

$$\left.\begin{aligned} \phi_q(z) &= e^{-qz} \phi_q(0) \\ U_q(z) &= e^{q(z-d)} U_q(d) \end{aligned}\right\}$$

Hence using (2.7),

$$\left.\begin{aligned} V_q(0) &= \phi_q(0) + U_q(0) \\ V_q'(0) &= -q\,\phi_q(0) + q\,U_q(0) \end{aligned}\right\}$$

Substitute in (2.15) gives

$$V_\rho'(0) = |q|^2 V_q + 4\pi \delta\rho_q$$
$$= -\rho V_\rho(0) + 2\rho U_\rho(0) \quad \ldots \quad (2.17)$$

Put (2.11) in (2.17) gives

$$|q|^2 V_q(\omega) + 4\pi \int dq_z' R_{\rho q_z q_z'}(\omega) V_{\rho q_z'}(\omega) = -\rho V_\rho(0) + 2\rho U_\rho(0)$$

Rewriting,

$$\int dq_z' E_{\rho q_z q_z'} V_{\rho q_z'}(\omega) = -\rho V_\rho(0) + 2\rho U_\rho(0) \quad \ldots \quad (2.18A)$$

where the matrix $E_{\rho q_z q_z'}$ is given by

$$E_{\rho q_z q_z'}(\omega) = |q|^2 \delta_{q_z q_z'} + 4\pi R_{\rho q_z q_z'}(\omega) \quad \ldots \quad (2.18B)$$

From (2.18A) we have in matrix notation,

$$V_q = \rho \sum_{q_z'} E^{-1}_{\rho, q_z q_z'} \left(2 U_\rho(0) - V_\rho(0)\right) \quad \ldots \quad (2.19)$$

Now, $\varepsilon_\rho^{-1}(\omega) = \rho \sum_{q_z'} E^{-1}_{\rho q_z q_z'}$

and applying (2.9) to (2.19) we have

$$\phi_\rho(0) = V_\rho(0) - U_\rho(0)$$
$$= \frac{1 - \varepsilon_\rho(\omega)}{1 + \varepsilon_\rho(\omega)} U_\rho(0)$$

This is the quantum analogue of the classical image theorem for a semi-infinite dielectric medium, which states that the ratio of the induced potential in the external region to the reflection of the source potential in the surface is weighted by the factor $R_\rho(\omega)$ where

$$R_{\rho}(\omega) = \frac{1 - \varepsilon_{\rho}(\omega)}{1 + \varepsilon_{\rho}(\omega)} \quad . \; . \; . \qquad (2.20)$$

Newns (1970) has given a detailed derivation of $R_{\rho, q_z, q_z'}(\omega)$ (in equation(2.18B)) for non-interacting electrons in the IBM and we quote his result in the form

$$R_{\rho q_z q_z'}(\omega) = \mathcal{D}_{\rho q_z}(\omega)\, \delta_{q_z q_z'} - A_{\rho q_z q_z'}(\omega) \; . \; . \; . \qquad (2.21A)$$

where the diagonal terms $D_{\rho q_z}(\omega)$ are related to the bulk RPA dielectric function thus:

$$\varepsilon^{RPA}(q, \omega) = \left(1 + 4\pi \frac{\mathcal{D}_{\rho, q_z}}{q^2}\right) \quad . \; . \; . \qquad (2.21B)$$

and the off-diagonal elements $A_{\rho q_z q_z'}(\omega)$ are more complex but obey the sum rule

$$\sum_{q_z'} A_{\rho, q_z q_z'}(\omega) = \mathcal{D}_{\rho, q_z}(\omega) \quad . \; . \; . \qquad (2.21C)$$

However for our SCISBM, these off-diagonal terms are neglected, and so

$$\varepsilon_{\rho}^{-1}(\omega) = \rho \sum_{q_z, q_z'} \left(\left(|q|^2 + 4\pi \mathcal{D}_{\rho, q_z} \right) \delta_{q_z q_z'} \right)^{-1} \; . \; . \; . \qquad (2.22)$$

Put equation (2.21B) in (2.22) and we get

$$\varepsilon_{\rho}^{-1}(\omega) = \frac{2\rho}{\pi} \int_0^{\infty} \frac{dq_z}{(\rho^2 + q_z^2)\, \varepsilon^{RPA}(q, \omega)} \quad . \; . \; . \qquad (2.23)$$

as in Ritchie and Marusak's 1966 paper. Thus the equations (2.20) and (2.23) give us our linear response function for the system in a well-defined mathematical form.

We now have a digression in which we define a slightly different retarded response function which enables us to

calculate some sum rules in a fairly simple way.

ANOTHER DEFINITION OF THE RESPONSE - FUNCTION : INTRODUCTION TO THE DYNAMIC FORM FACTOR.

Another form for the surface response function for a semi-infinite medium, assuming the existence of an external time-dependant potential which is applied as a perturbation to the system is defined as

$$* \quad R_{\varphi}(t) = \frac{2\pi i}{\varphi}\,\Theta(t)\langle 0|[\hat{\phi}_{\varphi}(0),\ \hat{\phi}_{-\varphi}(t)]|0\rangle \quad \ldots \quad (2.24)$$

where $\underline{\varphi}$ is a wave - vector parallel to the surface of the metal,

$\hat{\phi}_{\underline{\varphi}} = \sum_{i=1}^{N} e^{i\underline{\varphi}.\underline{x}_i + \varphi z_i}$

$\hat{\phi}_{\varphi}(t)$ is a density operator in the Heisenberg representation,

$|0\rangle$ is the ground state of the unperturbed metal surface and

$\langle 0|[\quad]|0\rangle$ meaning the expectation value with respect to the ground state of the system.

Physically, the first $\hat{\phi}$ in (2.24) corresponds to the perturbation while the second is linked to the probe into the system. We can rewrite (2.24) as

$$R_{\varphi}(t-t') = -\frac{2\pi i}{\varphi}\,\Theta(t-t')\int_{-\infty}^{0} dz\, e^{\varphi z}\int_{-\infty}^{0} dz'\, e^{\varphi z'}\langle 0|[\hat{\rho}_{-\underline{\varphi}}(z,t),\ \hat{\rho}_{\underline{\varphi}}(z',t')]|0\rangle \quad \ldots \quad (2.25A)$$

where

$$\rho_{\underline{\varphi}}(z) = \sum_{i} e^{-i\underline{\varphi}.\underline{x}_i}\,\delta(z - z_i) \quad \ldots \quad (2.25B)$$

* See Appendix D2 for relating to (2.20)

We now make a definition of the spectral density function of $R_\varphi(\omega)$, (written in the Fourier representation) as being proportional to the imaginery part of $R_\varphi(\omega)$ as follows:

$$S_\varphi(\omega) = -\frac{1}{\pi}\,\Im(\omega)\,R_\varphi(\omega) \quad \ldots \quad (2.26)$$

From (2.25A) and (2.26) we have

$$S_\varphi(\omega) = \frac{2\pi}{\varphi}\int_{-\infty}^{0} dz\, e^{\varphi z}\int_{-\infty}^{0} dz'\, e^{\varphi z'}\sum_n \delta(\omega+\varepsilon_0-\varepsilon_n)\times$$
$$\langle 0|\hat{\rho}_{-\varphi}(z)|n\rangle\langle n|\hat{\rho}_\varphi(z')|0\rangle \quad \ldots \quad (2.27)$$

where $|n\rangle$ is the excited state of the metal and surface with energy ε_n.

The $S_\varphi(\omega)$ is our two-dimensional frequency-dependent dynamic form factor corresponding to similar quantities defined for bulk systems (see, for example, Nozieres and Pines,1966). It is, in more physical terms, the coupling strength for solid excitations of frequency ω responding to an external perturbation of the form

In Lehmann representation we can write

$$R_\varphi(\omega) = \int_0^\infty d\omega'\, S_\varphi(\omega')\left\{\frac{1}{\omega-\omega'+i\delta} - \frac{1}{\omega+\omega'+i\delta}\right\} \quad \ldots \quad (2.28)$$

where $\delta > 0$

Using the standard result,

$$\lim_{\eta\to 0}\frac{1}{x-a+i\eta} = P\left(\frac{1}{x-a}\right) - i\pi\,\delta(x-a)$$

in (2.28) immediately gives

$$\mathrm{Im}\,R_\varphi(\omega) = -\pi\left\{S_\varphi(\omega) - S_\varphi(-\omega)\right\}$$

i.e. $\mathrm{Im}R_\varphi(\omega)$ is an odd function.

So far we have complete analogy with bulk systems as considered by Nozieres and Pines, 1966.

<u>Moments</u>

We define the nth moment of the system to be

$$\mu_n(\varphi) = \int_0^\infty \omega^n S_\varphi(\omega)\, d\omega \quad \ldots \quad (2.29)$$

where the special cases $n = -1$ corresponds to the perfect screening sum rule, and $n = +1$ corresponds to the f-sum rule. Put $\omega = 0$ in (2.28) gives

$$\int_0^\infty d\omega' \frac{S_\varphi(\omega')}{\omega'} = -\frac{1}{2} R_\varphi(0) \quad \ldots \quad (2.30)$$

By utilising the quantum analogue of the classical image theorem (see equation (2.20)) in the long wavelength limit

$$\lim_{\varphi \to 0} R_\varphi(0) = -1$$

as in the classical theory. Hence (2.30) becomes

$$\int_0^\infty d\omega' \frac{S_\varphi(\omega')}{\omega'} = 1/2 \quad \text{as} \quad \varphi \to 0 \quad \ldots (2.31)$$

Now consider the surface f-sum rule, or the case $n = +1$ in (2.29)

$$\mu_1(\varphi) = \int_0^\infty \omega S_\varphi(\omega)\, d\omega$$

$$= \sum_n \frac{2\pi}{\varphi} \int_{-\infty}^0 dz\, e^{\varphi z} \int_{-\infty}^0 dz'\, e^{\varphi z'} \langle 0 | \rho_{-\varphi}(z) H \rho_\varphi(z')$$

$$- H \rho_{-\varphi}(z) \rho_\varphi(z') | 0 \rangle \quad \ldots \quad (2.32)$$

(from (2.27))

where H is the Hamiltonian of the system, taken for simplicity to be of the form

$$H = \sum_i \frac{p_i^2}{2m} + V = \sum_i \frac{\nabla_i^2}{2m} + V$$

where p_i is the momentum of the ith particle of mass m and $V = V(\underline{r}_1, \quad \underline{r}_N)$ is a position-dependent potential with $r_i = (\underline{x}_i, z_i)$, $i = 1, \ldots N$.

We can rewrite (2.32) as

$$\mu_1(\varphi) = \frac{2\pi}{\varphi} \sum_n (\varepsilon_n - \varepsilon_0) \langle 0 | \eta_{-\varphi} | n \rangle \langle n | \eta_\varphi | 0 \rangle \ldots (2.33A)$$

where

$$\eta_\varphi = \sum_i e^{-i\underline{\varphi}.\underline{x}_i + \varphi z_i} \quad \ldots (2.33B)$$

Hence

$$\mu_1(\varphi) = \frac{\pi}{\varphi} \langle 0 | [\eta_{-\varphi}, H], \eta_\varphi] | 0 \rangle \quad \ldots (2.34$$

Since η_φ can be replaced by $\eta_{-\varphi}$ without alteration of symmetry of the problem. We make use of the Lemma in Appendix A2 to write (2.34) as

$$\mu_1(\varphi) = \frac{\pi}{2m\varphi} \langle 0 | 2 \sum_i \nabla_i e^{i\underline{\varphi}.\underline{x}_i + \varphi z_i} . \nabla_i e^{-i\underline{\varphi}.\underline{x}_i + \varphi z_i} | 0 \rangle$$

$$= \frac{\pi}{m\varphi} \sum_i \langle 0 | e^{2\varphi z_i} (i\underline{\varphi} + \hat{\underline{k}}\varphi) . (-i\underline{\varphi} + \hat{\underline{k}}\varphi) | 0 \rangle$$

where $\hat{\underline{k}}$ is the unit vector perpendicular to the metal surface.

$$\therefore \mu_1(\varphi) = \frac{2\pi\varphi}{m} \sum_i \langle 0 | e^{2\varphi z_i} | 0 \rangle$$

But $\rho(z) = \langle 0 | \sum_i \delta(z - z_i) | 0 \rangle$ is the substrate electron density at z

$$\Rightarrow \mu_1(\varphi) = \frac{2\pi\varphi}{m} \int_{-\infty}^{0} e^{2\varphi z} \rho(z)\, dz \quad \ldots (2.35)$$

As $Q \to 0$, we can approximate to a uniform charge density and obtain the limiting form

$$\lim_{\varphi \to 0} \mu_1(\varphi) = \frac{\pi n}{m} = \frac{1}{2}\omega_s^2 \quad . \; . \; . \quad (2.36)$$

where n= the number of electrons per unit volume,

$\omega_s = \omega_p/\sqrt{2}$

ω_p is the bulk plasma frequency.

Substitute the Ansatz,

$$S_\varphi(\omega) = C\,\delta(\omega - \omega_0) \quad . \quad . \quad . \quad (2.37A)$$

for the expressions μ_1, μ_{-1} in (2.31), (2.36) gives

$$\lim_{\varphi \to 0} S_\varphi(\omega) = \frac{\omega_s}{2}\,\delta(\omega - \omega_s) \quad . \; . \; . \quad (2.37B)$$

which immediately shows that if there is only a single excitation, then this excitation must be identified with the surface plasmon coupling intensity. Physically this means that the collective resonance is the only excitation in the system which can be detected outside the surface by an external probe situated at a distance large compared to the screening length.

Our results so far are extremely general and will therefore apply to any model of the electron system. The work is consistent with Gumhalter (1976, thesis).

In this thesis we are interested in calculating numerically the surface response function for the SCISBM.

EXPLICIT FORMULAE FOR THE DYNAMIC FORM FACTOR IN THE SCISBM.

Our work involves calculations within the RPA which is wellknown to yield good results in the high density regime (small values of r_s). We initially wish to calculate the dynamic structure factor $S_\varrho(\omega)$ which is rich in information about our system. In general, $S_\varrho(\omega)$ contains contributions from single quasiparticle - quasihole pair excitation, from multipair excitations and from longitudinal collective modes (the plasmons). For moderate to large values of Q in translationally invariant systems, the contributions from different modes of excitation cannot be disentangled and $S_\varrho(\omega)$ is spread more or less uniformly over the excitation frequencies. However for the long wavelength limit ($Q \to 0$) it is possible to clearly view the results of different excitations, as we shall see in the ensuing analysis.

From our previous formalism (equation 2.23) we have for the SCISBM

$$\varepsilon_\varrho^{-1}(\omega) = \frac{2\varrho}{\pi} \int_0^\infty \frac{dq_z}{\varepsilon_q^{RPA}(\omega)(\varrho^2+q_z^2)}$$

$$= \frac{2\varrho}{\pi} \int_0^\infty \frac{(\varepsilon_1 - i\varepsilon_2)}{(\varepsilon_1^2+\varepsilon_2^2)(\varrho^2+q_z^2)} dq_z \quad \ldots (2.38)$$

where $\varepsilon_q^{RPA}(\omega)$ is the bulk dielectric function of the three-dimensional wave vector $q=(\varrho,q_z)$ and $\varepsilon_1 = \varepsilon_1(q,\omega)$; $\varepsilon_2 = \varepsilon_2(q,\omega)$ are Lindhard's dielectric function given by (Nozieres and Pines, 1966, correcting by a factor of $\frac{1}{2}$ part of their expression for $\varepsilon_2(q,\omega)$) :

$$\varepsilon_1(q,\omega) = 1 + \frac{\lambda^2}{q^2}\left\{ \tfrac{1}{2} + \frac{p_F}{4q}\left[\left(\frac{(\omega+q^2/2)^2}{(qp_F)^2} - 1\right)\log\left|\frac{\omega - qp_F + q^2/2}{\omega + qp_F + q^2/2}\right| - \left(\frac{(\omega - q^2/2)^2}{(qp_F)^2} - 1\right)\log\left|\frac{\omega - qp_F - q^2/2}{\omega + qp_F - q^2/2}\right|\right]\right\} \quad \ldots (2.39A)$$

and

For $q \leq 2p_F$,

$$\varepsilon_2(q,\omega) = \left(\frac{\pi\lambda^2}{2q^3 p_F}\right)\omega \quad \ldots \quad \text{if} \quad \omega \leq qp_F - q^2/2 \quad \alpha$$

$$\frac{\pi\lambda^2 p_F}{4q^3}\left\{1 - \frac{(\omega - q^2/2)^2}{(qp_F)^2}\right\} \ldots \quad \text{if} \quad -\frac{q^2}{2} \leq \omega - qp_F \leq q^2/2 \quad \beta$$

$$0 \quad \ldots \quad \text{if} \quad \omega \geq qp_F + q^2/2 \equiv \gamma$$

For $q > 2p_F$,

$$\varepsilon_2(q,\omega) = \frac{\pi\lambda^2 p_F}{4q^3}\left\{1 - \frac{(\omega - q^2/2)^2}{(qp_F)^2}\right\} \ldots \quad \text{if} \quad \frac{q^2}{2} - qp_F \leq \omega \leq \frac{q^2}{2} + qp_F \quad \delta$$

$$0 \quad \ldots \quad \text{otherwise} \quad \gamma$$

The Greek letters at the end of the expression for $\varepsilon_2(q,\omega)$ (2.39B) indicate the different regions for ω bounded by the functional forms of q. This is illustrated in Fig. (2.2). For fixed ω - values ε_2 is non-zero within a finite range say q_A, q_B where $q_B > q_A$. In fact

$$q_A = -p_F + \sqrt{p_F^2 + 2\omega}$$

$$q_B = p_F + \sqrt{p_F^2 + 2\omega}$$

We work throughout in atomic units i.e. $\hbar = m = 1$,

$\lambda^2 = 3\omega_p^2/p_F^2 = 4p_F/\pi$ (the Fermi-Thomas screening wave vector)

$\omega_p = p_F^2\sqrt{\dfrac{4 \times 0.521 \times r_s}{3\pi}}$, (the bulk plasmon frequency)

(the Fermi-Thomas momentum

where r_s is the metallic density lying realistically in the range $1.8 \leq r_s \leq 5.6$.

In equation (2.20) we have shown that the linear response function $R_\varphi(\omega)$ valid for small perturbations may be written as

$$R_\varphi(\omega) = \frac{\varepsilon_\varphi^{-1}(\omega) - 1}{\varepsilon_\varphi^{-1}(\omega) + 1} \quad \ldots \quad (2.40)$$

which using (2.26) and (2.38) give

$$S_\varphi(\omega) = \begin{cases} -\dfrac{2}{\pi}\left\{\dfrac{E_2}{(E_1+1)^2 + E_2^2}\right\} & \ldots \ \omega > 0 \\ 0 & \ldots \ \text{otherwise} \end{cases} \quad (2.41)$$

where

$$E_1 = \frac{2\varphi}{\pi}\int_0^\infty \frac{\varepsilon_1}{(\varepsilon_1^2+\varepsilon_2^2)(\varphi^2+q_z^2)}\,dq_z \quad \ldots \quad (2.42A)$$

$$E_2 = -\frac{2\varphi}{\pi}\int_0^\infty \frac{\varepsilon_2}{(\varepsilon_1^2+\varepsilon_2^2)(\varphi^2+q_z^2)}\,dq_z \quad \ldots \quad (2.42B)$$

We note that for small ω-values, via a logarithmic expansion,

$$\varepsilon_1 \longrightarrow 1 + \lambda^2/q^2$$

and $\varepsilon_1 \xrightarrow{\omega \text{ large}} 1$ (actually $1 - \frac{\omega_p^2}{\omega^2}$), i.e. for large values of the frequency, the real part of the Lindhard's dielectric function approaches unity. Also

$$\varepsilon_1 \xrightarrow{q \text{ large}} 1 + O(1/q^3)$$

In (2.42B) the infinite integral in E_2 can be replaced by a finite one since ε_2 vanishes for large q values.

In the zero frequency limit but for finite Q we have (see Appendix B2)

$$S_\varphi'(0) = -\frac{\varphi}{\pi p_F \lambda^2}\left(1 + 2\log\varphi - \log\left(\frac{16\lambda^2 p_F^2}{4p_F^2+\lambda^2}\right)\right) \quad \ldots \quad (2.43)$$

which can be (and indeed is) used as a check on our work. We may also make an expansion of the spectral density function in ascending powers of ω for small Q, ω values:

$$\lim_{\substack{Q \ll \lambda \\ \omega \ll \omega_p}} S_Q(\omega) = a\omega + b\omega^2 + O(\omega^3) \quad \ldots \quad (2.44)$$

where

$$a = \frac{2Q}{\lambda^2 p_F \pi}\left(\log\left(\frac{2\lambda}{Q}\right) - \tfrac{1}{2}\right)$$

$$b = -\frac{2}{\pi\lambda^2 p_F^2}$$

a is easily obtained from (2.43) while b may be calculated by consideration of $S_Q''(0)$. The above equation shows the linear behaviour of $S_Q(\omega)$ for small values of ω ($\omega < Qp_F$)

Since we are concerned with the small Q-behaviour, let us for interest make an expansion of $\varepsilon_Q^{-1}(\omega)$ of the form

$$\varepsilon_Q^{-1}(\omega) \underset{\omega \gg Qp_F}{=} a_0(\omega) + \left(a_1(\omega) + i b_1(\omega)\right) Q \quad \ldots \quad (2.45)$$

ignoring terms of $O(Q^2)$ and higher. Then using (2.40) and (2.26) we have

$$S_Q(\omega) = -\frac{1}{\pi}\,\mathrm{Im}\,\frac{\varepsilon_Q^{-1}(\omega) - 1}{\varepsilon_Q^{-1}(\omega) + 1}$$

$$= -\frac{2Q}{\pi}\,\frac{b_1(\omega)}{\left(1 + a_0(\omega) + a_1(\omega)Q\right)^2 + \left(b_1(\omega)Q\right)^2} \quad \ldots \quad (2.46A)$$

Comparing the real and imaginery parts of equations (2.38) and (2.45) yields

$$b_1(\omega) = -\frac{2}{\pi}\int_0^\infty \frac{dq_z\, \varepsilon_2(0,\omega)}{\left(\varepsilon_1^2(0,\omega) + \varepsilon_2^2(0,\omega)\right) q_z^2} \quad \ldots \quad (2.46B)$$

and

$$a_1(\omega) = \frac{2}{\pi}\int_0^\infty \left(\frac{\dfrac{\varepsilon_1(0,\omega)}{\varepsilon_1^2(0,\omega) + \varepsilon_2^2(0,\omega)} - a_0}{q_z^2}\right) dq_z \quad \ldots \quad (2.46C)$$

and $$Q_0(\omega) = \left(1 - \frac{\omega_p^2}{\omega^2}\right)^{-1} = \frac{\omega^2}{\omega^2 - \omega_p^2} \quad \ldots \quad (2.46D)$$

Substitute (2.46D) into (2.46A) gives

$$\lim_{\substack{\omega \gg \varphi p_F \\ \varphi \text{ finite}}} S_\varphi(\omega) = -\frac{2\varphi}{\pi} \frac{b_1(\omega)(\omega^2 - \omega_p^2)^2}{\left[(2\omega^2 - \omega_p^2 + a_1(\omega)\varphi(\omega^2 - \omega_p^2))^2 + (b_1\varphi(\omega^2 - \omega_p^2))^2\right]} \quad (2.47$$

In fact $a_1(\omega)$ is the Hilbert Transform of $b_1(\omega)$: see Appendix C2. Thus in (2.47) we have obtained a simplified form of our dynamic structure factor for values of the frequency higher than our cut-off frequency Qp_F. For lower values of ω we anticipate the linear behaviour (equation (2.44)). We also note that as $\omega \to \omega_s = \frac{\omega_p}{\sqrt{2}}$, the surface plasmon, examination of the denominator in (2.47) (ignoring the Q^2 terms) shows a shooting up of $S_\varphi(\omega)$, indicating a delta-function type of behaviour as $Q \to 0$: see our Ansatz for $S_\varphi(\omega)$ in (2.37B).

Our (2.47) equation also clearly indicates

$$\lim_{\substack{\omega \to \omega_p \\ \varphi \ll \lambda}} S_\varphi(\omega) = 0 \quad \ldots \quad (2.48)$$

We make use of the sum rules on hand throughout to provide checks on our ensuing calculations (Equations 2.30 and 2.36).

DYNAMIC FORM FACTOR IN THE SCISBM: NUMERICAL RESULTS AND DISCUSSION

We have plotted several graphs of $S_Q(\omega)$ as a function of ω for various values of Q ($0.25\ p_F$, $0.5p_F$, p_F, $1.5\ p_F$, $2.0p_F$) for two values of the metallic density $r_s = 3.0, 5.0$ (Figs. 2.3 - 2.7). The Simpson's rule summation procedure used for the integrals, was seen to provide good convergent

results. For E_2 in (2.42B) we had a finite integration range (0,A) where

$$A = \sqrt{2p_F^2 + 2\omega - \varphi^2 + 2p_F\sqrt{p_F^2 + 2\omega}}$$

We split the integral E_1 in equation (2.42A) into two parts, (0, Uplim), and (Uplim, ∞) where Uplim $\gg 2p_F$ (we actually took Uplim = 12.0). The second integral was analytically handled, using asymptotic expansions for ϵ_1, ϵ_2 in the large q_z limit. The "plasmon region" where ϵ_1 and ϵ_2 simultaneously vanish (see Fig. 2.2) had to be carefully dealt with to prevent our integrals from blowing up. To prevent this from happening, we included a small 's' correction to $\epsilon_1^2 + \epsilon_2^2$ in the denominator of the integral (twice) and then extrapolated back linearly to obtain the correct integral. Parabolic extrapolations were attempted and compared with no significant difference to our results, showing that the linear approximation was sufficient for our purposes.

For small Q-values, there are three distinctive features of our spectral density curve $S_Q(\omega)$:

(I) The intial linear behaviour for small ω values. We notice a slight 'kink' occurring around the value $\omega = \omega_M = \varphi p_F$ before the curve shoots up at the surface plasmon and attribute this to the negative coefficient of ω^2 occurring in our expansion for $S_Q(\omega)$ in equation (2.44). Thus we have in the low frequency limit $0 < \omega < \varphi p_F$, the spectral function behaving linearly in ω; this relatively rapid rise at small ω leads to the well known result that a great many electron hole pairs can be excited near the Fermi level by a localised

perturbation giving rise to singular behaviour in the satellite spectra (Nozieres and Pines, 1966). Gumhalter and Newns (1975) have used the Ansatz

$$S_Q(\omega) = S_Q'(0)\,\omega\, e^{-\omega/\omega_m}$$

in this region.

(2) We note the sharp peak occurring around the surface plasmon ω_s. This corresponds to the δ - function type of behaviour for $S_Q(\omega)\left(=\frac{\omega_s}{2}\delta(\omega-\omega_s)\right)$. Due to the finiteness of our Q- values, the actual value of ω where the maximum occurs is slightly shifted to the right, giving us, quite naturally , the surface-plasmon dispersion which is discussed in the next section. These relations are plotted for both r_s = 3.0 and 5.0 in Figs. (2.9A and B).

(3) Another feature in evidence is the sharp dip or 'antiresonance' occurring in the region $\omega = \omega_p$. This also occurs in a recent work by Barton (1976) who emphasizes on separating out the different contributions due to bulk and surface plasmons. This is of course in expected agreement with our approximated version of $S_Q(\omega)$ given by (2.47) which we rewrite as

$$S_Q(\omega) = K_Q(\omega)\,(\omega^2 - \omega_p^2)^2$$

where $K_Q(\omega)$ is finite as $\omega \to \omega_p$.

Griffin and Zaremba (1973) have derived an expression for $S_Q(\omega)$ for inelastic scaterring in the Born approximation, applying a semi-classical limit of the quantum-mechanical RPA to a system of fermions bounded by infinite potential

barriers. But their form involves a peak at $\omega = \omega_p$ as well as $\omega = \omega_s$, for a system of electrons confined to a thick film. It would be interesting to see how their general expression for $S_Q(\omega)$ given by their equation (4.14) would compare with ours.

This phenomenon of antiresonance in the bulk plasmon demonstrates clearly the importance of the surface plasmon in our model and shows that our function $S_Q(\omega)$ is dominated by surface excitations but is "orthogonal" to bulk excitations. Physically this result is plausible since the spectral density belongs to the response function when both the source and probe are outside the surface.

We also note that in the small Q regime, good agreement was found numerically for our 'exact' $S_Q(\omega)$ and 'approximate' $S_Q(\omega)$ given by (2.47). At $Q = \frac{1}{4}p_F$ the two curves are so close that it is difficult to distinguish between them.

For $\omega \gg \omega_p$, we are left with a tail region dying off slowly to zero.

For larger values of Q ($=p_F$, $1.5p_F$, $2.0p_F$), $S_Q(\omega)$ is plotted in Figs.2.5 and 2.7 (for $r = 3.0, 5.0$ respectively) and we notice a change from the peaked characteristic to a more uniformly spread out behaviour. The dip at ω_p has disappeared at these higher wave-vector values. Hence we clearly see that the main contribution to $S_Q(\omega)$ occurs for $Q \leqslant p_F$.

Table (2.1) shows the results of our numerical checks via the two sum rules previously discussed. To check for μ_{-1} the graph $-\frac{1}{2}R_q(0) \sim q$ was plotted, in Fig, (2.8) where

$$R_q(0) = \text{Real}\left[\frac{\varepsilon_q^{-1}(0)-1}{\varepsilon_q^{-1}(0)+1}\right]$$

$$= \left[\frac{E_1^2 + E_2^2 - 1}{(E_1+1)^2 + E_2^2}\right]_{\omega=0}$$

Of course the numbers are rather subjective, depending on where the cut-off is taken in each case but we are nevertheless encouraged by the results. The numerically computed and theoretical figures are in satisfactory order of agreement. Introduction of the approximation to $S_Q(\omega)$ gave the sum rules to within 90% accuracy for $Q \sim O(1/4 p_F)$ at high metallic densities.

Before proceeding to the next chapter, we write a short section on surface plasmon dispersion relations below.

A COMMENT ON THE SURFACE PLASMON DISPERSION RELATION

Generally speaking, the presence of surfaces introduces new modes of plasma oscillations, in addition to the bulk one, with different properties and, in particular, different dispersion relations. The first theoretical observation of surface plasma oscillations were made by Ritchie (1957).

The semi-infinite electron gas with a perfectly reflecting boundary is one model of a metal surface which has been used in many calculations involving the RPA and hydrodynamical or quasiclassical RPA (i.e. that which neglects the quantum interference terms in the RPA). Feibelman (1971) has shown the importance

of the electron density profile at the surface in the dispersion relationship. He was also the first to show within the RPA that in the long wavelength limit $q \to 0$, the surface plasmon frequency $\omega_s = \omega_p/\sqrt{2}$ holds for a semi-infinite electron gas, independant of the exact electron density variation. The only assumption he made about the density was that it be self-consistent.

The imaginary part of the surface plasmon frequency $\omega_s(\varrho)$ is directly related to a Landau-type of damping originating in the decay of a surface plasmon into a particle hole pair (Newns, 1970) and may be partly due to inhomogeneities in the neighbourhood of the surface e.g. surface roughness (Raether, 1968; Ritchie, 1973) although it occurs for flat clean surfaces as well. Curves showing the variation of $\omega_2 \sim \varrho$ have been given by Ritchie and Marusak (1966) who use the same SCISBM as we do, and Beck (1971) who uses the IBM ie. the full quantum mechanical treatment.

In our model we are concerned with the real part of the dispersion. Let us assume an expansion of the form:

$$\omega_s(\varrho) = \alpha_0 + \alpha_1 \varrho + \alpha_2 \varrho^2 + \dots$$

Ritchie (1963) used a semi-classical hydrodynamical approach to the problem which yielded a linear term in his resulting equation. Ritchie and Marusak (1966) give graphs of $\omega_s(\varrho) \sim \varrho$ for the real part as a function of $Q/2p_F$ and obtain a linearity in behaviour.

It has been suggested (Ritchie, 1973) that the Q-dependance of ω_s could be tapped in a potentially interesting and useful manner to give us information regarding the surface dynamic response function. For our SCISBM we give in Figs. (2.9A & B) two graphs illustrating our surface plasmonic dispersion relations for r_s = 3.0, 3.0 respectively. We see that for small Q ($\ll \frac{1}{2}p$) our dispersion curve follow a decidedly linear behaviour with $\alpha_1 > 0$ although they assume a quadratic behaviour outside this Q-range. As expected, this linearity is in agreement with that predicted by Ritchie (1963) and Ritchie and Marusak (1966), the latter using exactly the same model as we do. But our results differ from those by Beck (1971) who in his pure quantum mechanical approach ends up with both the linear and quadratic terms in his dispersion formula for the same Q-range values. Some data from these three models discussed is displayed in Table (2.2) for comparative purposes.

Thus we see that our results for the Q-coefficient in the dispersion is in good order of agreement with Ritchie & Marusak, as expected, rather than Beck. The main reason we give for this is that the surface plasmon dispersion relation is sensitive to the electron-density profile at the surface (Bennett, 1970) although in any case for $Q \rightarrow 0$ it goes to $\omega_p/\sqrt{2}$. In our quasiclassical calculations (same as Ritchie and Marusak's, 1966) the density has a definite jump at the boundary,

whereas for the semi-infinite quantum mechanical RPA case, the electron density goes smoothly down to zero.

Krane and Raether (1976) have experimentally observed surface plasmon dispersion using high energy electron loss spectroscopy on aluminium and the results are notable for the initial dip occurring in the graph of $\omega_s(Q) \sim Q$ indicating that $\alpha_1 < 0$. This was earlier predicted by Bennett (1970) through a hydrodynamic approach, and later by Beck and Celli (1972) and Feibelman (1973) through a more realistic finite barrier model. Beck and Celli use a variational method while Feibelman incorporates self-consistent jellium values of the work function together with a surface diffuseness parameter, a, and illustrates the sensitivity of the dispersion to a . In the limiting case $a \to 0$, his results extrapolate back to those by Beck and Celli.

For interest we examine the perfect screening sum rule given by (2.30) using our small Q-approximation for $S_Q(\omega)$

i.e.

$$\int_0^\infty \frac{S_\varphi^{approx}(\omega)}{\omega}\, d\omega \underset{\varphi\to 0}{=} -\tfrac{1}{2} R_\varphi(0) = -\tfrac{1}{2}\left\{\frac{\epsilon_\varphi^{-1}(0)-1}{\epsilon_\varphi^{-1}(0)+1}\right\} \quad \text{from (2.40)}$$

$$= -\tfrac{1}{2}\left\{\frac{a_1(0)\varphi - 1}{a_1(0)\varphi + 1}\right\} \quad \text{where } a_1 \text{ is defined in (2.46C)}$$

$$\simeq \tfrac{1}{2}\left(1 - a_1(0)\varphi\right)^2$$

$$= \tfrac{1}{2}\left(1 - 2a_1(0)\varphi + O(\varphi^2)\right)$$

i.e. $$-\frac{2\varphi}{\pi}\int_0^\infty \frac{d\omega\, b_1(\omega)}{\omega\left((1+a_0(\omega)+a_1(\omega)\varphi)^2+(b_1(\omega)\varphi)^2\right)} \simeq \tfrac{1}{2} e^{-2a_1(0)\varphi}$$

for small φ - values. . . .(2.49)

The L.H.S. of the above equation can be quite easily checked to give consistent results for the zeroth-order term in Q, by calculating the residue near ω_s (actually given by the dispersion relation). We can rewrite the L.H.S. approximately as

$$-\frac{2\varphi}{\pi} b_1(\omega_s) \int_0^\infty \frac{d\omega\ (\omega_p^4/16)}{\omega\left[(\omega_s^2-\omega^2+\frac{\omega_p^2}{4}a_1\varphi)^2+(\frac{\omega_p^2}{4}b_1\varphi)^2\right]}$$

which has residues occurring at

$$\omega \simeq \pm\omega_s\left(1 + \tfrac{1}{4}\varphi\left(a_1 \pm i b_1\right)\right), \quad \text{by a binomial expansion.}$$

where a_1, b_1 are evaluated at $\omega = \omega_s$. . . . . (2.50

Taking an appropriate contour in the upper half of the complex plane and calculating the two residues at $\omega = \pm\omega_s(1+\tfrac{1}{4}\varphi(a_1+ib_1$ and using Cauchy's Integral formula gives the required answer of $\frac{1}{2}$ to be the value of our integral.

The equation (2.50) is the same as that given by Newns (1970) in his equation (91). To relate the Q-coefficient viz. in $R_Q(0)$ to physical quantities, consider a static point charge ($e = 1$) applied at the point (0,0,d) outside the surface of the metal. Then the response of the system will be such as to produce an image charge equal in magnitude but opposite in sign at the mirror point (0,0,-d) inside the metal. This is in accordance with classical Physics and is valid provided d is larger than the characteristic screening length of the metal, which is of the order of the inverse Fermi-Thomas wave-vector . Take the virtual image charge density to be of the form

$$\rho_\varphi(\underline{x}, z) = e^{i\underline{\varphi}\cdot\underline{x}}\,\delta(z-d)$$

Now the potential due to the charge satisfies Poisson's equation:

$$\nabla^2\phi = 4\pi\rho_\varphi(\underline{x}, z)$$

which solves to give the potential of the image charge to be

$$\phi_{im}(z,\omega) = \frac{2\pi}{\varphi}\, e^{-\varphi|z+d|}\, R_\varphi(\omega)$$

Take $\omega = 0$ limit and the exponential form for $R_\varphi(\omega)$,

$$\phi_{im}(z,0) \underset{\varphi \ll d}{=} \frac{2\pi}{\varphi}\, e^{-\varphi z}\, e^{-\varphi(d+2a_1(0))}$$

The "effective surface" is seen to be at $z = -a_1(0)$. Thus in the case of adsorption where d is microscopic, the simple classical formula may be used as a first approximation for adsorbed species of relatively large radius e.g. adsorbed caesium, provided d is interpreted as the distance from an

effective image plane. In our model for $r_s = 3.0$, from gradient measurements of $\log R_q(0) \sim Q$ we obtain $a_1(0) = 1.16$ a.u. $\simeq 0.61$ Å (since 1a.u. = 0.529Å) in excellent agreement with Newns (1970) graph in his Fig.7 which is a plot of $d \sim r_s$ for the truncated electron gas. A point of interest is to note that a change of sign of the Q-coefficient in $R_q(0)$ results in a similar change in sign of the Q-coefficient in the dispersion relationship. The numerical results in our calculation for $r_s = 3.0, 5.0$, give $a_1(0) = 1.2, 1.5$, $a_1(\omega_s) = 4.4, 6.0$ which strongly suggests the relation

$$a_1(0) \propto a_1(\omega_s)$$

or distance of effective image plane from the surface $\propto$ Q-coefficient of the surface plasmon dispersion formula.

This gives some information to us connecting the surface plasmon dispersion relationship from a purely abstract formula to a concrete physical concept involving the static surface response function. It is of interest to note that this argument accounts for the sign of the surface plasmon dispersion eg. in the ISBM and jellium models both $a_1(0)$ and $a_1(\omega_s)$ are positive and negative respectively (Newns, 1977). We leave this as a tentative suggestion rather than an obvious statement of fact.

With this we conclude Chapter I. We believe our graphs of $S_q(\omega)$ to be the first of its kind to be published, which naturally leaves little or no scope for direct comparison with other work. In the next Chapter we proceed to discuss

the intrinsic satellite spectrum of an adsorbed atom, a quantity which can be directly compared with experimental data rapidly emerging from various laboratories scattered in different parts of the world at the present time.

APPENDIX A2

(1) **LEMMA:** $\sum_{ijk} [[f_i, -\nabla_j^2], g_k] = 2\nabla_i f_i . \nabla_i g_i$

where f, g are functions of position alone.

PROOF: Let ψ be a wavefunction depending upon position co-ordinate alone, and let

$$\mathcal{G} = \sum_{ijk} [[f_i, -\nabla_j^2], g_k]$$

$$\therefore \mathcal{G}\psi = -(f_i \nabla_j^2 g_k - \nabla_j^2 f_i g_k - g_k f_i \nabla_j^2 + g_k \nabla_j^2 f_i)\psi$$

$$= -(f_i \nabla_j^2 (g_k \psi) - \nabla_j^2 (f_i g_k \psi - g_k f_i \nabla_j^2 \psi + g_k \nabla_j^2 (f_i \psi))$$

Using the standard result that

$$\nabla^2 (ab) = a\nabla^2 b + b\nabla^2 a + 2\nabla a . \nabla b$$

for scalars a,b, gives

$$\mathcal{G}\psi = -\{f_i \nabla_j^2 (g_k \psi) - f_i \nabla_j^2 (g_k \psi) - g_k \psi \nabla_j^2 f_i - 2\nabla_j f_i . \nabla_j (g_k \psi) - g_k f_i \nabla_j^2 \psi + g_k f_i \nabla_j^2 \psi + g_k \psi \nabla_j^2 f_i + 2 g_k \nabla_j f_i . \nabla_j \psi\}$$

Now i = j, otherwise $\mathcal{G}\psi = 0$

$$\therefore \mathcal{G}\psi = 2(\nabla_i f_i . \nabla_i (g_k \psi) - g_k \nabla_i f_i . \nabla_i \psi)$$

$$= 2\nabla_i f_i (\psi \nabla_i g_k + g_k \nabla_i \psi) - 2 g_k \nabla_i f_i \nabla_i \psi$$

Now i = k, otherwise again $\mathcal{G}\psi = 0$.

$$\therefore \mathcal{G}\psi = 2\nabla_i f_i . \nabla_i g_i \quad , \text{ as required.}$$

This result is used in equation (2.34)

(2) <u>Statement of Green's second identity or symmetrical theorem (one version).</u>

If f and g are scaler functions of position with continuous derivatives of at least second order, and V is the volume enclosed by a closed surface S, then :

$$\iiint_V (f\nabla^2 g - g\nabla^2 f)\,dv = \iint_S (f\nabla g - g\nabla f)\cdot d\underline{s}$$

APPENDIX B2

$$S_\varrho(\omega) = -\frac{2}{\pi}\left\{\frac{E_2}{(E_1+1)^2+E_2^2}\right\} \quad \ldots \quad \text{see } (2.41)$$

$$\therefore \quad \frac{dS_\varrho(\omega)}{d\omega} = -\frac{2}{\pi}\left\{\frac{\left((E_1+1)^2+E_2^2\right)dE_2/d\omega - E_2\left(2(E_1+1)dE_1/d\omega + 2E_2\,dE_2/d\omega\right)}{\left((E_1+1)^2+E_2^2\right)^2}\right\}$$

But at $\omega = 0$, $E_2 = 0$

$$\therefore \quad S_\varrho'(0) = -\frac{2}{\pi}\left.\frac{dE_2/d\omega}{(1+E_1)^2}\right|_{\omega=0} \quad \ldots \quad (B2.1)$$

We use the Fermi-Thomas approximation that

$$\varepsilon^{RPA}_{q_1}(0) \simeq 1 + \lambda^2/|q|^2$$

$$\therefore \quad E_1(0) \simeq \frac{2\varrho}{\pi}\int_0^\infty \frac{dq_z}{(\varrho^2+q_z^2)\,\varepsilon_{q_1}(0)}$$ ignoring $\varepsilon_{q_2}^2$ terms which are of order ω^2.

$$= \frac{2\varrho}{\pi}\int_0^\infty \frac{dq_z}{(\varrho^2+q_z^2+\lambda^2)}$$

$$= \frac{\varrho}{\sqrt{\varrho^2+\lambda^2}}$$

$$\underset{=}{\varrho\to 0} \quad \frac{\varrho}{\lambda}.$$

Now

$$E_2 \underset{=}{\omega\to 0} -\frac{2\varrho}{\pi}\int_0^\infty \frac{dq_z\;\varepsilon_2(\omega)}{(\varrho^2+q_z^2)\,\varepsilon_1^2}$$

$$\simeq -\frac{\lambda^2\omega\varrho}{p_F}\int_0^{2p_F}\frac{dq_z}{(\varrho^2+q_z^2+\lambda^2)^2\sqrt{\varrho^2+q_z^2}}.$$

since

$$\varepsilon_2(\omega) = \frac{\pi\lambda^2\omega}{2p_F\,(\varrho^2+q_z^2)^{3/2}}$$ in the region $\omega < qp_F - q^2/2$

and taking $2p_F$ as our cut-off.

We can rewrite E as

$$E_2 \overset{\omega\to 0}{=} \frac{\lambda\omega\varphi}{2p_F}\frac{d}{d\lambda}\int_0^{2p_F}\frac{dq_z}{(\varphi^2+q_z^2+\lambda^2)\sqrt{\varphi^2+q_z^2}}$$

Now use the substitution

$$y = \frac{q_z}{\sqrt{\varphi^2+q_z^2}} \Rightarrow \frac{dy}{dq_z} = \frac{\varphi^2}{(\varphi^2+q_z^2)^{3/2}}$$

$$\therefore \quad E_2 = \frac{\omega\varphi\lambda}{2p_F}\frac{d}{d\lambda}\frac{1}{\lambda^2}\int_0^{\frac{2p_F}{\sqrt{\varphi^2+4p_F^2}}}\frac{dy}{\left(\frac{\varphi^2+\lambda^2}{\lambda^2}\right)-y^2}$$

$$= \frac{\omega\varphi\lambda}{4p_F}\frac{d}{d\lambda}\left[\frac{1}{\lambda\sqrt{\varphi^2+\lambda^2}}\log\frac{(\sqrt{\varphi^2+\lambda^2}+K\lambda)}{(\sqrt{\varphi^2+\lambda^2}-K\lambda)}\right]$$

where

$$K = \frac{2p_F}{\sqrt{\varphi^2+4p_F^2}}$$

This reduces exactly to

$$E_2 \overset{\omega\to 0}{=} \frac{\omega\varphi}{4p_F}\left[\frac{2K\varphi^2}{(\varphi^2+\lambda^2)(\varphi^2+\lambda^2-K^2\lambda^2)} - \frac{(\varphi^2+2\lambda^2)}{\lambda^2(\varphi^2+\lambda^2)}\log\left(\frac{\sqrt{\varphi^2+\lambda^2}+K\lambda}{\sqrt{\varphi^2+\lambda^2}-K\lambda}\right)\right]$$

Expanding out the logarithmic term and making suitable approximations (for small $Q \ll \lambda$, $K \simeq 1$) we obtain

$$\lim_{\omega\to 0} E_2 = \frac{\omega\varphi}{2p_F\lambda^2}\left(1 - 2\log\left(\frac{4\lambda p_F}{\varphi}\right) - \log\left(\frac{2}{2\lambda^2+8p_F^2}\right)\right)$$

Substituting back into (B2.1) we get

$$S_\varphi'(0) = -\frac{\varphi}{\pi p_F\lambda^2}\left(1 + 2\log\varphi - \log\left(\frac{16\lambda^2p_F^2}{\lambda^2+4p_F^2}\right)\right)$$

as required.

Using $\lambda \ll 2p_F$, this reduces to

$$S_\varphi'(0) = -\frac{\varphi}{\pi p_F\lambda^2}\left(1 + 2\log\varphi - 2\log(2\lambda)\right)$$

as in Gumhalter (1976)

APPENDIX C2

We assume an expansion for $\varepsilon_q^{-1}(\omega)$ of the form

$$\varepsilon_q^{-1}(\omega) = (a_0 + a_1 q + a_2 q^2 + \dots) + i(b_0 + b_1 q + b_2 q^2 + \dots)$$

$$= E_1 + i E_2 \qquad \dots \qquad (C2.1)$$

Using the standard Kramer's Kronig relation (see Ichimaru's or Messiah's book),

$$E_1(q,\omega) = 1 - \frac{1}{\pi}\int_{-\infty}^{\infty} d\omega' \, E_2(q,\omega') \, P\left(\frac{1}{\omega-\omega'}\right) \quad \dots \quad (C2.2A)$$

$$E_2(q,\omega) = \frac{1}{\pi}\int_{-\infty}^{\infty} d\omega' \left\{ E_1(q,\omega') - 1 \right\} P\left(\frac{1}{\omega-\omega'}\right) \quad \dots \quad (C2.2B)$$

Since we have split E_1, E_2 into a series of ascending powers in Q, we equate the relevant co-efficients of Q (assuming this can be done) to obtain

$$a_r(\omega) = 1 - \frac{1}{\pi}\int_{-\infty}^{\infty} d\omega' \, b_r(\omega') \, P\left(\frac{1}{\omega-\omega'}\right) \quad \dots \quad (C2.3A)$$

$$b_r(\omega) = \frac{1}{\pi}\int_{-\infty}^{\infty} d\omega' \left(a_r(\omega') - 1\right) P\left(\frac{1}{\omega-\omega'}\right) \quad \dots \quad (C2.3B)$$

$\forall \quad r = 0, 1, 2, \dots$,

e.g.

$$\left.\begin{aligned} a_0(\omega) &= \omega^2/(\omega^2 - \omega_p^2) \qquad \dots \quad (C2.4A) \\ b_0(\omega) &= \frac{\pi\omega^2}{2\omega_p}\left\{ \delta(\omega-\omega_p) - \delta(\omega+\omega_p) \right\} \qquad \dots \quad (C2.4B) \end{aligned}\right\}$$

can easily be seen to satisfy (C2.3)

We know $$Q_1(\omega) = \frac{2}{\pi}\int_0^\infty \frac{\left(\frac{\varepsilon_1}{|\varepsilon|^2} - a_0\right)}{q_z^2} dq_z \qquad \ldots (C2.5A)$$

To obtain $b_1(\omega)$, we have

$$-\frac{\pi\omega^2}{2\omega_p}\delta(\omega - \omega_p) + b_1(\omega)\,\varrho = -\frac{2\varrho}{\pi}\int_0^\infty \frac{\varepsilon_2 \; dq_z}{|\varepsilon|^2(\varrho^2 + q_z^2)}$$

ignoring $\delta(\omega+\omega_p)$ since we are concerned with $\omega > 0$ terms.

$$\Rightarrow \quad b_1\varrho = -\frac{2\varrho}{\pi}\int_0^\infty \frac{\varepsilon_2\, dq_z}{|\varepsilon|^2(\varrho^2+q_z^2)} + \frac{2\varrho}{\pi}\cdot\frac{\pi\omega^2}{2\omega_p}\delta(\omega-\omega_p)\int_0^\infty \frac{dq_z}{(\varrho^2+q_z^2)}$$

$$\therefore \lim_{\varrho\to 0} b_1(\omega) = \frac{2}{\pi}\int_0^\infty \frac{\left(\frac{\pi\omega^2}{2\omega_p}\delta(\omega-\omega_p) - \frac{\varepsilon_2}{|\varepsilon|^2}\right)}{q_z^2} dq_z. \qquad \ldots (C2.5B)$$

Inspection of (C2.5A) and (C2.5B) show them to be Hilbert Transforms of each other. When $\omega \neq \omega_p$, by definition $\delta(\omega-\omega_p)=0$. But around the plasmon frequency (C2.5B) holds. One can replace the delta function by a function $\phi_{q_z}(\omega-\omega_p)$ i.e.

$$\delta(\omega-\omega_p) \longrightarrow \frac{1}{2\sqrt{\pi}\,q_z}\, e^{-(\omega-\omega_p)^2/(4q_z^2)}$$

which is a Gaussian or normal probability function with the properties

$$\int_{-\infty}^{\infty} \phi_{q_z}(\omega-\omega_p)\, d\omega = 1.$$

$$\lim_{q_z\to 0}\int_{-\infty}^{\infty} \phi_{q_z}(\omega-\omega_p)\, f(\omega)\, d\omega = f(\omega_p)$$

(see Butkov's 'Mathematical Physics' p. 231).

The first part of the integral in (C2.5B) then becomes $\frac{\omega^2}{\sqrt{\pi}\,\omega_p(\omega-\omega_p)^2}$, indicating the singularity at ω_p.

APPENDIX D2

AIM : To relate the Kubo formula for $R_\varphi(\omega)$ given by equation (2.5) with the expression in (2.24).

Method : We know from the image theorem that

$$R_\varphi(\omega) = \left.\frac{V_\varphi^{im}(z,\omega)}{U_\varphi(z,\omega)}\right|_{z=0}$$

$$= \left\{ \int_{-\infty}^{0} dz' \frac{2\pi}{\varphi} e^{\varphi z'} \delta\rho_\varphi(z',\omega) \right\} \Big/ \frac{2\pi}{\varphi} e^{-\varphi d}$$

From equation (2.11), using appropriate Fourier transform ($\underline{X} \to \underline{Q}$) we have

$$R_\varphi(\omega) = \frac{2\pi}{\varphi} \int_{-\infty}^{0} dz' \int_{-\infty}^{0} dz'' e^{\varphi z'} e^{-\varphi z''} R_\varphi(z', z'', \omega)$$

Substitute in the commutator expression for $R_\varphi(z', z'', \omega)$ (see 2.5) and we get

$$R_\varphi(\omega) = \frac{2\pi i}{\varphi} \int_{-\infty}^{0} dz' e^{\varphi z'} \int_{-\infty}^{0} dz'' e^{\varphi z''} \left[\rho_\varphi(z',\omega), \rho_{-\varphi}(z'',\omega) \right]$$

where $\rho_\varphi(z) = \sum_i e^{-i\underline{\varphi}.\underline{x}_i} \delta(z - z_i)$

as in (2.25) and assuming

$$\rho(\underline{r}) = \sum_i \delta(\underline{r} - \underline{r}_i).$$

FIG 2.1

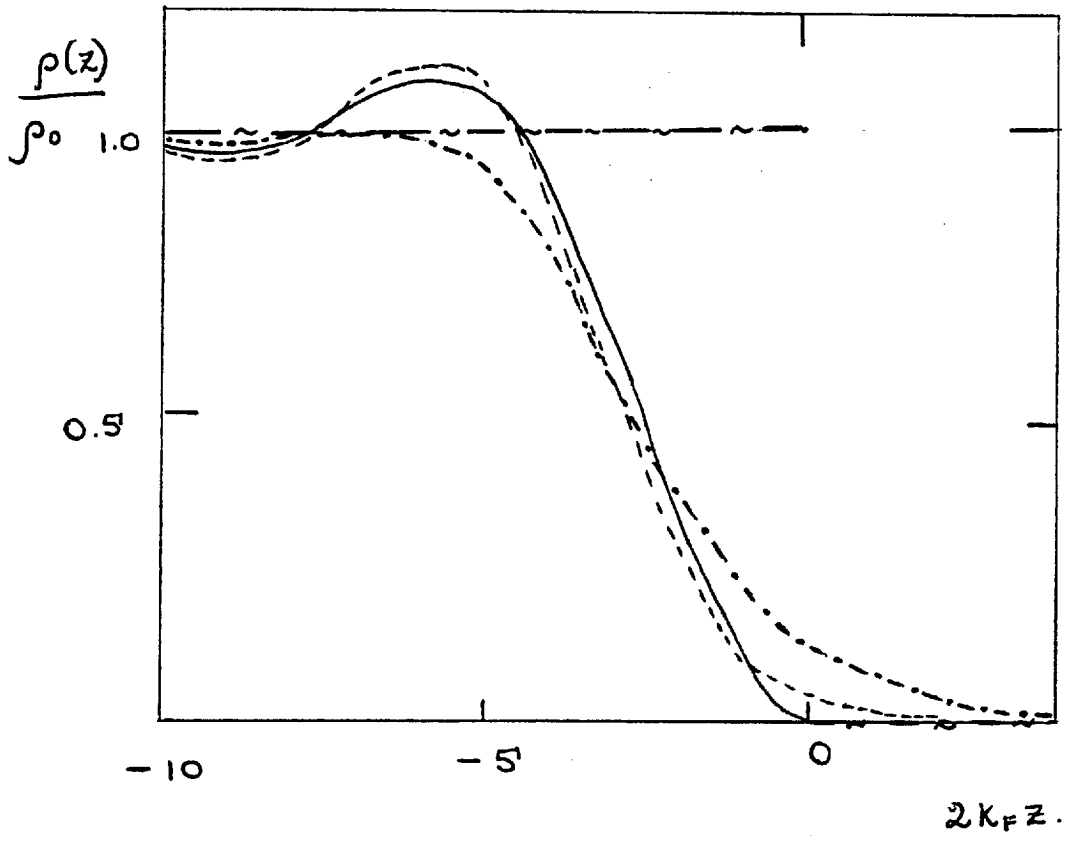

——— IBM

—~—~ SCISBM

------ $r_s = 5.0$ (LANG'S SELF-CONSISTENT CALCULATION)

-·—·—·- $r_s = 2.0$ (LANG'S SELF-CONSISTENT CALCULATION)

THE FIGURE SHOWS THE CHARGE DENSITY OF THE ELECTRON GAS AT THE METAL SURFACE

FIG (2.2).

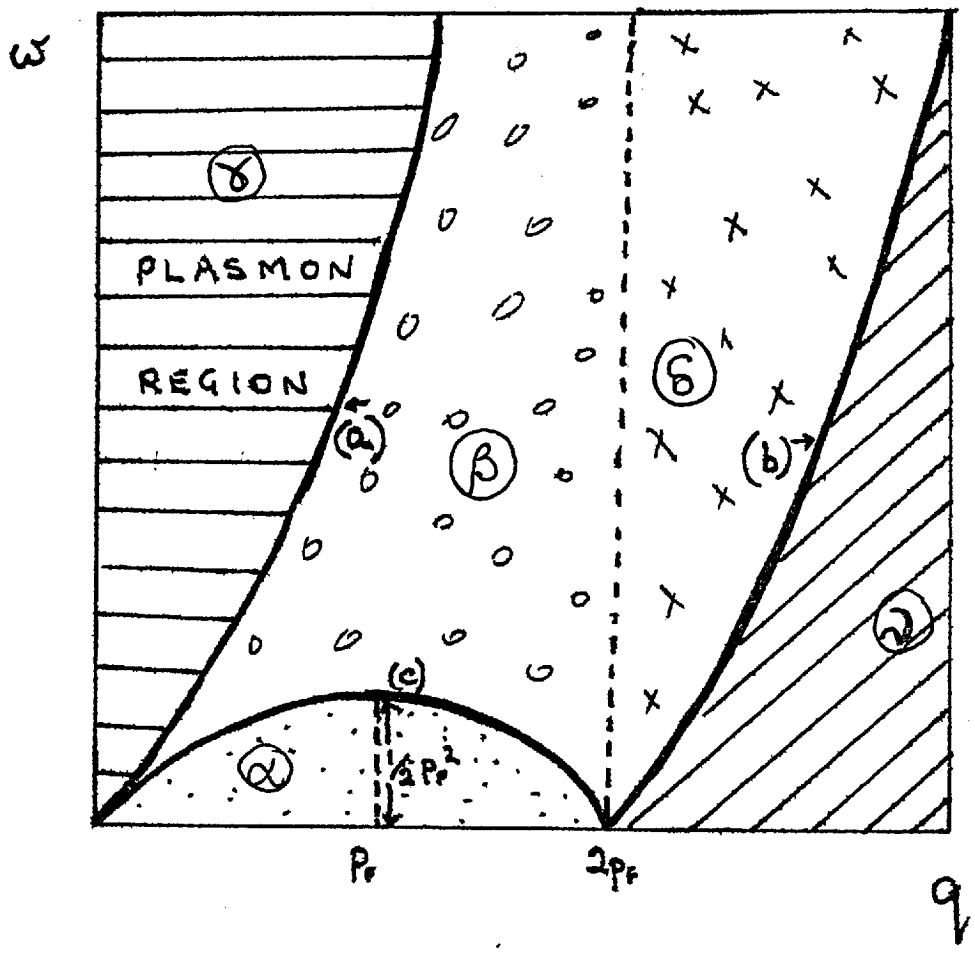

CURVE (a) : $\omega = q^2/2 + q p_F$

CURVE (b) : $\omega = q^2/2 - q p_F$

CURVE (c) $\omega = q p_F - q^2/2$

ILLUSTRATION OF THE DIFFERENT REGIONS OF VARIATION FOR $E_2(q, \omega)$ AS GIVEN BY (2.39B).

FIG (2.3)

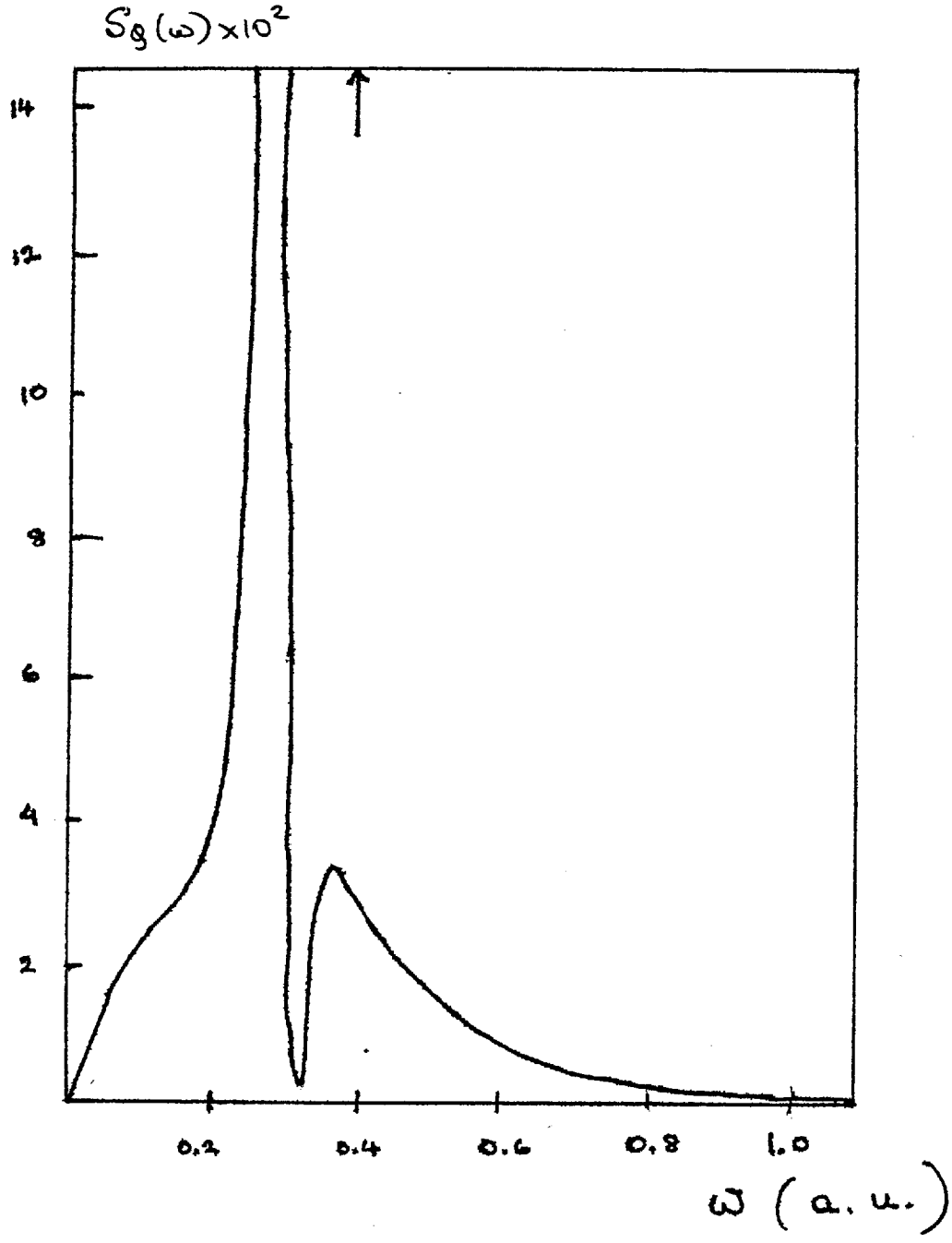

$r_s = 3.0, \quad q = 0.25\, p_F.$

A PLOT OF THE DYNAMIC FORM FACTOR AS A FUNCTION OF ω (GIVEN BY EQU. (2.41))

FIG 2.4.

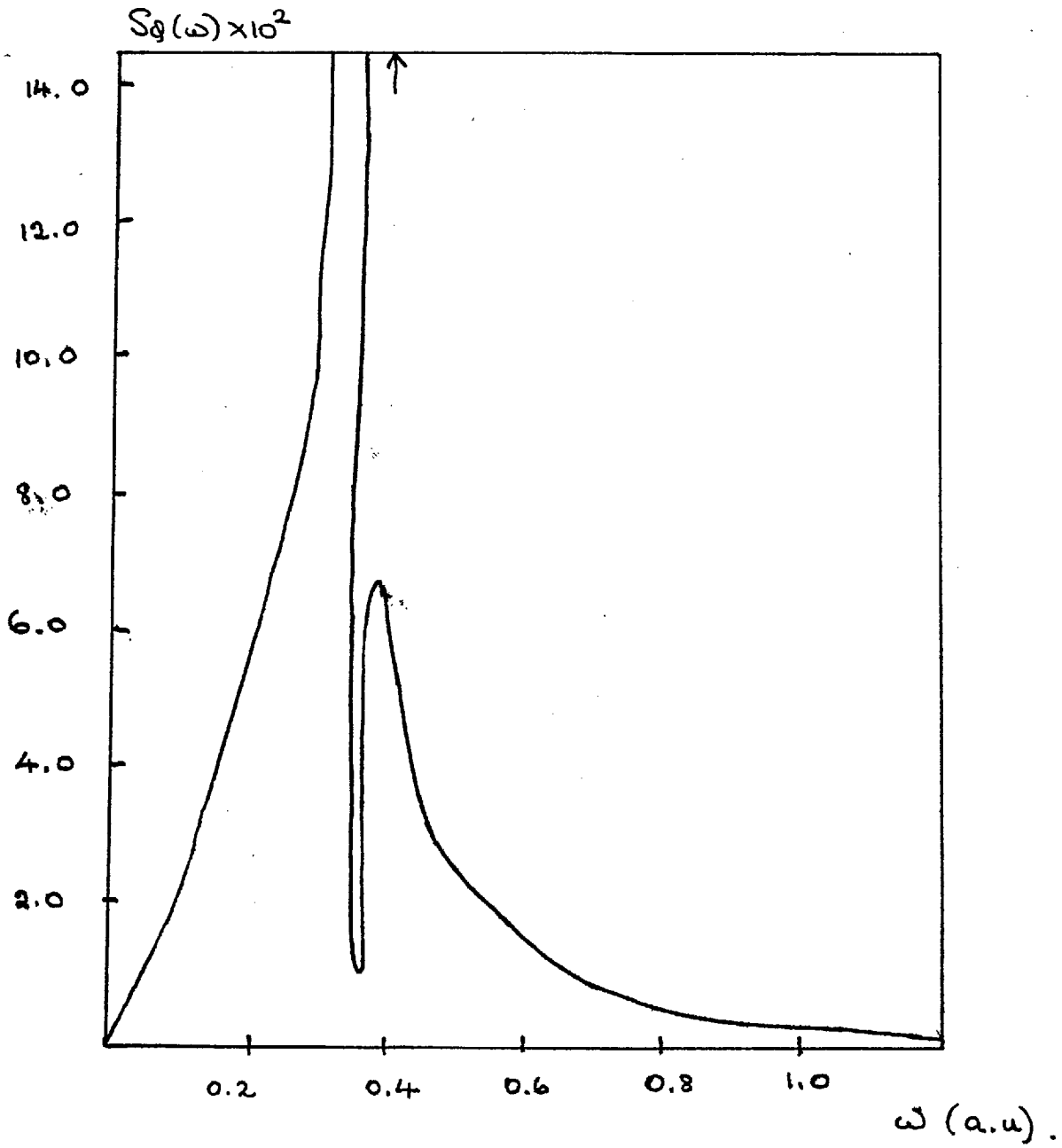

$r_s = 3.0$, $q = 0.5 p_F$.

A PLOT OF THE DYNAMIC FORM FACTOR AS A FUNCTION OF ω (AS GIVEN BY (2.41))

FIG (2.5)

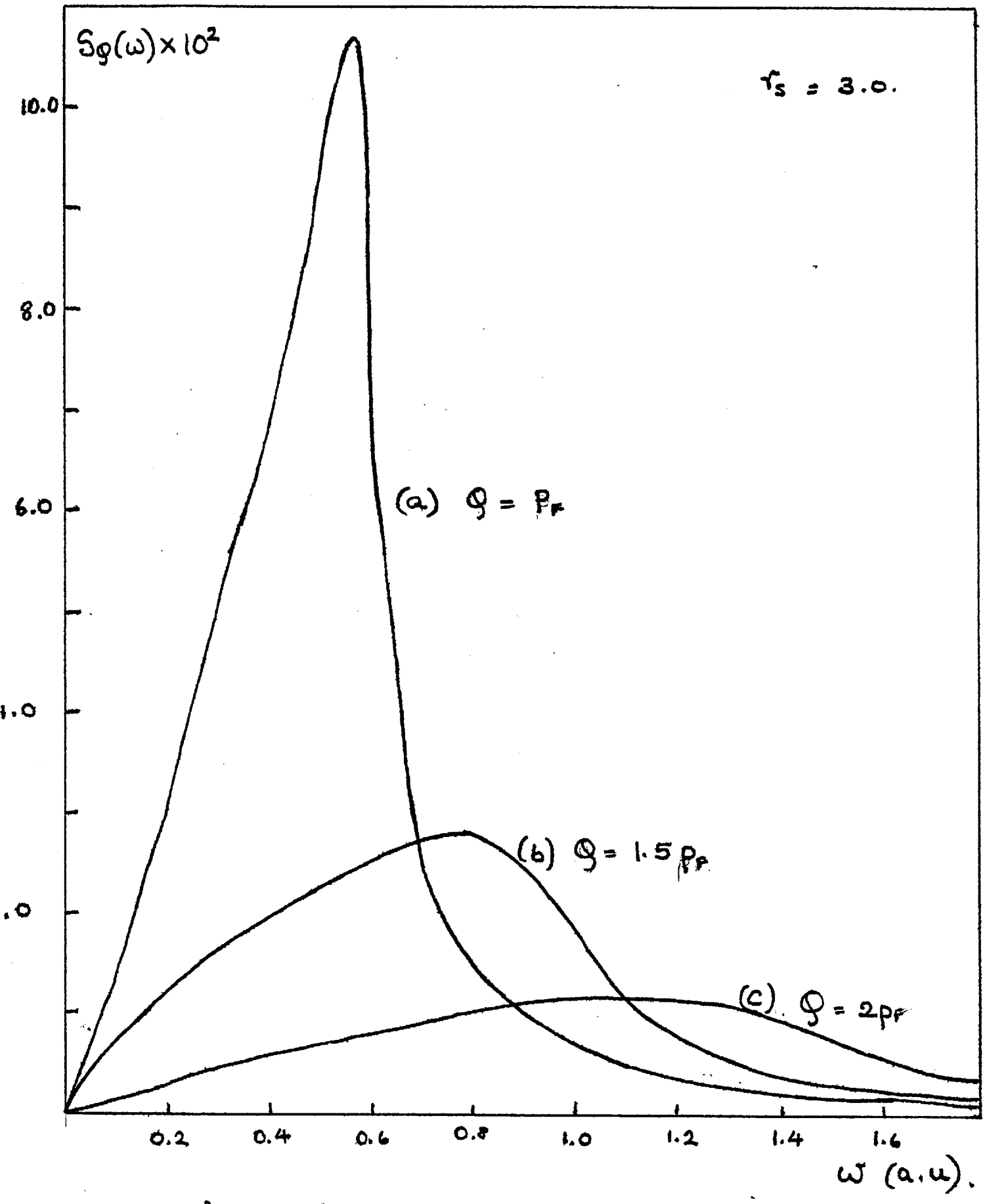

A PLOT OF THE DYNAMIC FORM FACTOR AS A FUNCTION OF ω (GIVEN BY EQ. 2.41)

FIG (2.6)

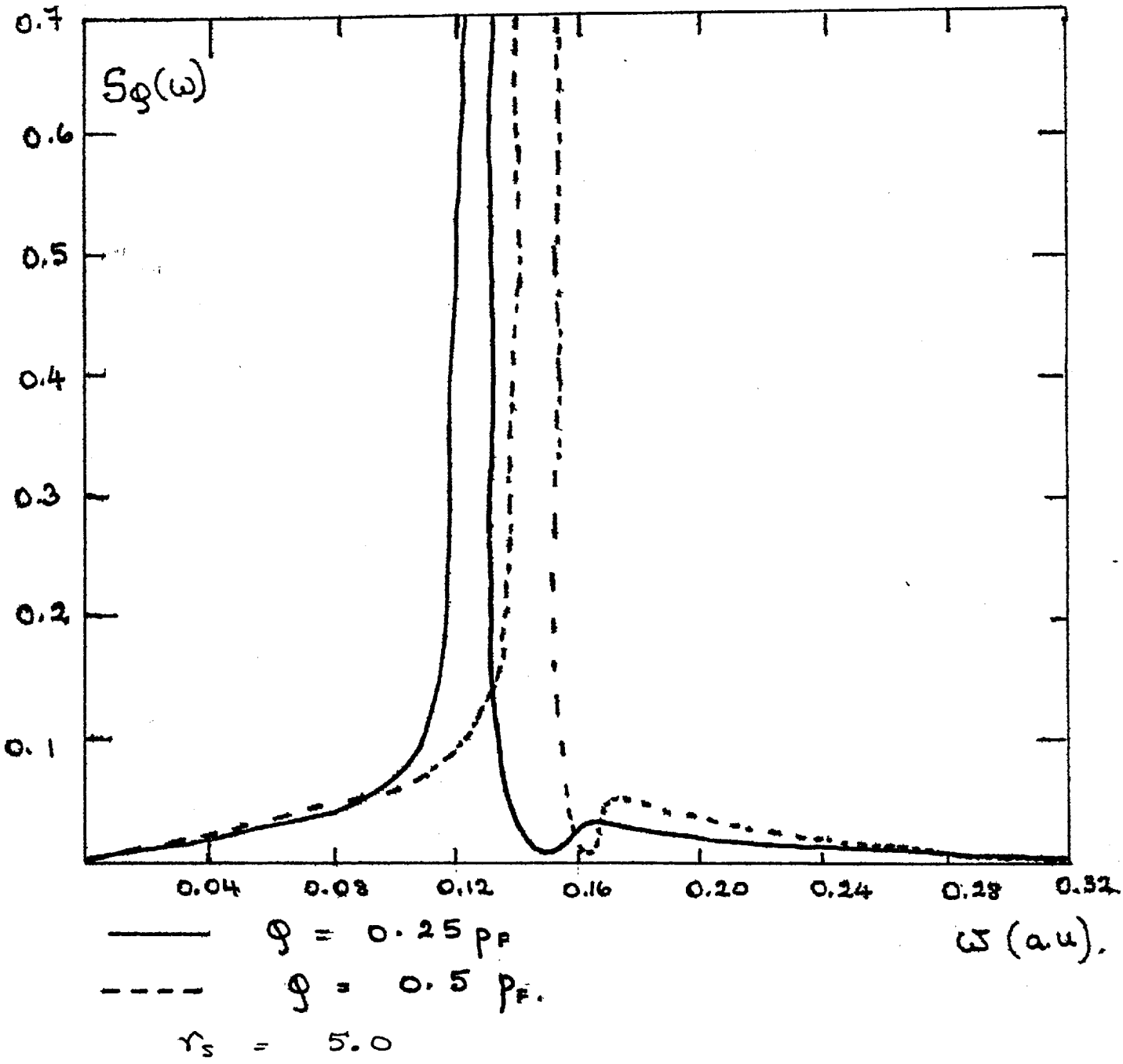

A PLOT OF THE DYNAMIC FORM FACTOR AS A FUNCTION OF ω (given by 2.41).

FIG (2.7)

A PLOT OF THE DYNAMIC FORM FACTOR AS A FUNCTION OF ω (Equ: 2.41)

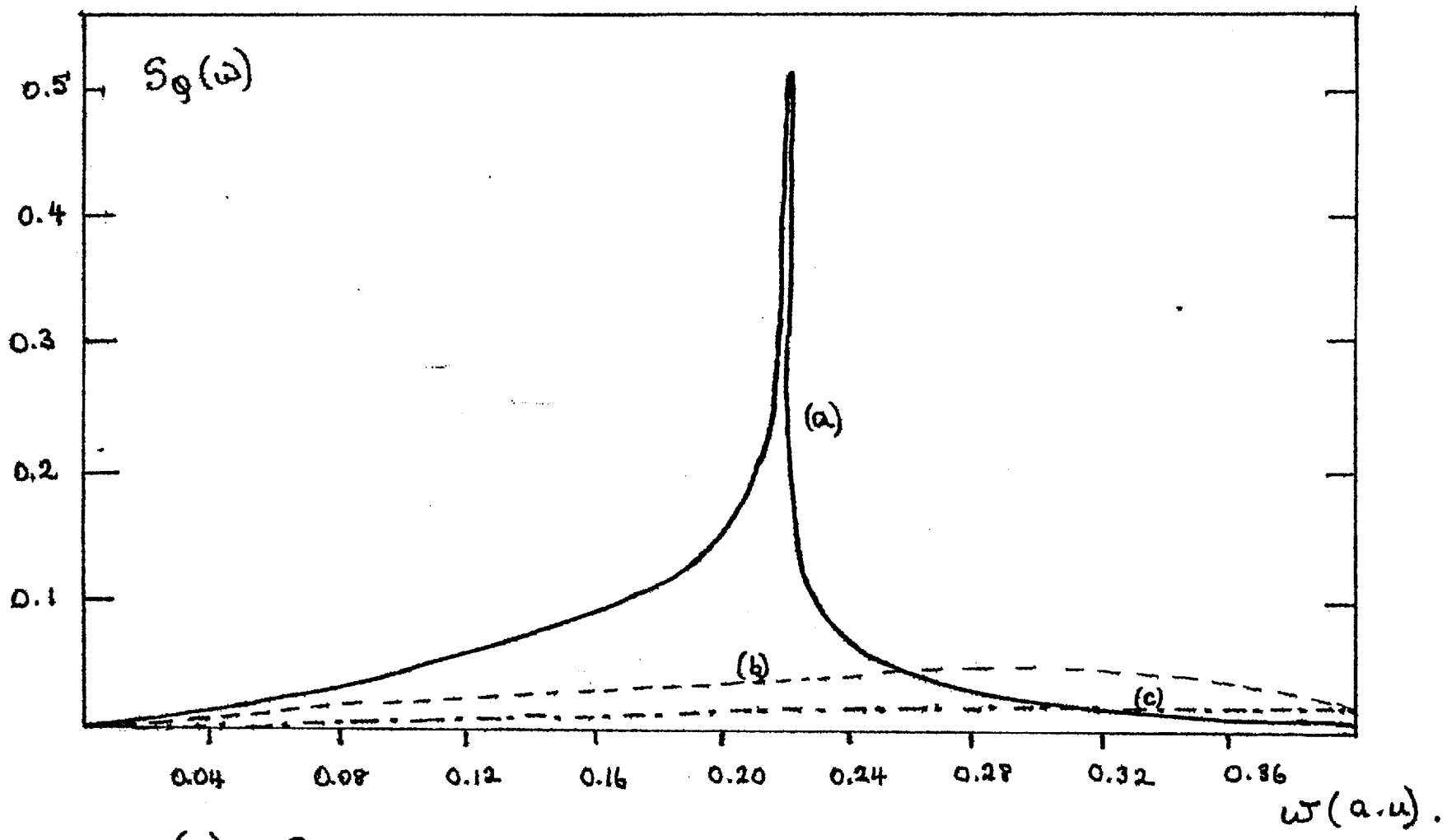

(a) $q = p_F$
(b) $q = 1.5\, p_F$
(c) $q = 2.0\, p_F$

$r_s = 5.0$

FIG (2-8)

A PLOT OF THE STATIC RESPONSE FUNCTION AS A FUNCTION OF φ.

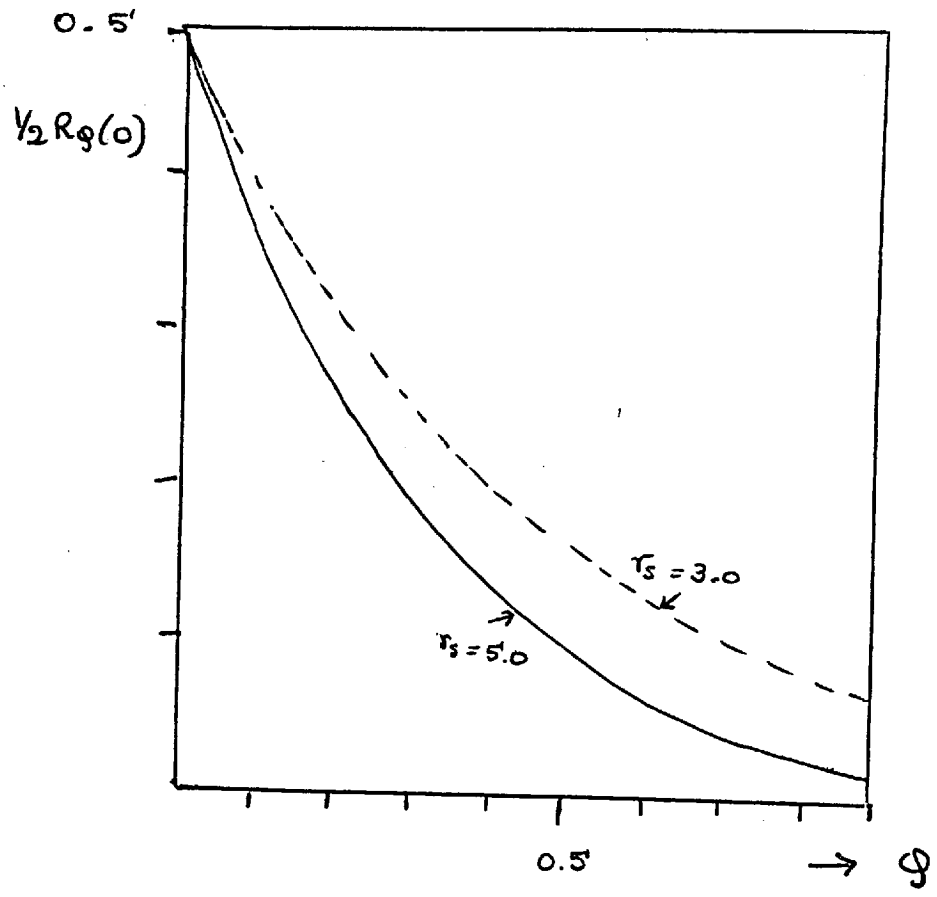

FIG (2.9)

A PLOT OF THE DISPERSION RELATION OBTAINED.

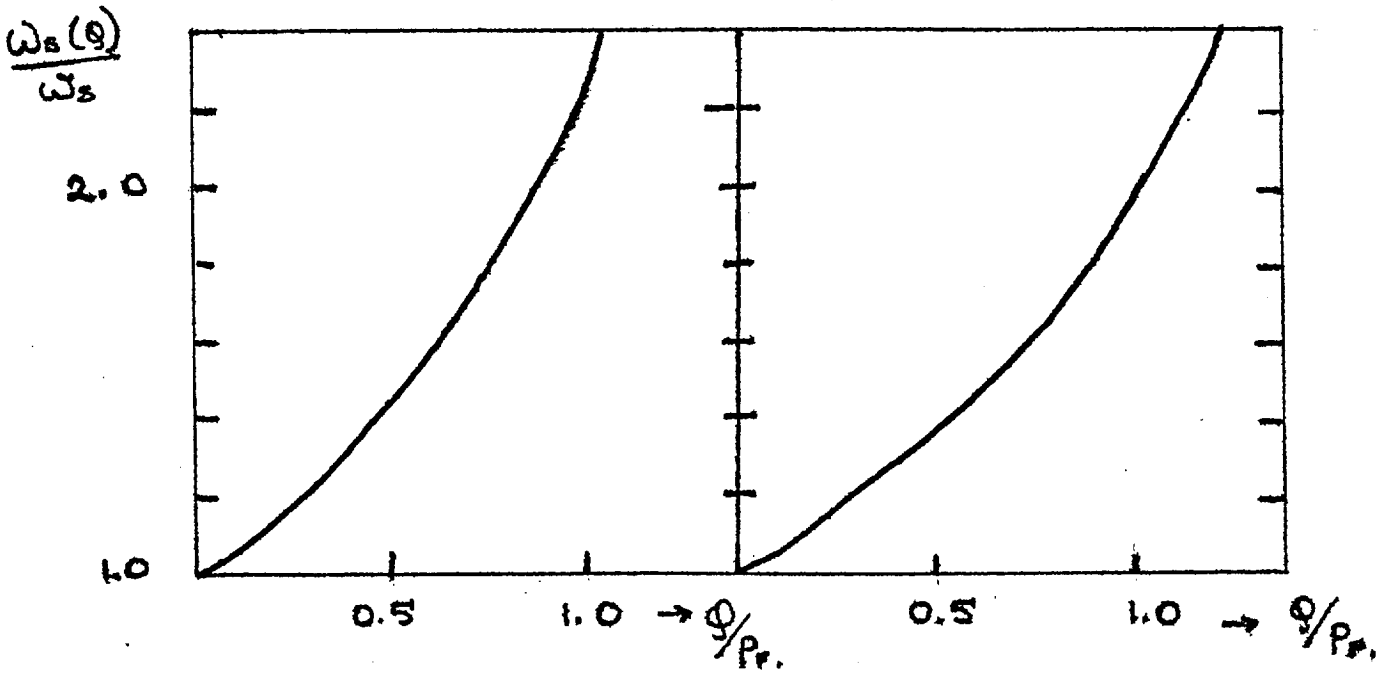

(A) $\gamma_s = 3.0$ (B) $\gamma_s = 5.0$

TABLE (2.1)

q	$I_1^{Calculated} = \int_0^\infty \omega S_q(\omega)\, d\omega$	$I_1^{"Expected"} = \frac{1}{4}\omega_p^2$	$I_{-1}^{Calculated} = \int_0^\infty \frac{S_q(\omega)}{\omega} d\omega$	$I_{-1}^{"Expected"} = \frac{1}{2}R_q(0)$	$\left(I_1/I_{-1}\right)^{Calculated}$	$\left(I_1/I_{-1}\right)^{"Expected"}$
0.16	0.026	0.0278	0.35	0.34	0.0743	0.089
0.192	0.029	0.0278	0.32	0.32	0.0906	0.087
0.32	0.026	0.0278	0.252	0.24	0.103	0.116
0.384	0.026	0.0278	0.209	0.21	0.124	0.132
0.64	0.0296	0.0278	0.098	0.12	0.302	0.232

A COMPARISON OF NUMERICAL CALCULATIONS WITH THE EXPECTED SUM RULES. FOR $r_s = 3.0$

TABLE (2.2)

COMPARISON OF LINEAR DISPERSION TERM OF THIS WORK WITH THOSE BY RITCHIE AND MAROSAK (1966) AND BECK (1971).

	r_s	α_1	RATIO
SCISBM THIS WORK	3.0	0.717	$\alpha_1^{r_s=3} / \alpha_1^{r_s=5}$
	5.0	0.640	= 1.12
(SCISBM) RITCHIE/ MAROSAK ('66) $\alpha_1 = \frac{1}{0.938}\sqrt{\frac{6}{5r_s}}$	3.0	0.674	$\alpha_1^{r_s=3} / \alpha_1^{r_s=5}$
	5.0	0.522	= 1.29
(ISBM) BECK (1971)	1.5	0.401	
	3.4	0.307	$\alpha_1^{r_s=3.4} / \alpha_1^{r_s=6}$
	6.0	0.230	= 1.33

CHAPTER III

THE XPS SPECTRA OF PHYSISORBED ATOMS

The aim of this chapter is to discuss and give numerical calculations of the intrinsic satellite spectrum $N_+(\omega)$ for the core level of an adsorbed atom residing on a metal surface. Gadzuk (1975) has given an informative review on the electronic and geometrical properties of surfaces with adsorbed gas monolayers using both field and photoemission theory (FEED, XPS, UPS).

We are mainly concerned with X-ray photoemission spectroscopy (XPS) as opposed to ultra-violet photoelectron spectroscopy (UPS). The photoemission of electrons occurs when a solid is irradiated by photons with energy $\hbar\omega > \phi$ where ϕ is the work-function, some of which are consequently emitted from the solid. The energy distribution of the ejected electron is related to the electronic states of the solid both before and after photon absorption (and hence hole creation). Now the XPS method is an experimental technique which is being rapidly developed for probing the electronic structure of adsorbed species. The experimentally measured spectral density curves are closely related to the spectral densities of adsorbate orbitals.

In particular, we focus our attention on the excitation of the core level of the adsorbed atom. In photoemission where an electron is swiftly ejected from the orbital,

a screening effect is caused by the interaction of the hole left behind with the substrate electrons, causing readjustment and giving rise to subsequent relaxation effects appearing in the measured spectra. The concept of the relaxation shift (i.e. the characteristic shift of the adsorbate energy levels relative to the gas-phase levels) may be understood by considering the very slow or 'adiabatic' removal of an electron from the core. Its energy level then suffers an upward shift that is relative to the gas phase level, and this is termed the relaxed level. It is an inherent consequence of energy conservation, since the Coulomb interaction between the hole charge and remaining polarized electrons effectively lowers the total energy of the ionized system. Hence the ejected electron must emerge with a greater energy than would be inferred by a 'frozen' electron picture.

On the other hand, intrinsic satellites make an appearance for the sudden removal of the electron. Thus we can essentially summarise as follows :

a) The relaxation shift is due to the static response of the electron gas to the core hole potential, wheras

b) The 'shake-up' or satellite effects occur due to the dynamic response.

These two processes, far from being independant, are connected through the Kramers-Kronig relation given by (2.30), rewriting as

$$R_\rho(0) \propto \int \mathrm{Im}\, \frac{R_\rho(\omega)}{\omega}\, d\omega$$

To zero-order, this adsorbate screening energy is just the quantum mechanical generalisation of a classical image potential shift viz. $v = e^2/4d$, which is the work needed to remove an electron adiabatically to infinity.

Before proceeding on to the mathematical formalism of our problem, let us briefly distinguish between the terms ' intrinsic' and 'extrinsic' as follows :

1) The intrinsic satellite structure (or shake up effect as it is sometimes called) is the result of the screening of the suddenly created core hole by the conduction or valence electrons,

   whereas

2) The extrinsic structure arises from the energy loss of the escaping electron via plasmon excitation.

For high energies of the escaping electrons these two processes become independant. The coupling of fast photoelectrons to substrate excitations is inversely proportional to their velocity and thus one expects that the effects of the intrinsic interactions to be dominant (Harris, 1975) in the observed spectra. Mathematically we can distinguish between these two types of spectra by a factor of the inverse frequency, ω^{-1} , where the intrinsic loss spectrum contains an additional factor of ω^{-1} relative to the extrinsic spectrum. This is in accordance with Ballu, Lecante and Newns (1976) (note the ω^2 appearing in the denominator of the forthcoming equation 3.16). Thus although intrinsic and extrinsic plasmon emission yields satellite at the same energies, their relative contribution

or intensity is different, thus permitting their separation.

MATHEMATICAL FORMALISM

Basically we wish to derive an expression for the imaginary part of the Green's function in our model which is directly related to the density of states $N_+(\omega)$ of an adsorbate orbital as follows:

$$N_+(\omega) = -\frac{1}{\pi} \operatorname{Im} G(\omega - i\eta) \quad \ldots (3.1)$$

where G is the core Green's function in the representation and η is infinitesimally positive. For simplicity the absorbed orbital is taken to be spherical with centre located at (0,0,d) outside the surface. We focus our attention on the spectral density of weakly bound adsorbates involving finite screening length, relaxation shifts, line asymmetries and shake-up effects. Our calculations are believed to be applicable to long lifetime adsorbate levels of physisorbed species such as rare gas atoms e.g. Xenon (Xe) and Neon (Ne).

Let us write the Hamiltonian in the form :

$$H = \varepsilon_c n_c + H_M + e n_c \hat{\phi}(d) \quad \ldots (3.2A)$$

where the index c denotes the core level of the adatom, H_M denotes the Hamiltonian for the metal, $n = c^\dagger c$ where $c^\dagger, c$ are creation and destruction operators e.g. c destroys an electron with energy ε_c in the core state $|c\rangle$. Assume the metal and adatom densities and wave-functions do not overlap. So the only coupling between them is electrostatic in nature (given by the third term in (3.2A) where e is the charge

on the adatom. This represents the Coulomb interaction between the adatom electron and metal electrons. n_c commutes with H_H but $\hat{\phi}(d)$ does not, since H_H contains terms involving kinetic energy.

Let $\underline{r}_d = (0,0,d)$ denote the position of our adatom and $\underline{r}_i$ be the position of the ith electron in the metal substrate. Then $\hat{\phi}(d)$ can be written as

$$\hat{\phi}(d) = \frac{1}{2} \sum_{i=1}^{N} \frac{1}{|\underline{r}_d - \underline{r}_i|}$$

where N is the total number of electrons in the metal and e = 1.

Due to the orientation of the Cartesian framework system, we can drop the modulus sign and rewrite in Fourier transform notation as

$$\hat{\phi}(d) = \frac{1}{2\pi^2} \sum_{i=1}^{N} \int \frac{dq\, e^{i\underline{q}\cdot(\underline{r}_d - \underline{r}_i)}}{2q^2} \qquad \text{where } \underline{q} = (\underline{\varphi}, q_z)$$

$$= \frac{1}{4\pi^2} \sum_{i=1}^{N} \int d^2\varphi\, e^{i\underline{\varphi}\cdot(\underline{x}_d - \underline{x}_i)} \int dq_z \frac{e^{iq_z(d - z_i)}}{(\varphi^2 + q_z^2)}$$

By converting to polar coordinates we can show that the integral over q_z becomes (Gradshtein and Ryshik)

$$\hat{\phi}(d) = \frac{2\pi}{4\pi^2} \sum_{i=1}^{N} \int d^2\varphi \frac{e^{i\underline{\varphi}\cdot(\underline{x}_d - \underline{x}_i)}\, e^{-\varphi|d - z_i|}}{\varphi}$$

$$= \frac{1}{2\pi} \int d^2\varphi\, \hat{\phi}_\varphi\, e^{-\varphi d}$$

using the definition of $\hat{\phi}_\varphi$ given in (2.24) and since $\underline{x}_d = (0,0)$

Now use

$$\int d^2\varphi \longrightarrow \frac{4\pi^2}{A} \sum_{\varphi}$$

where A is the unit area.

$$\therefore \quad \phi(d) = 2\pi \sum_{\varphi} \frac{\hat{\phi}_{\varphi} e^{-\varphi d}}{\varphi}$$

This now gives us a well defined Hamiltonian in (3.2A).

We define Green's function for the adatom core orbital as

$$G_c = -i \langle 0 | T\, c(t)\, c^{+}(0) | 0 \rangle \quad \ldots \quad (3.3A)$$

where $|0\rangle$ is the ground state of the full Hamiltonian H, and T is the time ordering operator (from any standard many-body book e.g. Abrikosov et al, 1963).

Use the equation of motion for the operator c(t) :

$$dc/dt = i\,[c, H]$$

For convenience, take $\varepsilon_c = 0$ in H in (3.2A), then by taking e = 1, we have

$$\dot{c}(t) = ic \sum_{\varphi} \left(\frac{2\pi}{\varphi}\right) e^{-\varphi d}\, \phi_{\varphi}$$

$$\therefore \quad c(t) = c(0) \exp\left\{ i \sum_{\varphi} \frac{2\pi}{\varphi} e^{-\varphi d} \int_0^t \phi_{\varphi}(t)\, dt \right\} \quad \ldots (3.3B)$$

Substitute (3.3B) in (3.3A) gives

$$G_c = -i\, \Theta(t) \langle 0 | \exp\left\{ i \sum_{\varphi} \frac{2\pi}{\varphi} e^{-\varphi d} \int_0^t \phi_{\varphi}(t)\, dt \right\} | 0 \rangle \quad \ldots (3.3C)$$

using the properties of the fermion operators c, c^{+}.

Suppose first of all that ϕ_{φ} has the property of a Bose displacement operator. This seems to be equivalent to the RPA in the present problem. We use the theorem stating that $\langle \exp(i(\alpha b + \alpha^{*} b^{+})) \rangle = \exp \langle -\frac{1}{2} \alpha \alpha^{*} \rangle$ where b, b^{+} are Boson operators with coefficients α, α^{*} respectively (proof found in standard quantum mechanics text books e.g. Messiah).

Hence we can rewrite (3.3C) as

$$\left.\begin{aligned} G_c &= -i\,\Theta(t)\exp\{C(t)\} \qquad \text{where} \\ C(t) &= -\frac{1}{2}\sum_{\varphi\varphi'}\frac{(2\pi)^2}{\varphi\varphi'}\,e^{-d(\varphi+\varphi')}\int_0^t dt_1\int_0^t dt_2\,\langle\phi_\varphi(t_1)\,\phi_{-\varphi'}(t_2)\rangle \end{aligned}\right\} \quad (3.3D)$$

and the $-i\Theta(t)$ in front of G is Green's function for the non-interacting electron. Using the property that

$$\int_0^t\int_0^t dt_1\,dt_2\,f(t_1,t_2) = 2\,\Theta(t_1-t_2)\int_0^t dt_1\int_0^{t_1} dt_2\,f(t_1,t_2)$$

provided $f(t_1, t_2) = f(t_2, t_1)$, and writing $\phi_{-\varphi'} = \phi_{-\varphi}\,\delta_{\varphi\varphi'}$ and

$$V_\varphi^2 = \sum_\varphi\left(\frac{2\pi}{\varphi}\right)e^{-2\varphi d} \qquad \ldots (3.4)$$

$$\therefore\quad C(t) = -\sum_\varphi\left(\frac{2\pi}{\varphi}\right)V_\varphi^2\int_0^t dt_1\int_0^{t_1} dt_2\,\Theta(t_1-t_2)\langle\phi_\varphi(t_1)\,\phi_{-\varphi}(t_2)\rangle \qquad \ldots (3.5A)$$

Recall definition (2.24) for the linear response $R_\varphi(t)$

The time representation of the surface response function is

$$R_\varphi(t_1,t_2) = R_\varphi(t_1-t_2) = -i\,\Theta(t_1-t_2)\int_0^\infty d\omega\,S_\varphi(\omega)\,e^{-i\omega(t_1-t_2)}$$
$$- i\,\Theta(t_2-t_1)\int_0^\infty d\omega\,S_\varphi(\omega)\,e^{i\omega(t_1-t_2)}$$

Substituting in (3.5A) and utilising the time ordering effects gives us

$$C(t) = -\sum_\varphi V_\varphi^2\int_0^t dt_1\int_0^{t_1} dt_2\int_0^\infty d\omega\,S_\varphi(\omega)\,e^{-i\omega(t_1-t_2)} \qquad \ldots (3.5B)$$

$$= -\sum_\varphi V_\varphi^2\int_0^\infty d\omega\,\frac{S_\varphi(\omega)}{\omega}\left(1-e^{-i\omega t}-i\omega t\right) \ldots (3.5C)$$

Rewrite (3.5C) as

$$C(t) = -\sum_{q} V_q^2 \int_0^\infty d\omega\, S_q(\omega) \left\{ C_1(\omega) + C_2(\omega) \right\} \quad \ldots (3.5D)$$

where

$$C_1(\omega) = \left(1 - e^{-i\omega t}\right) / \omega^2$$

$$C_2(\omega) = -it / \omega \, .$$

Our method is similar to that by Doniach and Sunjic (1969). Methods for the derivation of an expression for $N_+(\omega)$ have been given via Feynmann diagram techniques, discussed in detail by Nozieres and Dominicis (1969), subsequently by Langreth (1970), Gumhalter (Thesis, 1976), and Brenig (1975).

Then the first part of the integral involving $c_1(\omega)$ describes the transient or instantaneous response of the substrate electrons to the applied perturbation i.e. if a hole is created in the adatom orbital and then the interaction Hamiltonian H' is suddenly switched off, this term describes the readjustment of the system in the absence of the localised perturbation. This $c_1(\omega)$ term thus gives rise to relaxation or shake-up satellites where in this sudden limit the wave functions of the electrons in the ion core are a continuous function of time viz. they do not change with the perturbation. The second term involving $c_2(\omega)$ in the integral (3.5D) is the adiabatic (or 'long time ') response of the substrate electrons to the applied perturbation.

Now from equations (3.1, 3.5A, 3.5C) we have

$$N_+(\omega) = -\frac{1}{\pi}\,\mathrm{Real}\int_{-\infty}^{0} dt\, e^{i(\omega-v-i\eta)t + c'(t)} \qquad \ldots (3.6A)$$

where

$$v = \sum_{\varrho}{}' V_\varrho^2 \int d\omega \frac{S_\varrho(\omega)}{\omega}$$

$$= -\frac{1}{2}\sum_{\varrho}{}' V_\varrho^2 R_\varrho(0) \quad \text{using the perfect screening sum rule} \qquad \ldots (3.6B)$$

In the classical limit $v \simeq e^2/4d$ (this is for small Q- or large d-approximation). This is the static interaction energy of a point charge at the adatom with the surface.

C'(t) is just C(t) as in (3.5D) without the adiabatic term $C_2(\omega)$ i.e.

$$c'(t) = -\sum_{\varrho}{}' V_\varrho^2 \int_0^\infty d\omega \frac{S_\varrho(\omega)}{\omega^2}\left(1 - e^{-i\omega t}\right) \qquad \ldots (3.6C)$$

Making the approximation

$$e^{c'} = 1 + c'$$

in equation (3.6A) we have

$$N_+(\omega) = -\frac{1}{\pi}\,\mathrm{Re}\int_{-\infty}^{0} dt\; e^{i(\omega-v-i\eta)t}\,(1+C'(t))$$

$$= -\frac{1}{\pi}\,\mathrm{Re}\;\frac{e^{i(\omega-v-i\eta)t}}{i(\omega-v-i\eta)}\Bigg|_{-\infty}^{0} + J(\omega)$$

$$\therefore\quad N_+(\omega) = \delta(\omega-v) + J(\omega) \qquad \ldots \qquad (3.6D)$$

where

$$J(\omega) = -\frac{1}{\pi}\,\mathrm{Re}\int_{-\infty}^{0} dt\; e^{i(\omega-v-i\eta)t}\sum_{\rho} V_\rho^2\int_0^\infty d\omega'\,\frac{S_\rho(\omega')}{(\omega')^2}\left(1-e^{-i\omega' t}\right)$$

Interchanging the order of summation and integration,

$$J(\omega) = -\frac{1}{\pi}\,\mathrm{Re}\sum_{\rho} V_\rho^2\int_0^\infty d\omega'\,\frac{S_\rho(\omega')}{(\omega')^2}\int_{-\infty}^{0} dt\; e^{i(\omega-v-i\eta)t}\left(1-e^{-i\omega' t}\right)$$

$$= -\frac{1}{\pi}\,\mathrm{Re}\sum_{\rho}\frac{V_\rho^2}{i}\int_0^\infty d\omega'\,\frac{S_\rho(\omega')}{(\omega')^2}\left[\frac{1}{\omega-v-i\eta} - \frac{1}{\omega-v-\omega'-i\eta}\right] \ldots \qquad (3.6E)$$

Thus from (3.6D), (3.6E)

$$N_+(\omega) \overset{\omega\neq v}{=} \sum_{\rho} \frac{V_\rho^2\, S_\rho(\omega-v)}{(\omega-v)^2} \qquad \ldots\ldots (3.7)$$

since the term $\frac{1}{\omega-v-i\eta}$ only has non-zero imaginary part for ω equals v from the standard result that

$$\lim_{\eta\to 0}\frac{1}{\omega-v\pm i\eta} = P\left(\frac{1}{\omega-v}\right) \mp i\pi\,\delta(\omega-v)$$

Now consider the case $\omega-v\to 0$. To obtain an analytical form for $N_+(\omega)$ we make use of the Ansatz for $S_\rho(\omega)$

$$S_\rho(\omega) = \omega e^{-\omega/\omega_m} S_\rho'(0) \qquad \ldots\ldots (3.8)$$

which is valid for $\omega<\omega_M$, where $\omega_M = P_F/2d$. Put (3.8) in (3.6C) gives

$$e'(t) = -\sum_{\varphi} V_{\varphi}^{2} S_{\varphi}'(0) \int_{0}^{\infty} \frac{d\omega}{\omega} (1 - e^{-i\omega t}) e^{-\omega/\omega_m}$$

$$= -\gamma \log(1 + i\omega_m t) \qquad \ldots (3.9A)$$

where

$$\gamma = \sum_{\varphi} V_{\varphi}^{2} S_{\varphi}'(0) \qquad \ldots (3.9B)$$

and we have made use of Frullani's Integral which states

$$\log t = \int_{0}^{\infty} \frac{(e^{-x} - e^{-xt})}{x} dx \qquad \text{if} \quad re(t) > 0$$

Substituting (3.9A) in (3.6A) we get

$$N_{+}(\omega) = \frac{1}{2\pi} \int_{-\infty}^{\infty} dt \, \frac{e^{i(\omega - v)t}}{(1 + i\omega_m t)^{\gamma}} \qquad \ldots (3.10)$$

This can be evaluated exactly via a contour integration (see Appendix A3) to yield

$$N_{+}(\omega) \overset{\omega \to v}{=} \frac{e^{-(\omega - v)/\omega_m} (\omega - v)^{-1+\gamma}}{\Gamma(\gamma)\, \omega_m^{\gamma}} \Theta(\omega - v) \qquad \ldots (3.11)$$

where

$$\gamma = \log_e (1.59 \lambda d) / (8 d^2 p_F^2)$$

and $\Gamma(\gamma)$ is the Gamma Function. (Gumhalter and Newns, 1975)

For convenience we have taken the unperturbed adatom energy ε_a equal to zero

Substituting (3.4) for V_{φ}^{2} in (3.7) and using

$$\sum_{\varphi} \longrightarrow \int 2\pi\varphi \, d\varphi$$

gives

$$N_{+}(\omega) \overset{\omega \to v}{=} \frac{1}{(\omega - v)^2} \int_{0}^{\infty} d\varphi \, e^{-2\varphi d} S_{\varphi}(\omega - v) \qquad \ldots (3.12)$$

which is our perturbational result for the density of occupied

states of the adatom in the Born approximation. Thus for values of the frequency away from v, this is just the Laplace Transform with respect to the spctral density of states $S_{\rho}(\omega)$. Examination of (3.11) shows an expected sharp cut-off of the density around $\omega = v$. This divergence is called the infra-red catastrophe and arises as an inherent consequence of the 'Anderson Orthogonality Block' which occurs whenever a large system responds to a transient localised perturbation (Anderson,1967). For very large values of d,

$$\lim_{d \to \infty} \gamma(d) = 0$$

which indicates a delta function type of behaviour experienced by our spectral density near $\omega = v$. Around the electron-hole continuum we can easily calculate the first moment contribution to $N_{+}(\omega)$ around the line $\omega = v$ i.e.

$$\mu_1^{N} = \int_0^{\infty} \frac{(\omega - v)^{\gamma} e^{-(\omega - v)/\omega_m}}{\Gamma(\gamma)\, \omega_m^{\gamma}} d\omega$$

$$= \gamma \omega_m$$

$$= \frac{1}{4\lambda^2 d^2} \log(1.59 \lambda d) \qquad \ldots (3.13)$$

μ_1^{N} thus depends on the distance d and the Fermi-Thomas wave vector λ, alone. This static type of behaviour is in order as we are concerned here with the spectral density behaviour in the static limit viz. $\omega \to 0$. Now the sudden (or irreversible) approximation for switching on the core hole, appropriate for our intrinsic satellites, gives the 'zero work' sum rule which states that the first

moment of the core XPS spectrum lies at the gas-phase position of the core level. This is easily seen from (3.7):

$$\int_0^\infty (\omega - \nu)\, N_+(\omega)\, d\omega = -\tfrac{1}{2} \sum_\varrho V_\varrho^2 R_\varrho(0)$$

$$= \nu \qquad \ldots (3.14)$$

Alternatively if we use the Ansatz for $S_\varrho(\omega)$ appropriate around the surface plasmon,

$$S_\varrho(\omega) = \tfrac{1}{2}\omega_s\, \delta(\omega - \omega_s)$$

in (3.12) and integrate over ω from zero to infinity,

$$\int_0^\infty N_+(\omega)\, d\omega = \nu/\omega_s \qquad \ldots (3.15)$$

which gives us the strength of the satellite peak due to the surface plasmon relative to the elastic peak in Born approximation (we take $\omega = 0$ to be the elastic threshold). This is a good check which we make use of in our ensuing numerical calculations of $N_+(\omega)$. Our results apply to electron propagators. Similar results involving minor modifications (change of sign in t) can be made for hole propagators to calculate the density of unoccupied deep states (Langreth,1970; Gumhalter,1976). We do not elaborate further on this.

NUMERICAL PROCEDURE AND RESULTS

We work in the region $\omega > 0$. From the previous section we summarise the formula used for $N_+(\omega)$ as follows:

$$N_+(\omega) = \left.\begin{array}{ll} \dfrac{e^{-\omega/\omega_m}\,(\omega)^{\gamma-1}}{\Gamma(\gamma)\;\omega_m^{\gamma}} & \cdots\ \omega < \omega_m \\[2ex] \dfrac{1}{\omega^2}\displaystyle\int_0^{\infty} d\varphi\, e^{-2\varphi d}\, S_\varphi(\omega) & \cdots\ \omega > \omega_m \end{array}\right\} \cdots (3.16)$$

where we have taken, for simplicity,

$$\vartheta = -\tfrac{1}{2}\sum_{\varphi} V_\varphi^2\, R_\varphi(0) = 0$$

which involves just a shift of the origin for ω. ω_M is our 'cut-off' frequency equal to $P_F/2d$ which separates the electron-hole continuum from the plasmon region and the γ parameter has been previously defined (see equation (3.11)). In the region $\omega < \omega_M$ we use the approximate version of $N_+(\omega)$ obtained by use of a simple exponential Ansatz for $S_\varphi(\omega)$, while for larger values of ω, the problem reduces to simply evaluating the Laplace Transform of $S_\varphi(\omega)$. The behaviour of the spectral density function, $S_\varphi(\omega)$, was plotted for different r_s and Q values in Chapter I. To facilitate computer calculations we used the small Q-approximation for $S_\varphi(\omega)$ given by equation (2.47) in equation (3.16) above, which is valid upto values of the bulk plasmon frequency ω_p. We do not extend our calculations beyond this value of the frequency. As we are mainly interested in the behaviour around the surface plasmon, this justifies our approximation used.

We have carried out the numerical evaluation of $N_+(\omega)$

given by equation (3.16) for the values of the metallic densities r_s = 3.0, 5.0 and two values ofthe adatom radius d = 2.5, 4.0. The graphs are plotted in Figs. (3.3), (3.4) as functions of increasing frequency ω where all quantities are in atomic units. The small d-values and the low electron densities considered are in effect to maximise the non-classical behaviour of the system in which we are interested. Two distinct features of interest arise in our curves:

(1) The small ω -behaviour or the divergence occurring in as $\omega \to 0$. This is a non-classical phenomenon and is basically the infra-red singularity of power law type $\frac{1}{\omega^{1-\gamma}}$ (since $\gamma < 1$ within the range of metallic densities r_s = 1 to 8 and d = 1 to 8, from Gumhalter's thesis, Table 1). For small γ , $N_+(\omega) \sim \gamma/\omega$. This divergence in the Born approximation limit is due to the linearity of $S_\rho(\omega)$ for small ω -values (as previously discussed in Chapter II). Suppose that in a general model

$$S_\rho(\omega) = a\,\omega^n$$

where a is a constant and $n > 0$. Then by considering the ' non-shift ' part of the integral in $N_+(\omega)$ i.e. that involving $c_1(\omega)$ in equation (3.5D) we find that for $n < 1$ the integral diverges at the origin giving an infinite contribution whereby the problem is insoluble, and we call this a 'super catastrophe'. For values of $n > 2$ the low frequency modes give little contribution and so we have no catastrophe. But for n = 1, the integral is convergent and logarithmic in behaviour

and results in the infra-red catastrophe. Mahan (1967) suggested that the X-ray spectra of metals should be singular near the threshold according to the power law $\omega^{-\nu}$ where ν is a dimensionless coupling parameter describing the interaction between the conduction electrons and deep hole left behind. He did this by approximating a series to an exponential and calculating the first terms of a perturbation expansion, which gave a power law rather than a logarithmic singularity. Nozieres et al (1969) confirmed Mahan's prediction of threshold singularity within a more accurate many-body approach and suggest that a large coupling strength ν may lead to a zero amplitude at the threshold instead of a divergence through a broadening of the spectral density function. We are,however, concerned with the weak coupling limit.

In 1970, Doniach and Sunjic discussed the photo-emission scattering cross-section which, in an asymptotic limit for long times, reduced to an expression proportional to $\frac{1}{\omega^{1-\alpha}}$ where $\alpha < 1$ is related to the phase shift for scattering of conduction electrons from the hole potential. In practice, one cannot see the small ω-divergence due to the finite lifetime of the core hole except as an asymmetry in an otherwise symmetrical lineshape of the 'elastic peak'.

In our computer curve calculations in this small

ω-region we obtained excellent agreement with the Ansatz approximation for $N_+(\omega)$ and our approximation for $N_+(\omega)$ (using the $S_g(\omega)$ approximation) as well as with the $N_+(\omega)$ calculated using the "exact" form of $S_g(\omega)$ given by equation (2.41) in the last chapter.

Around the surface plasmon region far too much computer time was being wasted to obtain adequate convergence using the "exact" $S_g(\omega)$, hence our resort to the simplified version for $S_g(\omega)$.

(2) The second distinctive feature of the graphs is the behaviour at the surface plasmon, which we see by noting the change of scale applied is a remarkably narrow satellite with width only of the order of $0.1\omega_s$ It is interesting to see the resulting asymmetry occurring in the surface plasmon peak. This is due to the positive surface plasmon dispersion in this model as discussed in the last chapter, so that the surface plasmon resonance lies in the region $\omega > \omega_s$. The form of the peak of $N_+(\omega)$ for $\omega > \omega_s$ is approximately exponential, a result predicted by Harris (1975), although our curve contains information on the damping and intensity fall-off effects.

Checks were made on the calculations throughout by evaluating the area under the surface plasmon peak in $N_+(\omega)$, and $\omega N_+(\omega)$ by a Simpson's rule procedure and the results

are set out in the comparative table 3.1. From this table we see that 55-70% of the classical intensity v/ω_s is found in the calculated satellite (p_1) although of course the cut-offs taken are entirely subjective (tail corrections are not allowed for). The area under the surface plasmon peak involved in the first moment of $N_+(\omega)$ given by p_2 in the table gives about 57-76% of our numerical estimates of v.

As d increases we note that the peak of the curve shifts down as expected and there is a tendency for the peak to narrow down i.e. the surface plasmon width seems to have some inverse power relationship with the adatom radius d. Referring to equation (3.16) we see from the factor e^{-Qd} that as d increases, Q correspondingly decreases and so the frequency dispersion relation ω_Q approaches the surface plasmon frequency ω_s, thus narrowing the satellite.

CALCULATION OF XPS SATELLITES FOR TRANSITION METALS VIA A WAVE-INDEPENDANT PICTURE

Let us assume that $S_Q(\omega) = S(\omega)$ i.e. that the spectral density is independant of the wave-vector Q. Then from (3.16) we have

$$N_+^{\text{Intrinsic}}(\omega) = \frac{1}{2d\omega^2} \cdot S(\omega)$$

$$= \frac{1}{2d\omega^2}\left[\frac{2}{\pi}\,\mathrm{Im}\,\frac{1}{1+\varepsilon(\omega)}\right] \quad \ldots \quad (3.17)$$

which is just the linearised form of (3.16) in the limit $Q \to 0$ but at finite ω. In their 1976 paper, Ballu et al plot a graph of the extrinsic $\frac{1}{\omega}\,\mathrm{Im}\left(\frac{1}{1+\varepsilon(\omega)}\right) \sim \omega$ for molybdenum and draw attention to the surface plasmon peak occurring around ω = 1.35eV or 0.045a.u. This should be an observable satellite in the XPS spectra from core levels of suitable adsorbed atoms.

Using the data on the dielectric function from Weaver et al (1974) we have made a plot of $N_+(\omega) \sim \omega$ given by equation (3.17), for molybdenum and tantalum in Figs. 3.5A and 3.6A, taking d = 4.0 au. For molybdenum we notice the surface plasmon peak at ω = 0.045 au. , (1.23 eV) and other weaker peaks at = 0.34 au., 0.72 au. (i.e. 9.25 eV and 19.6 eV respectively) which agrees well with experimental results where peaks are observed at 1.35 eV, 10.1 eV and 19.0 eV (Ballu et al, 1976). An estimation of the area under the main surface plasmon peak is 0.11, using cut-offs at ω = 0.02 and 0.10 which are

purely subjective. This is an encouraging result as we expect that for xenon on molybdenum this satellite should be about 10% of the total area under the curve. The area under this peak in a plot of $\omega N_+(\omega) \sim \omega$ is about 0.05 which is approximately 80% of the classically expected result $\frac{1}{4d}$ (= 0.0625 for d = 4.0).

Examination of Fig. (3.6A) for xenon on tantalum shows a surface plasmon peak occurring at ω = 0.062 au. (1.68 eV) and other weaker peaks at ω = 0.27 au., 0.46 au. and 0.58 au. (7.34 eV, 12.5 eV and 15.8 eV respectively. The area occurring under the main peak is 0.09 between the cut-offs ω = 0.03 and 0.11. Again the 10% of the total area under the curve occurring in the main satellite is encouraging.

Fig. (3.7) gives a similar plot for the intrinsic spectrum of silver with d still equal to 4.0 au. The data for $S(\omega)$ is taken from the 1962 paper by Ehrenreich and Phillips where the real and imaginary parts of the dielectric constant for silver are plotted. The surface plasmon peak is pronouncedly sharper than that observed in the calculations for molybdenum and tantalum in Figs. (3.5A) and (3.6A) and occurs at ω = 8.5 au. (231 eV). An analytical areal estimation under this peak gives a result of 0.19 which is rather high compared with the previous two cases above.

For the three cases just discussed, subjective difficulties occurred in accurate estimation of the data from the small graphs in the various papers as $\omega \to 0$ and so we avoid going too near this point.

Next we convolute the expression for $N_+(\omega)$ given by equation (3.17) as follows :

$$N_+^c(p) = \frac{\Delta}{\pi} \int_0^\infty \frac{d\omega\, N_+(\omega)}{(p-\omega)^2 + \Delta^2} \quad \ldots \quad (3.18)$$

and further define

$$N_+'(p) = N_+^c(p) + \frac{\Delta}{\pi(\Delta^2 + p^2)} \quad \ldots \quad (3.19).$$

where the Δ parameter is measured from the paper by Kai Siegbahn et al (19) as the width of their intensity curve at half the maximum for xenon $3d_{5/2}$ Δ = 0.55 eV (0.02 au.). We evaluate the integral in (3.18) numerically, using a suitable upper limit ($\sim 10\,\Delta$) which should give sufficient accuracy. By using the already computed data points for $N_+(\omega)$ for molybdenum in Fig.(3.5A) we can plot out results for $N_+^c(p)$ and $N_+'(p)$ as a function of p in Figs. (3.5B) and (3.5C). We notice that the first surface plasmon peak present for molybdenum in $N_+(\omega)$ still appears in $N_+^c(p)$ but is wiped out in $N_+'(p)$ by simply adding on of the Lorentzian, although the weaker peaks do still appear.

Similar calculations were done with the tantalum data giving the same results (which are not displayed).

Generally speaking, the experimental XPS spectra do not agree with the predictions of intrinsic plasmons. In 1975, Pardee et al carried out an analysis of the surface and bulk plasmon contributions accompanying core level X-ray photoemission and found negligible intrinsic plasmon production for aluminium and magnesium 2s lines but did find dominant extrinsic plasmon lines.

Yates and Erikson (1974) have made an experimental XPS study of Xenon ($d \simeq 2.5$ a.u.) physisorbed on tungsten (111) at temperature 120°K. Their results show possibly the first observed surface plasmon satellites in the XPS adatom spectra, which occurs approximately at $\omega_s = 0.15$a.u.

In 1976, Bradshaw et al report on the first clear observation of the coupling of a surface plasmon to an adsorbate core level for oxygen ($d \simeq 1.38$a.u.) on aluminium (100) ($r_s \simeq 2.07$). The satellite occurs at 10. 9 eV or 0.4 a.u. corresponding to the aluminium surface plasmon. A similar surface plasmon satellite was observed for oxygen adsorbed on polycrystalline magnesium ($r_s \simeq 3.0$) at 7. 8eV or 0. 29 a.u. They present a theory which separates out the extrinsic, intrinsic and interference effects and find a value of 0. 4eV$\simeq$0.015 a.u. for the relaxation shift, which is small compared with ours : See table 3.1, $\nu \simeq 0.06$, but it must be remembered that this is for $r_s = 3.0$ whereas for aluminium $r_s = 2.07$.

It is difficult to make any further comparison due to lack of clarity and blurring effects in the available data. In our results the surface plasmon

peak is remarkable for the appearing asymmetry and also for the narrowness of the satellite. Unfortunately, none of these features have been clearly observed experimentally. However, perhaps too much emphasis should not be placed on this asymmetric behaviour as the model has neglected many important interactions which may act so as to obscure this asymmetry e.g. the internal excitations of the atom and the vibrational degrees of freedom, Gadzuk (1976).

At the first glance, our model may appear to be deceptively simple. But it is important to realise that the three items viz.

1. small ω-behaviour (infra-red divergence),
2. surface plasmon excitation,
3. relaxation shifts

are woven together to create a rich and intricate fabric within $N_+(\omega)$.

APPENDIX A3

Equation (3.10) may be evaluated exactly by considering the closed contour $\mathcal{C}$ in the complex t-plane as illustrated in Fig. (3.1). The point of singularity in equation (3.10) occurs at $t = i/\omega_m$ which is taken outside $\mathcal{C}$ by considering the cuts given by L_1, L_2. $\mathcal{S}_1$, $\mathcal{S}_2$ are arcs of the semi-circle of radius R, $\mathcal{S}_3$ is a circle of radius ρ and centre $(0, i/\omega_m)$ and L_3 is a diagonal of the $\mathcal{S}$ circle passing through the real t-axis.

Cauchy's Integral Theorem states that for a complex function f(z),

$$f(z) = \int_{L_3} + \int_{\mathcal{S}_1} + \int_{L_1} + \int_{\mathcal{S}_3} + \int_{L_2} + \int_{\mathcal{S}_2}$$
$$= 0$$

provided there are no poles inside the contour. It can easily be shown that as $R \to \infty$, $\rho \to 0$ the integrals around $\mathcal{S}_1$, $\mathcal{S}_2$, $\mathcal{S}_3$ are equal to zero. This leaves us with the integrals over L_1, L_2, L_3. But the integral over L_3 is just the one we wish to evaluate. Taking the real parts,

$$I_{L_3} = -\mathrm{Re}\left(I_{L_1} + I_{L_2}\right)$$

Put $t = ir$ along L_1,

$t = ire^{2\pi i}$ along L_2

gives

$$I_{L_3} = -\mathrm{Re}\left\{\int_{\infty}^{\gamma\omega_m} \frac{ie^{-(\omega-v)r}}{(1-r\omega_m)^{\gamma}}\,dr + \int_{\gamma\omega_m}^{\infty} \frac{ie^{-(\omega-v)re^{2\pi i}}}{(1-r\omega_m e^{2\pi i})^{\gamma}}.e^{2\pi i}\,dr\right\}$$

Put $xe^{2\pi i} = 1 - r\omega_m e^{2\pi i}$ in the second integral.

$$\therefore\ I_{L_3} = +\,\mathcal{J}_m \frac{e^{2\pi i(1-\gamma)}}{\omega_m} \int_{-\infty}^{0} \frac{dx\ e^{-(\omega-v)(1-x)/\omega_m}}{x^{\gamma}}$$

Substitute $x = -\left(\frac{\omega_m}{\omega - v}\right) y$

$$\therefore\ I_{L_3} = \mathcal{J}_m \frac{(-1)^{-\gamma} e^{2\pi i(1-\gamma)} \cdot e^{-(\omega-v)/\omega_m} \cdot (\omega-v)^{\gamma-1}}{\omega_m^{\gamma}} \int_0^{\infty} e^{-y} y^{-\gamma}\, dy.$$

This integral is just $\Gamma(1-\gamma)$. We use the relation

$$\frac{\pi}{\sin \pi\gamma} = \Gamma(\gamma)\,\Gamma(1-\gamma)$$

to get

$$I_{L_3} = \frac{2\pi\ e^{-(\omega-v)/\omega_m}\ (\omega-v)^{\gamma-1}}{\omega_m^{\gamma}\ \Gamma(\gamma)} \quad \ldots \quad (A3.1)$$

as required.

<u>AIM</u> : To show $\gamma = \log_e(1.59\,\lambda d)/8d^2\rho_F^2$

We know $\gamma(d) = \sum_{\varphi}{}' V_\varphi^2\, S_\varphi'(0)$

from equation (3.9B). We use the approximation

$$S_\varphi'(0) \underset{\varphi \ll \lambda}{=} -\frac{\varphi}{\pi p_F \lambda^2}\left(1 - 2\log\left(\frac{2\lambda}{\varphi}\right)\right) \quad \ldots \quad (A3.2)$$

(See Appendix B2)

$$\therefore\ \gamma(d) = \frac{1}{(2\pi)^2} \int_0^{\infty} 2\pi\varphi\, d\varphi \cdot \frac{2\pi}{\varphi} e^{-2\varphi d} \cdot S_\varphi'(0) \quad \ldots \quad (A3.3)$$

Put (A3.2) in (A3.3) and integrate by parts to get

$$\gamma(d) = -\frac{1}{2\pi p_F \lambda^2 d^2}\left(3/2 + \sigma - \log(4d\lambda)\right)$$

where $$\sigma = \int_0^\infty e^{-x} \log(x)\, dx$$

which reduces to the required form using an approximation for σ.

FIG.3.1

THE CLOSED CONTOUR USED TO EVALUATE THE COMPLEX INTEGRAL IN EQUATION (3.10) - SEE APPENDIX A3

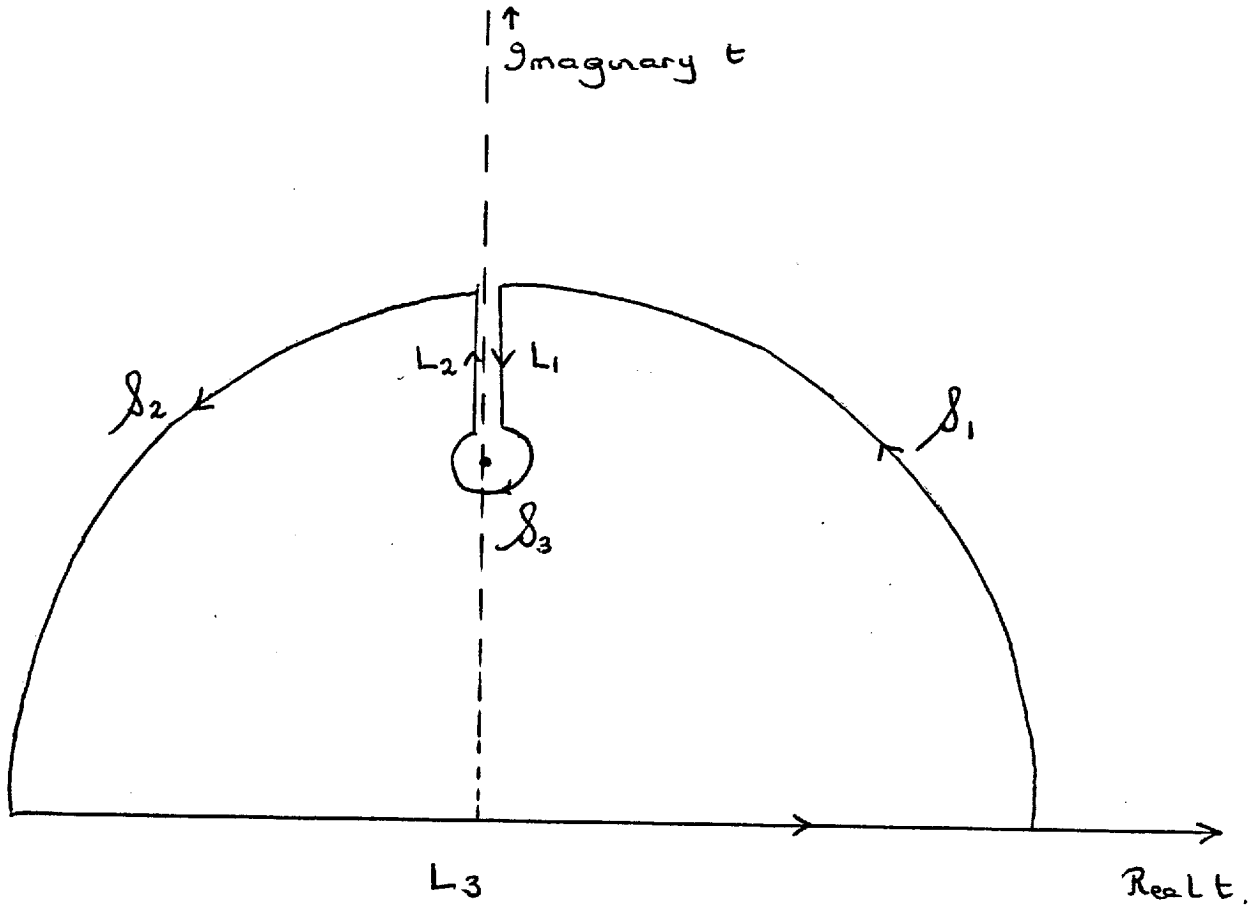

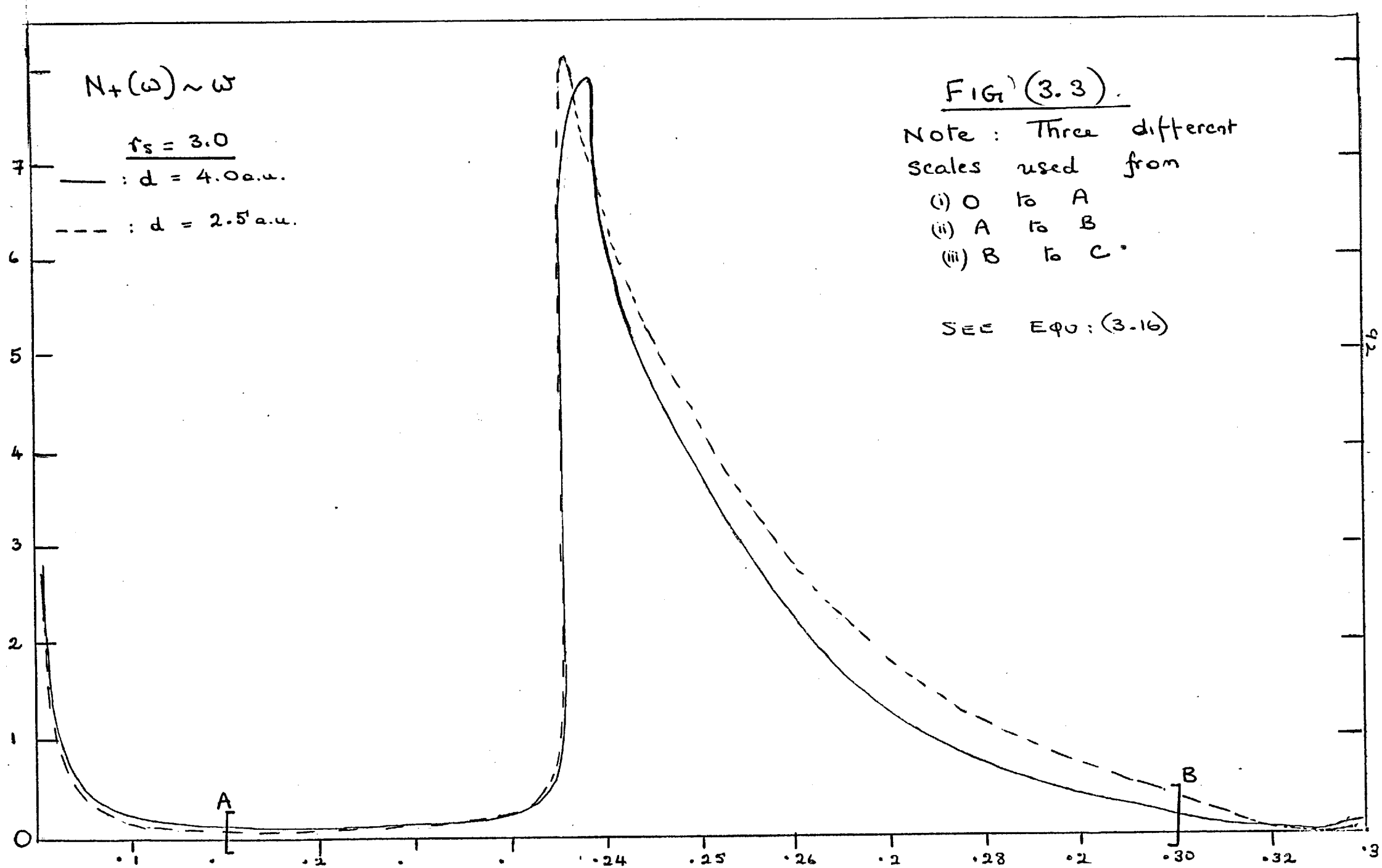
$N_+(\omega) \sim \omega$
$r_s = 3.0$
—— : d = 4.0 a.u.
- - - : d = 2.5 a.u.
FIG (3.3).
Note : Three different scales used from
(i) O to A
(ii) A to B
(iii) B to C.
SEE EQU : (3.16)
A
B
O
1
2
3
4
5
6
7
·1
·2
·24
·25
·26
·28
·30
·32
·3

FIG 3.4.

See Equ. (3.16)

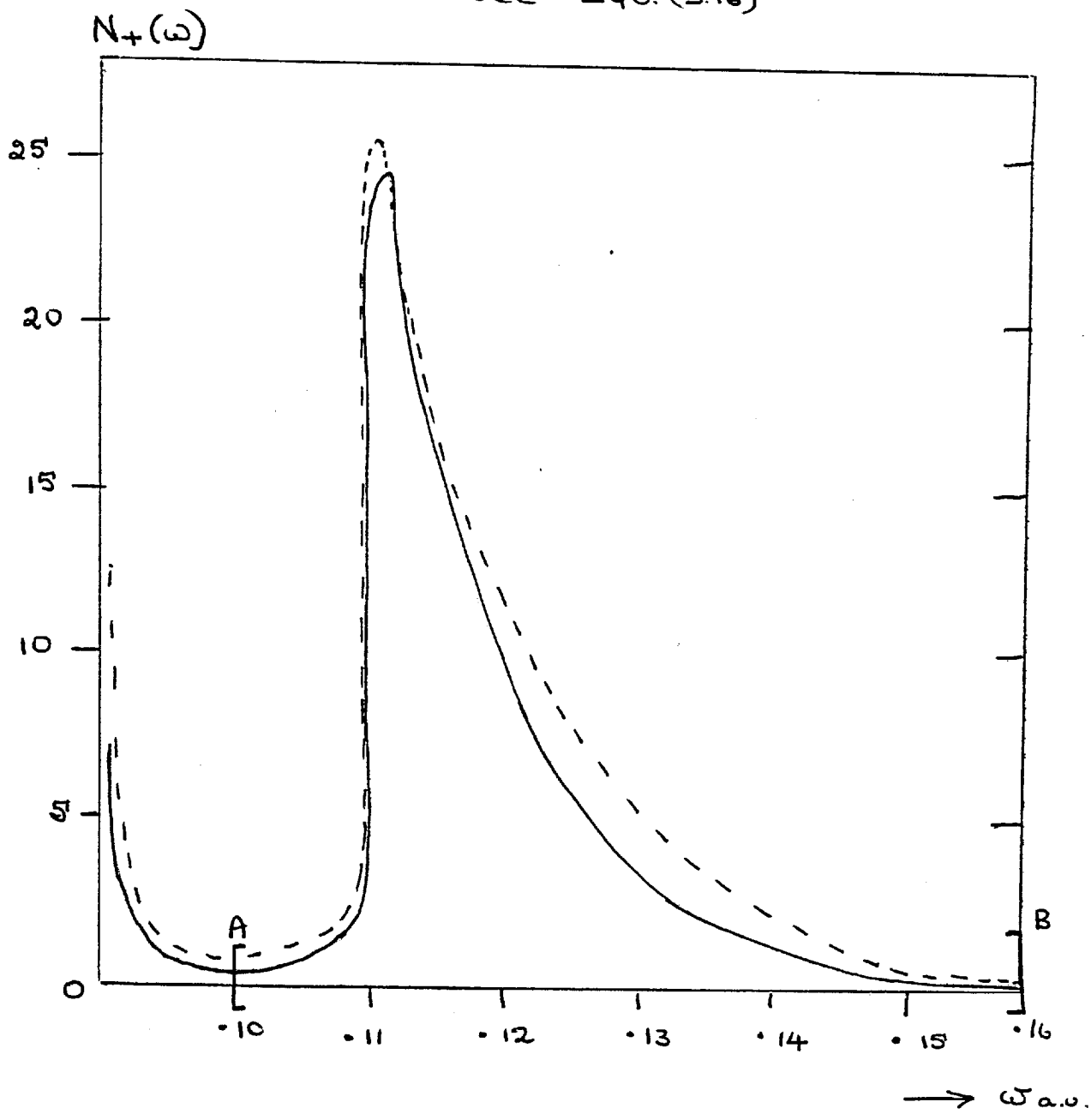

——— d = 4.0 a.u

- - - - d = 2.5 a.u.

Note scale change in [A, B]

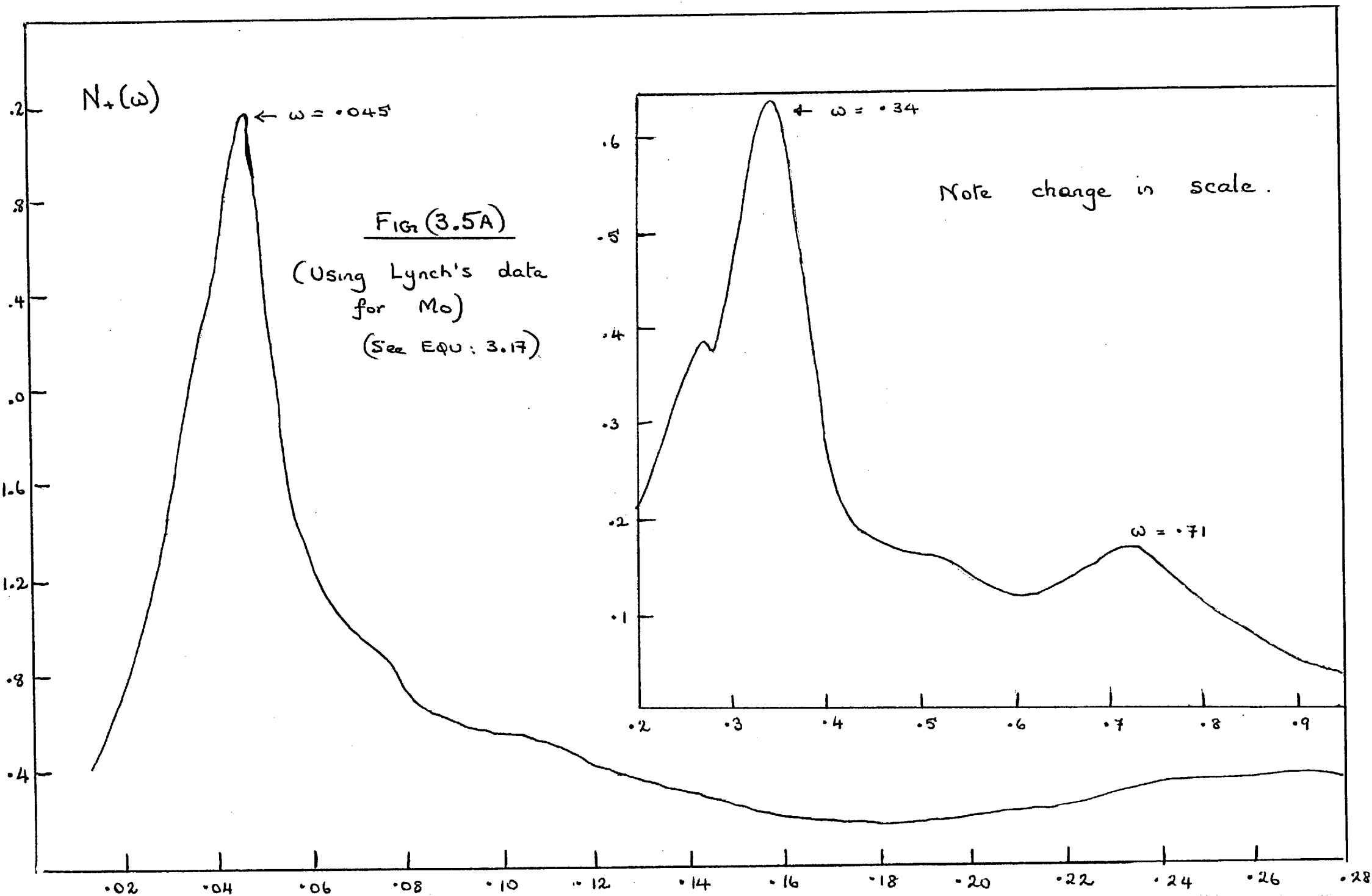
$N_+(\omega)$
← ω = ·045
FIG (3.5A)
(Using Lynch's data for Mo)
(See EQU: 3.17)
← ω = ·34
Note change in scale.
ω = ·71
·2
·8
·4
·0
1·6
1·2
·8
·4
·6
·5
·4
·3
·2
·1
·02
·04
·06
·08
·10
·12
·14
·16
·18
·20
·22
·24
·26
·28
·2
·3
·4
·5
·6
·7
·8
·9

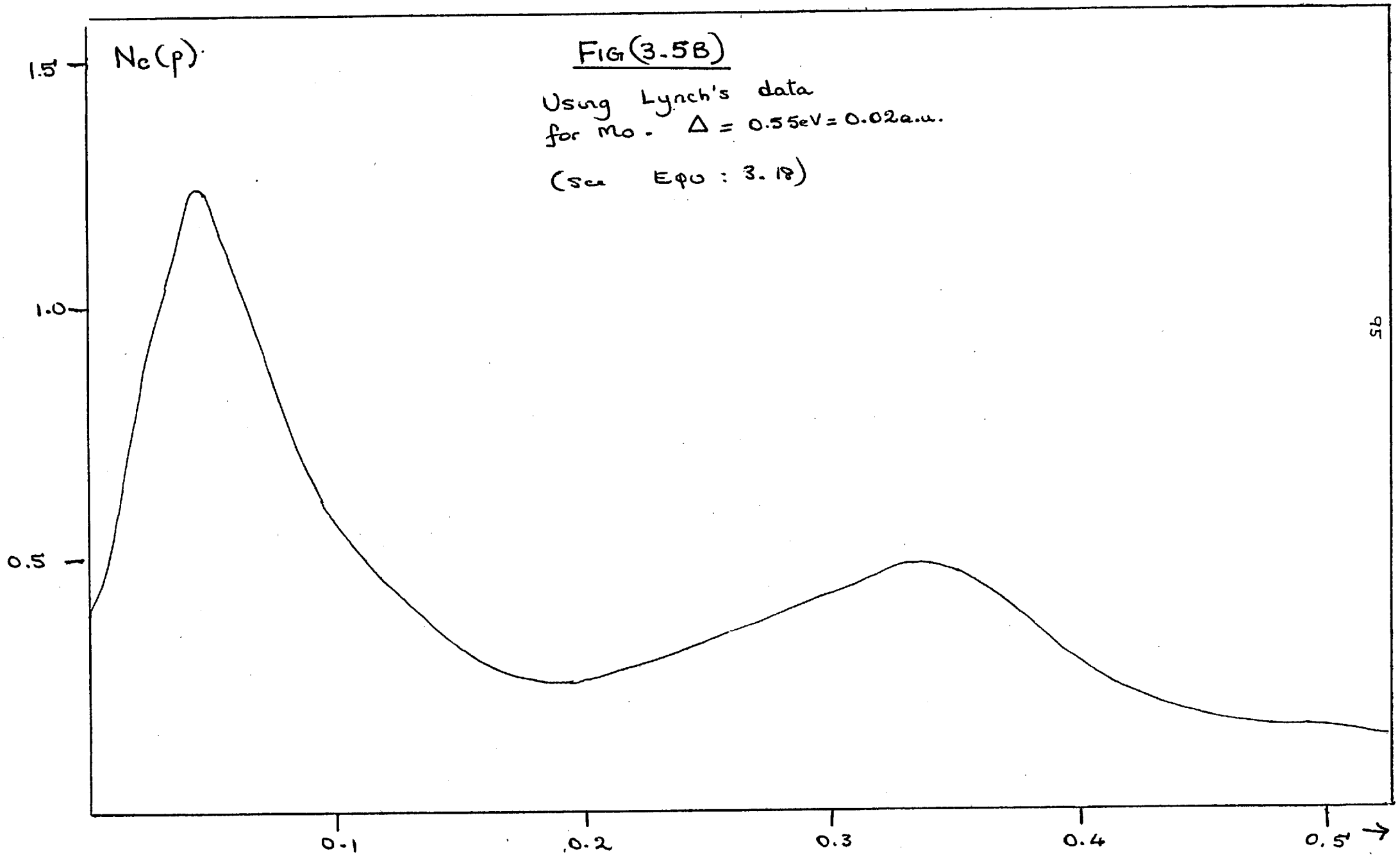

FIG (3.5B)

Using Lynch's data for Mo. $\Delta = 0.55\,eV = 0.02\,a.u.$

(see Eqn : 3.18)

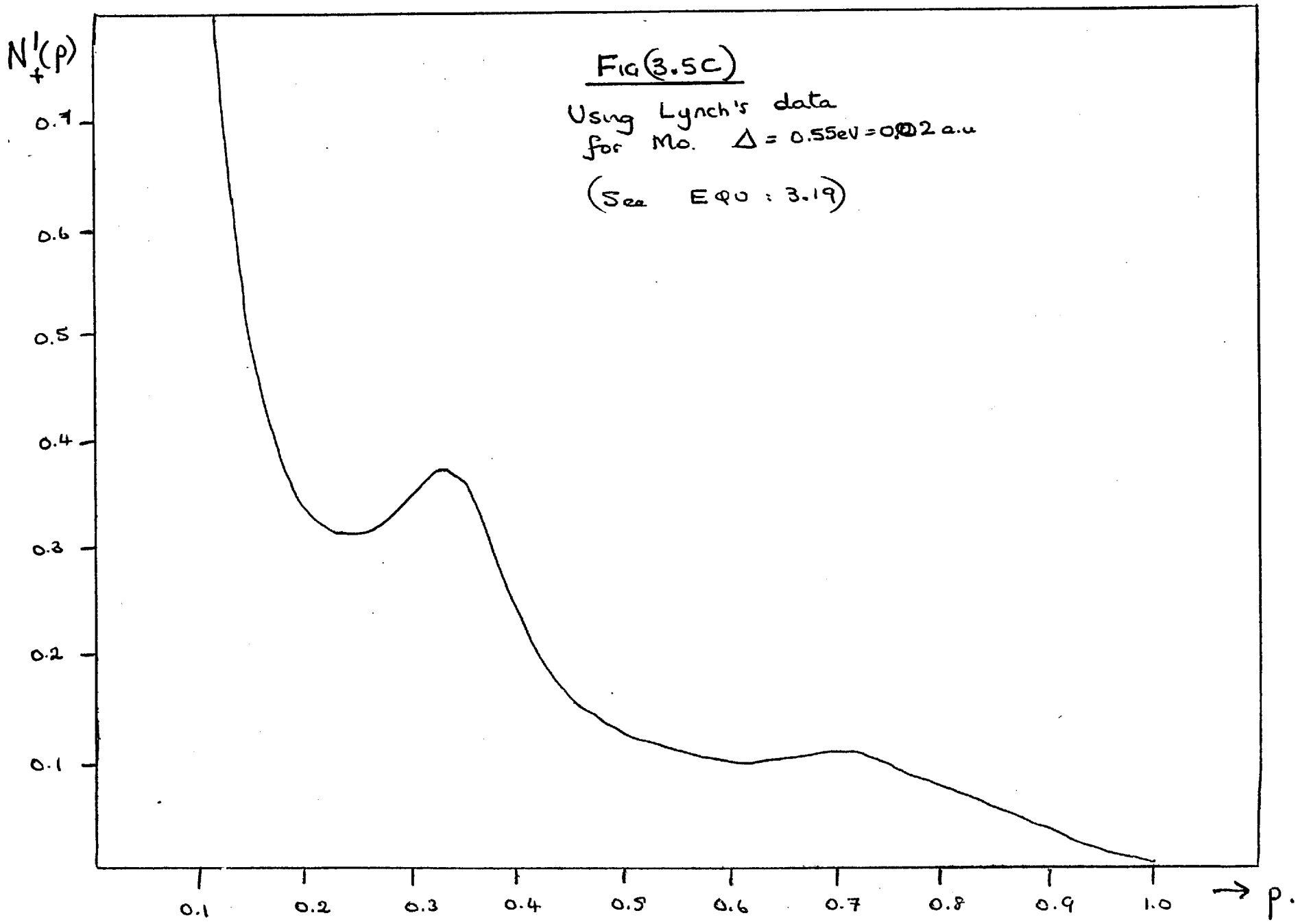

Fig (3.5c)

Using Lynch's data for Mo. $\Delta = 0.55\,eV = 0.02$ a.u

(See EQU : 3.19)

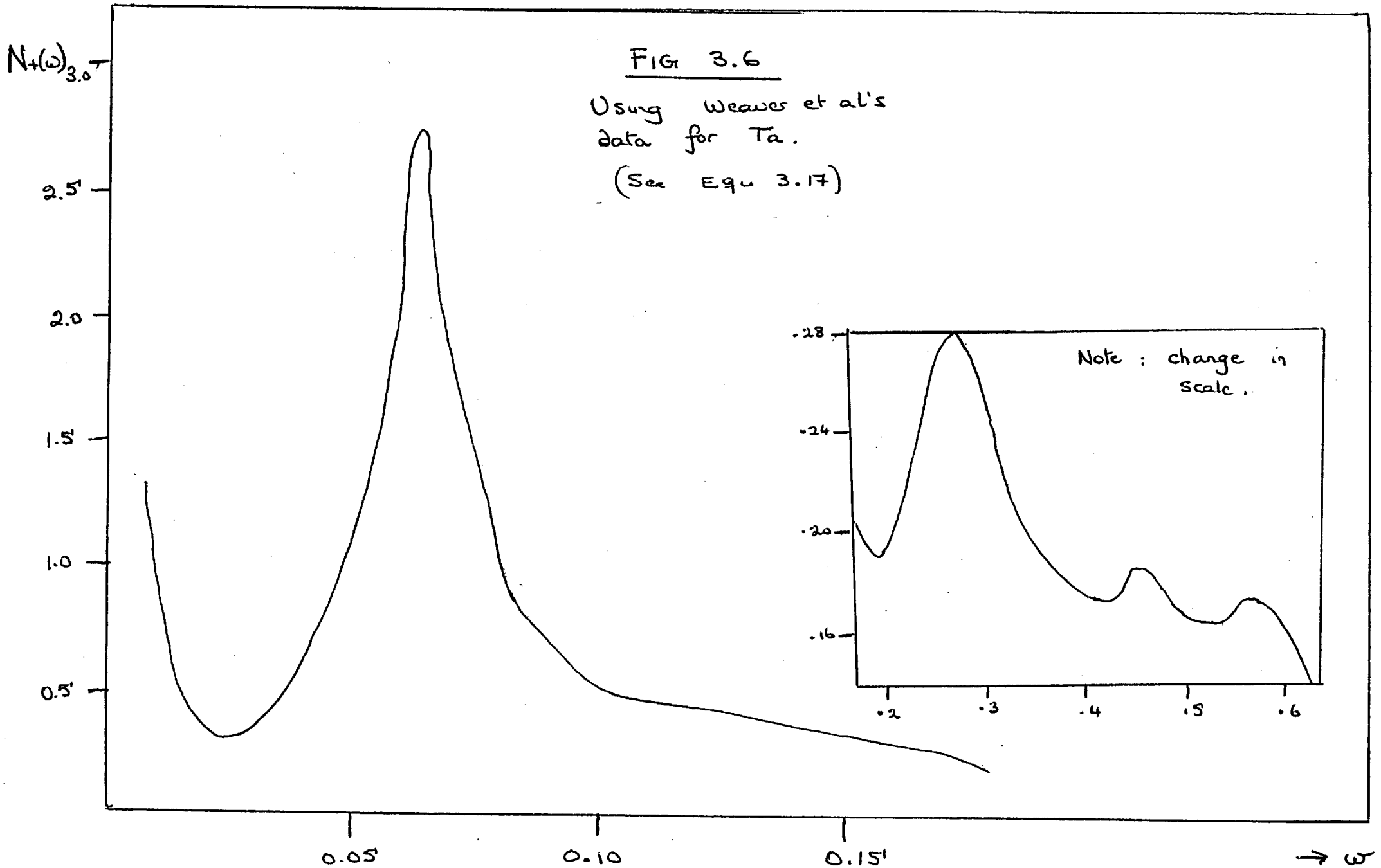

FIG 3.6

Using Weaver et al's data for Ta.

(See Equ 3.17)

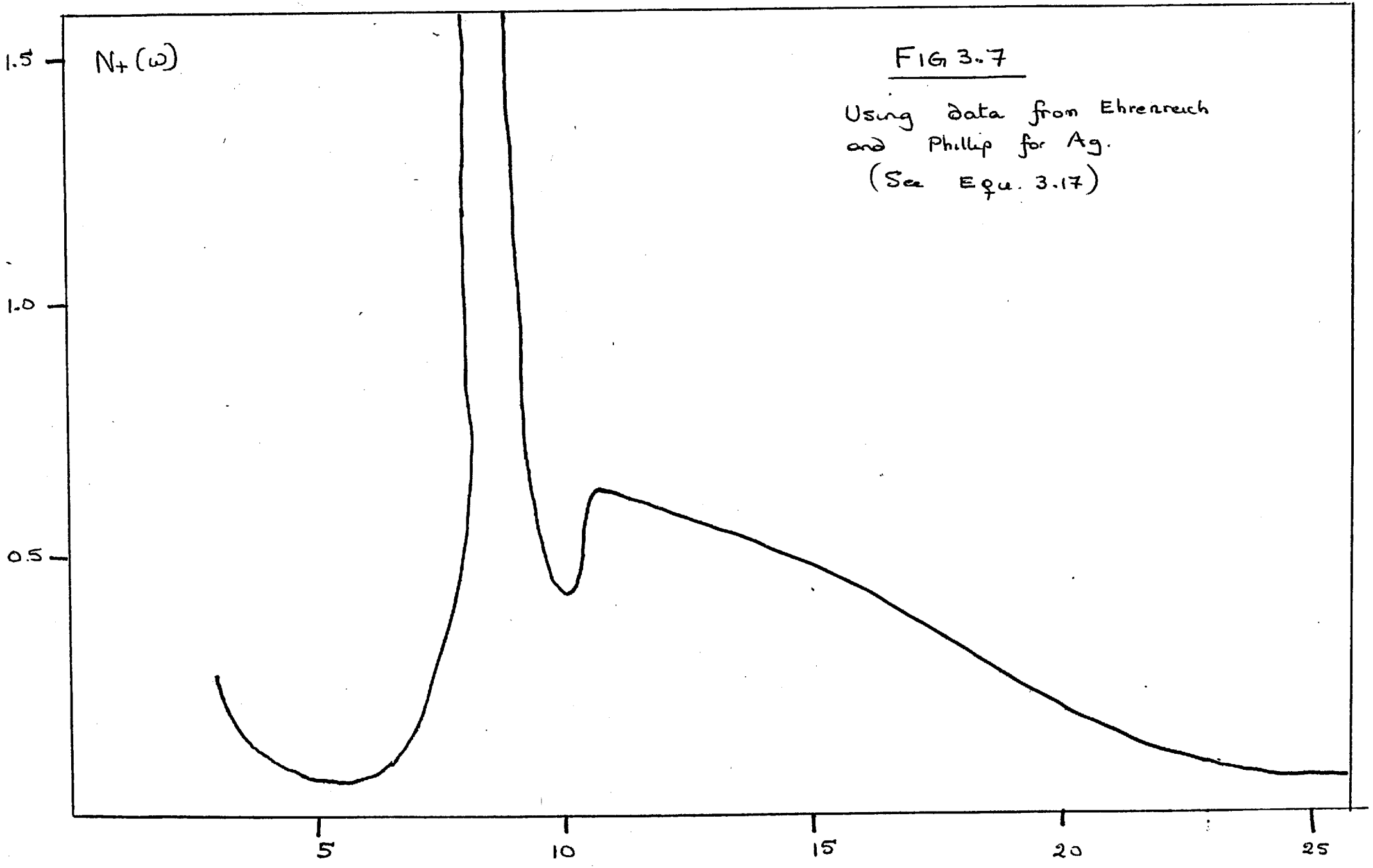

FIG 3.7

Using data from Ehrenreich and Phillip for Ag.
(See Equ. 3.17)

TABLE (3.1)

r_s	ω_s	d	ϑ	ϑ/ω_s	$p_1^{calc.}$	$p_2^{calc.}$
3.0	0.24	4.0	0.049	0.21	0.125	0.032
3.0	0.24	2.5	0.069	0.29	0.16	0.04
5.0	0.11	4.0	0.045	0.41	0.30	0.034
5.0	0.11	2.5	0.062	0.54	0.35	0.034

ALL QUANTITIES ARE IN ATOMIC UNITS.

$\vartheta = -\frac{1}{2}\int_0^\infty R_g(0)\, e^{-2\varphi d}\, d\varphi$

p_1^{calc} is the calculated area under the surface plasmon satellite in $N_+(\omega) \sim \omega$

p_2^{cal} is the calculated area under the surface plasmon satellite in $N_+(\omega)\times\omega \sim \omega$

CHAPTER IV

THE STATIC SPIN SUSCEPTIBILITY AND MAGNETIZATION OF SURFACE ENHANCED ITINERANT ELECTRONS

A General Introduction

As mentioned in the introduction, the latter half of this thesis concerns itself with properties involving the static spin susceptibility of a metal surface, for a nearly magnetic exchange enhanced material. Initial interest in this particular susceptibility with respect to the surface was stimulated by Beal-Monod et al in 1972 and subsequent work has yielded interesting results in the one-dimensional analysis so far carried out e.g. Zaremba and Griffin, 1973 and 1975 ; Muscat et al 1975 and 1976 ; Schiach 1976, Perdew 1977. Indeed the magnitude of the surface spin susceptibility is significant in some treatments in the theory of chemisorption and catalysis (Schrieffer and Gomer 1971 ; Suhl et al 1970). More details of the work done over the last five years is given in the next section.

Let us commence by making a general classification for the three magnetic states in a system viz. diamagnetic, paramagnetic and ferromagnetic as follows :

1. Diamagnetic materials have a negative magnetic susceptibility of the order 10^{-6} which is temperature independant e.g. inert gases, hydrogen, many metals and organic compounds.

It tends to occur in materials with closed shells.

All substances have a basic diamagnetism term which is nearly always weak and very often overshadowed by a much larger

2. paramagnetic susceptibility, in which the response is positive e.g. the alkali metals, most gases, soluble salts of iron and oxygen.

In the least complicated case of the alkali elements e.g. Li, Na, K, Rb and Cs, is seen a temperature independant weak paramagnetic susceptibility. The explanation is due to the essentially non-temperature dependance of the well known free electron gas (which has a parabolic density of states) Pauli susceptibility given by

$$\chi_p = 2\mu_B^2 N(\varepsilon_F)$$

where μ_B is the Bohr magneton and

$N(\varepsilon_F)$ is the density of states at the Fermi level.

However, for most transition metals (characterised by incomplete 3d-shells) and rare earth metals (characterised by incomplete 4f-shells) are much more strongly paramagnetic than the alkali metals with a significant temperature-dependant susceptibility. Experiments on palladium yield an enhancement factor of approximately 12 to the Pauli susceptibility. This is due essentially to the electron-electron

interaction (exchange and correlation) which was neglected in the χ_p calculation. These enhanced systems may also show a temperature dependance (as indeed palladium does). It is also thought that orbital angular momentum may have some contribution to the susceptibility and hence enhancement (Kubo et al, 1956).

Where there is a temperature dependance of the susceptibility in paramagnetic materials, it tends to follow the inverse temperature Curie law e.g. for rare earth metals.

3. ferromagnetism occurs for positive values of the susceptibility and for temperatures below Curie point, the Curie-Weiss law for susceptibility applies. For higher temperature, paramagnetism prevails. Examples are nickel and iron.

Further details and references may be found in Crangle,1976; Heck, 1974; Culitty, 1972; White 1970; Wohlfarth, 1976.

In experiments it is important to distinguish between various contributions to the susceptibility, although this is often a difficult task. In 1964, Clogston et al have shown how the total susceptibility, χ, for platinum may be thought of as a sum of separate susceptibilities due to the various contributions via spin paramagnetism and diamagnetism due to the core.

The d-electrons are considered in a tight-binding approximation, and it is this effect which is dominant in the total susceptibility, the s-spin contribution being smaller partly due to the smaller density of states. The exchange interactions act appreciably on the spin part of the susceptibility which justifies our forthcoming involvement with this.

Just how a system of interacting electrons respond to a magnetic field is a many body problem with all its attendant difficulties. One model which has been much used is the Hubbard model which in the single band approximation has a Hamiltonian of the form:

$$H = \sum_{ij} t_{ij} c_{i\sigma}^{+} c_{j\sigma} + \tfrac{1}{2} I \sum_{i,\sigma} n_{i\sigma} n_{i-\sigma}$$

where t_{ij} is the hopping term between electrons at sites i,j,

$c_{i\sigma}^{+}$ is a creation operator for a Wannier state,

$c_{i\sigma}$ is a destruction operator for a Wannier state.

(Hubbard,1963).

The second term represents the electron-electron interaction, where I is the intra-atomic Coulomb integral. Calculations in the Hartree-Fock approximation yield (Izuyama et al,1963)

$$\chi = \chi_P / (1 - I N(\epsilon_F))$$

showing an enhanced type of Pauli susceptibility previously mentioned. Divergence occurs when $\bar{I} = IN(\epsilon_F) = 0$. This condition for ferromagnetic instability is the Stoner criterion. We are concerned in this thesis with paramagnetic materials with $\bar{I} < 1$.

Our study is concerned with itinerant electron behaviour as opposed to a localised model. The latter

assumes that the particles reside on lattice sites with a well defined local spin $\underline{S}$. The well-known Heisenberg model works well for rare earth metals (White,1970) whose localised moments are due to partially filled f-shells which are tightly bound to the atomic nucleus.

However transition metals are better characterised by an itinerant electron model in a description of their magnetic properties. This is clear from the saturation moments which correspond to non-integral numbers of spins per atom eg. for the ferromagnetic metals iron,cobalt and nickel these are 2.2, 1.72 & 0.61 respectively. Also the properties of observed large electronic specific heats and d-electron contributions to the electrical conductivity indicate the supremacy of the itinerant over the localised model for transition metals (Herring, 1966, Chapter IV).

Systems in which there occurs a strongly enhanced static spin susceptibility are often labelled 'exchange enhanced' or 'almost ferromagnetic' systems. Our interest in the second half of this thesis lies in the study of the paramagnetic properties of bounded Fermi systems characterised by a strongly enhanced static spin susceptibility. Examples of nearly ferromagnetic systems are liquid helium^3 (the only Fermi liquid found in nature), palladium, and certain transition metal alloys eg. palladium-rhodium and rhodium-nickel. It should be emphasised that the exchange interaction is of quantum

mechanical origin tied up with the concept of the indistinguishability of identical quantum particles and the antisymmetry requirement for the state function of an assembly of fermions eg. electrons. In other words the Pauli exclusion principle is manifested in the interaction (and higher order mechanisms). These concepts were first developed by Heisenberg,1928; and formed the basis of subsequent theoretical work.

Let us now conclude this very general introduction and proceed to discuss recent work that is of immediate significance to our problem.

A REVIEW OF RECENT WORK - Introduction to our particular problem.

We now discuss recent work done that is directly relevant to our problem. It is only over the last five years that interest has abounded in the examination of surface effects on the magnetic response of an itinerant electron gas. Mills, Beal-Monod and Weiner in 1972, (hereafter referred to as MBW)first drew attention to the fact that the behaviour of itinerant electron materials that are strongly paramagnetic (due to large exchange enhancement or the temperature being near the magnetic ordering temperature) differ near the surface to that in the bulk. They showed that in the RPA for an exchange-enhanced paramagnet the surface susceptibility does not display the enhancement found in the bulk, by using an approximation to the non-interacting spin susceptibility in the presence of a surface. This consists of replacing the bare susceptibility of the bulk material plus terms due to the reflection of electrons from the surface, by the bare bulk susceptibility alone. A further approximation was then used for this bare bulk susceptibility which did not yield a surface enhancement.

In 1973, WBM (ie. Weiner et al as above) included the effects of the reflection terms through an oscillatory

approximation and found an additional enhancement near the surface greater than that in the bulk. In both these papers a tight binding model of electrons was used. WBM find a divergence susceptibility for values of the interaction $\bar{I}$ less than or equal to unity i.e. the RPA calculation of the surface susceptibility results in a surface phase transition occurrence before the bulk phase transition. Some doubt however has been cast upon their choice of parameters used as corresponding to an unphysical situation (Newns, 1977).

Weiner (1973, Boston Conference) found the susceptibility of the surface to diverge for $\bar{I} < 1$, almost universally as a function of crystal structure, surface orientation and Fermi energy. He predicted a surface magnetic phase transition while the bulk is still paramagnetic for $\bar{I} \simeq 0.9$ a value for which the RPA is quite reliable in the bulk.

In 1972, Beal-Monod, Kumar and Suhl conducted a numerical investigation of the surface magnetization as a function of both the interaction I and distance from the surface of the metal for different widths of thin metallic films. They find the surface magnetization undergoing enhancement to the same degree as the bulk magnetization when using the exact expression for the susceptibility at zero interaction, , obtained from the free electron bands and which includes the surface oscillatory terms. Their results are notable for the large peak in the magnetization occurring at the value $2p_F z = 4.5$. It is found that as $\bar{I} \to 1$, this peak grows

faster than $(1-\bar{I})^{-1}$ which is apparently related to the fact that the free particle spin susceptibility is largest at the position of this peak.

The three different approaches observed above show that the results are extremely sensitive to the ways in which the surface contributions are taken care of.

In his thesis (1974), Zaremba makes a study of the variation in susceptibility for the free electron model of bounded Fermi systems using a finite range of interaction of the form

$$I(\underline{r}) = I \frac{\kappa^2}{4\pi|\underline{r}|} e^{-\kappa|\underline{r}|}$$

as opposed to the zero-range ($\kappa \to \infty$) interactions so far considered. His results which apply to metallic films predict the occurrence of a surface phase transition at $\bar{I}_s = 0.985$ but they are extremely sensitive to the value of the finite range $\eta = 1/\kappa$, taken (confirmed analytically by Muscat, 1975). In particular, the large quantum oscillations found by previous workers are significantly reduced in magnitude, in fact almost washed out, when η is of the order of the Fermi-Thomas screening length and the anomalous surface phase transition does not occur for $\bar{I} < 1$.

Muscat et al (1975) re-examine the degree of enhancement of the spin susceptibility near the surface of a nearly magnetic exchange enhanced metal when a uniform field and a field localised near the surface are applied, using a zero-

range interaction and free electron model. Their results show a strongly enhanced magnetization near the surface as compared with the bulk and predict the existence of ferromagnetic instability for values of the electron - electron interaction for which the bulk is still paramagnetic, i.e. $\bar{I}_s$ =0.985, in agreement with Zaremba's 1974 work. The large peak at $2p_F z$=4.5 is present as in Beal-Monod et al (1972).

Muscat (1976) performed numerical calculations of a paramagnetic metal within a finite barrier potential (V) model of the metallic surface in contrast to the ISBM discussed above. For large values of V($\sim$2) he finds that there is still an enhancement of the magnetization near the surface although the large peak is shifted from $2p_F z \simeq 4.5$ for $V = \infty$ to $2p_F z \simeq 3.5$ for V = 2.0. Consequently there is ferromagnetic instability at the surface occurring at values $0.985 < \bar{I}_s < 1$ which are V-dependant. For smaller values of V, no surface instability can be estimated.

The most recent work we know of relating to surface magnetization calculation of itinerant paramagnets is by Schiach (1976) who considers the surface response to a uniform static magnetic field, by using approximations for the non-interacting electron susceptibility, χ°, and a finite range exchange interaction as Zaremba and Griffin (1973). The first approximation used is to neglect the non-diagonal terms in χ° and simplify the remaining

diagonal ones, while the second involves a simplifying of the off-diagonal terms by a separable non-oscillating scheme (also considered by Muscat et al, 1975). The result is that like MBW, no quantum oscillations are observed in the magnetization - there is no surface phase transition.

So far all the work done on this problem of surface enhanced magnetization has been limited to the static and one-dimensional cases given by $\omega = 0$ and $\underline{Q} = 0$.

To conclude this section, we give a brief scan of the present situation. The importance of the properties of the static spin susceptibility of paramagnets via the exchange coupling parameter $\bar{I}$ has become increasingly clear over the last few years. Work has been carried out on the variation of the surface susceptibility in metallic films using various approximations for the non-interacting electron susceptibility. Some approximations give a smaller surface than bulk enhancement (MBW, 1972). However exact RPA calculations for the ISBM (as well as the finite potential barrier model) find that a surface phase transition exists for $\bar{I} < 1$ at which the surface susceptibility diverges. This has also been shown through use of a tight binding model (Weiner, 1973).

Aim and Motivation

Our concern for the second half of this thesis is to extend the work discussed above to a more realistic situation in three dimensions i.e. for finite $\underline{Q}$ and $\omega = 0$.

Only the instability at $\underline{Q}$ equals zero has been studied so far. As noted by Ying et al (1976), although for a simple band structure the bulk instability always occurs first at $\underline{Q} = \underline{0}$, this is not necessarily the case for the surface region which requires a separate study.

A prime motivation for the study is the importance of the localised static surface susceptibility in chemisorption problems (Schrieffer and Gomer, 1971). Here the spin of an atom adsorbed on the surface is assumed to be coupled to the spin fluctuations of the solid via a short range exchange interaction. In this problem the perturbing field is not only localised near the surface but also localised about a point in the surface plane, and so the localised susceptibility discussed by Muscat et al (1975) is only an approximation.

Through simple qualitative arguments (as well as further detailed analysis), Schreiffer and Gomer arrive at an expression for ΔE, the strength of the induced covalent bond, formed by the coupling of an induced spin density in the solid in the bonding region to the adatom spin. ΔE takes the form

$$\Delta E \propto -J^2 \chi_{\text{localised}}.$$

where J is the exchange interaction between the adatom and single metal atom (for further details see Chapter I).

To date (within our knowledge) Schiach (1976) alone has calculated this ΔE as a function of adatom position, using approximation schemes for χ^{o}. We expand his calculations by using the exact RPA expression.

DESCRIPTION OF OUR MODEL WITH ITS MATHEMATICAL PROPERTIES

The geometry of the situation is still that of a semi-infinite metal with its surface in the x-y plane and the z-axis being perpendicular to this surface. In the real space co-ordinate system $\underline{r} = (\underline{X}, z)$ maps on to $\underline{q} = (\underline{Q}, q_z)$ within the Fourier space framework. We now work with the infinite square barrier model in which the density profile of the electrons varies as a function of z given by equation (2.1) i.e. it has a Friedel oscillatory behaviour. We use the Fourier cosine transform of a function $f(\underline{r})$ as defined in equation (2.9).

Now the magnetization for a paramagnetic system in the presence of a magnetic field $H(r,t)$ is generally defined by

$$m(\underline{r}, t) = \int \chi(\underline{r}, \underline{r}', t, t') H(\underline{r}', t') \, d\underline{r}' \, dt' \quad \ldots (4.1)$$

where the transverse susceptibility is given by the Kubo-like formula:

$$\chi(\underline{r}, \underline{r}', t, t') = i\Theta(t-t') \langle [S^{+}(\underline{r}, t), S^{-}(\underline{r}', t')] \rangle \quad \ldots (4.2)$$

where $S^{+}(\underline{r},t)$ is the spin-raising operator,

$S^{-}(\underline{r},t)$ is the spin-lowering operator at position $\underline{r}$ and time t and

Θ is the ordinary step-function.

Due to translational invariance in all co-ordinates excepting the ones perpendicular to the surface we use the following transformation

$$\chi(\underline{q}, q_z, q_z', \omega) = \iiint d^2(\underline{x}-\underline{x}')\, d(t-t')\, dz\, dz'\, \chi(\underline{r}, \underline{r}', t, t') \times e^{i\omega(t-t')} \cos(q_z z)\cos(q_z' z') \quad \ldots (4.3)$$

where $\underline{X}=(x,y)$, $\underline{Q} = (q_x, q_y)$.

It is of importance to realise that paramagnetic susceptibility of a system of electrons is the same as the response function involving the dielectric constant i.e. equation (4.3)is identical to (2.12) when there is no electron - electron interaction. Now for the case of a non-interacting degenerate electron gas, Newns (1970), (Beck and Celli in an equivalent formalism in the same year) has shown in detailed analysis that in the ISBM :

$$\chi^0(\underline{q}, q_z, q_z', \omega) = D_{q, q_z}(\omega)\, \delta_{q_z q_z'} - A_{q, q_z, q_z'}(\omega) \quad \ldots (4.4A)$$

i.e. as a sum of diagonal ($q_z = q_z'$) and non-diagonal ($q_z \neq q_z'$) elements which obey the sum rule

$$D_{q q_z}(\omega) = \int A_{q, q_z q_z'}\, dq_z' \quad \ldots (4.4B)$$

This is physically feasible since the electronic wavefunctions vanish at z = 0 and so

$$\int \chi^0(q, q_z, q_z', \omega)\, dq_z' = 0 \quad \ldots (4.4C)$$

For the static case $\omega = 0$ in which we are interested, we

use Newns's expressions (1970) for $D_{\varrho q_z}$ and $A_{\varrho q_z q_z'}$ written in a non-dimensional form as follows :

$$D_{\varrho q_z}(0) = \frac{1}{2} + \frac{1-|q|^2}{4|q|}\log\left|\frac{1+|q|}{1-|q|}\right| \quad \ldots\ldots \quad (4.4D)$$

where we have replaced

$$q_z \rightarrow q_z/2p_F$$

$$q_z' \rightarrow q_z'/2p_F$$

$$\varrho \rightarrow \varrho/2p_F$$

This is the usual Lindhard function for an infinite medium. The correction due to the presence of the surface is given by :

(I) if $q_z < q_z'$

$$A_{\varrho q_z q_z'}(0) = \begin{cases} 0 & \ldots\ldots \text{ if } q_z' > 1+q_z \\ \frac{1}{2\varrho^2}\left[\varrho^2 + q_z q_z' - \left\{q_z^2 q_z'^2 + \varrho^2(q_z^2+q_z'^2+\varrho^2-1)\right\}^{1/2}\right] & \ldots\ldots \text{ if } 1-q_z < q_z' < 1+q_z \\ 1 & \ldots\ldots \text{ if } 1/2 - \mathrm{Re}(1/4-\varrho^2)^{1/2} < q_z < 1+q_z' \\ & \quad \underline{\text{or}}\ q_z' < \mathrm{Re}\,\varrho\left[(1-q_z^2-\varrho^2)/(\varrho^2+q_z^2)\right]^{1/2} \\ \frac{1}{2\varrho^2}\left[\varrho^2 - \left\{q_z^2 q_z'^2 + \varrho^2(q_z^2+q_z'^2+\varrho^2-1)\right\}^{1/2}\right] & \ldots\ldots \text{ if } q_z < 1/2 - \mathrm{Re}(1/4-\varrho^2)^{1/2} \\ & \quad \underline{\text{and}}\ \mathrm{Re}\,\varrho\left[(1-q_z^2-\varrho^2)/(\varrho^2+q_z^2)\right]^{1/2} < q_z' < 1-q_z \end{cases}$$

(II) if $q_z > q_z'$ then

$$A_{\varrho q_z q_z'} = A_{\varrho q_z' q_z} \quad \ldots\ldots (4.4E)$$

This is the corrected version of the formula given by Newns (1970). It comes from the quantum mechanical interference between impinging and reflected electrons and is strongly dependant on the assumed properties of the surface. Graphs illustrating the various regions of $A_{\varsigma q_z q_z'}$ as written in equation (4,4E) are given in Figs. (4.1 A,B,C) for clarity.

For interest we plot the behaviour of χ° given in (4.4A).

Fig. (4.2) shows the variation of $D_{\varsigma q_z}(0)$ with q_z given by equation (4.4D) for two values of Q differing by a factor of ten viz. Q = 0.04 and Q = 0.4. But the maximum difference between the two curves is by about 5% (which occurs as $q_z \rightarrow 0$) and there is negligible difference for large values of q_z ($q_z > 2$).

Figs. (4.3) to (4.5) illustrate graphically the non-uniform part $A_{\varsigma q_z q_z'} \sim q_z'$ (for fixed Q, q_z values) given by equation (4.4E). This is important only in giving a correct description for perturbations in the surface region. In Fig. (4.3) we take Q = 0.1 and let q_z run over the values 0.0, 0.5, 0.9, 1.0, 1.02 and 2.0. The behaviour is in good agreement with graphs by Muscat et al (1975) who in fact consider the limit Q = 0. We note the points of singularity are (0,1) and (1,0) and it is this singular behaviour which is responsible for dominant Friedel oscillations in the surface response function (Beck and Celli, 1970).

Similar curves are drawn in Fig. (4.4) for Q = 0.5

and we note the change in behaviour for $q_z = 0.9$, 1.0, 1.02 as $q_z' \to 0$.

In Fig. (4.5), we take Q = 1.0 and again see a noticeable change in behaviour with all the curves shrinking in height by as much as 50% in some cases ($q_z = 0.5$, 0.9). The dotted curve on this figure is for Q = 2.0 and $q_z = 0.0$, showing that for this and higher values of the Fourier wave-vector contributions from $A_{Qq_zq_z'}$ become less and less important. Physically this means that the further away from the surface we go, the contributions to the Friedel-type of oscillations dwindle down (see Fig. 2.1).

Physical Significance of χ^o

The non-interacting response matrix χ^o as defined in (4.4) can be interpreted physically through the schematic diagrams in Fig.(4.6 i, ii, iii, iv) which translates the effects into real space. The first sketch illustrates the direct propagation of an electron at $\underline{r}$ and a hole at $\underline{r}'$. This arises from the diagonal term D which is identical to the well-known response function of a non-interacting Fermi gas subject to periodic boundary conditions. If this were not so, the effect of the boundary would be to modify the response deep within the gas, which is not expected even in the absence of any Coulomb interactions between the particles.

In fact the total effect of a disturbance at $\underline{r}'$ giving rise to a response at $\underline{r}$ just below the surface can be regarded as a sum total of the different multiple reflections involved at the boundary : these are sketched in Fig.(4.6ii , iii, iv) and the quantum mechanical treatment of the dynamics of particles impinging on and reflecting from the surface is displayed in the quantum interference effects in χ° which are inherent in its non-diagonal part A (Beck and Celli,1970) and gives rise to the oscillatory behaviour in χ° . This same oscillatory property is reflected in the electron density profile given in Fig.(2.1).

These high momentum transfer processes through the multiple reflections on the bounding surface are essential features in a study of the magnetization near the surface.

Let us conclude this section by a description of some properties of χ° . From (4.4) it is easily seen that χ° is invariant under interchange of its arguments q_z, q_z' i.e.

$$\chi^{\circ}(\rho, q_z, q_z') = \chi^{\circ}(\rho, q_z', q_z)$$

since the non-diagonal terms A are symmetric with respect to q_z, q_z'. In real space, this takes over as :

$$\chi^{\circ}(x, z, z') = \chi^{\circ}(x, z', z)$$

In fact this symmetricity readily extends to the complete

response χ , by writing the Bethe-Salpeter equation for χ (see equation (4.6) in the next section) in matrix notation as :

$$\chi = \chi^{\circ} + \chi^{\circ} I \chi \Rightarrow \chi = (1 - \chi^{\circ} I)^{-1} \chi^{\circ}$$

$$\therefore \chi^{T} = \chi^{\circ} + \chi^{T} I^{T} \chi^{\circ} \Rightarrow \chi^{T} = \chi^{\circ} (1 - \chi^{\circ} I^{T})^{-1}$$

since $\chi^{0} = \chi^{\circ T}$ where T denotes the transpose of the matrix. Thus assuming $(1 - \chi^{\circ} I)$ is symmetric i.e. $I = I^{T}$, and that $(1 - \chi^{\circ} I)^{-1}$ exists, we have :

$$\chi = \chi^{T}$$

Also, for film geometry if l is the width of the film,

$$\chi^{\circ}(x, z, z') = \chi^{\circ}(x, l - z, l - z')$$

$$\chi(x, z, z') = \chi(x, l - z, l - z')$$

which just reflects the inversion symmetry about the mid-plane of the film.

Derivation of the RPA Integral Equation for the Static Magnetization.

We now wish to derive an RPA integral equation for the magnetization of the form :

$$m(\underline{r}) = m^{\circ}(\underline{r}) + \bar{I} \int \chi^{\circ}(\underline{r},\underline{r}')\, m(\underline{r}')\, d\underline{r}' \quad \ldots (4.5A)$$

where the static limit $\omega = 0$ is assumed throughout and the electron-electron exchange interaction is of the form :

$$I(\underline{s}_1 - \underline{s}_2) = \bar{I}\, \delta(\underline{s}_1 - \underline{s}_2) \quad \ldots (4.5B)$$

between electrons at sites $\underline{s}_1$, $\underline{s}_2$ i.e. we take a zero-range form for the interaction, and $\bar{I}$ is assumed to be non-dimensional,

and

$$m^{\circ}(\underline{r}) = \int \chi^{\circ}(\underline{r},\underline{r}')\, h(\underline{r}')\, d\underline{r}' \quad \ldots (4.5C)$$

is the magnetization at zero interaction. All quantities are made dimensionless by factoring out $N(\varepsilon_F)$, the density of states at the Fermi level e.g. $h \rightarrow HN(\varepsilon_F)$.

One possible path of procedure is to start with the definition of in equation (4.2) and by use of a suitable Hamiltonian in second quantized form derive the equation of motion of the system through evaluation of relevant commutators. Then by using a standard procedure in RPA, we can linearize this equation of motion by replacing pairs of creation and destruction operators by their

expectation values which then results in a truncated equation of motion which will assume the form :

$$\chi(\underline{r},\underline{r}',\omega) = \chi^{\circ}(\underline{r},\underline{r}',\omega) + \bar{I}\int d\underline{r}''\chi^{\circ}(\underline{r},\underline{r}'',\omega)\chi(\underline{r}'',\underline{r}',\omega) \quad \ldots (4.6)$$

using (4.5B).

This is the method used by MBW (1973) in their tight-binding model. Substitution of (4.6) in (4.1) would give us the required form of (4.5A). For present purposes we shall give only the simplest derivation of the RPA integral equation for the magnetization m(r) in terms of m (r) -- see equation 4.5C.

The interacting electron problem reduces essentially to the previous non-interacting electron problem discussed in Chapter II with the interaction entering via an 'effective' field as follows.

In the RPA, the response $\delta\rho$ to a system is given by

$$\delta\rho(\underline{r},t) = \int_0^t dt' \int d\underline{r}' \chi^{\circ}(\underline{r},\underline{r}',t,t')V(\underline{r}',t) \quad \ldots (4.7)$$

which is the same as equation (2.4). Through the application of an appropriate Fourier transform defined in (2.6), we can write

$$\delta\rho_{\uparrow}(\underline{r},\omega) = \int d\underline{r}' \chi^{\circ}(\underline{r},\underline{r}',\omega) V_{\uparrow}(\underline{r}',\omega) \quad \ldots (4.8A)$$

where the index $\uparrow$ denotes the response for up-spin electrons . Similarly, we can write

$$\delta\rho_{\downarrow}(\underline{r},\omega) = \int d\underline{r}' \chi^{\circ}(\underline{r},\underline{r}',\omega) V_{\downarrow}(\underline{r}',\omega) \quad \ldots (4.8B)$$

for down-spin electrons.

But the magnetization of a system is defined as the difference between the total number of up-spin and down-spin electrons. Hence by subtracting (4.8B) from (4.8A), we arrive at the local magnetization at the point $\underline{r}$:

$$m(\underline{r},\omega) = \int d\underline{r}'\, \chi^{\circ}(\underline{r},\underline{r}',\omega)\left(V_{\uparrow} - V_{\downarrow}\right) \quad \ldots (4.9)$$

We now introduce the concept of a molecular field which postulates that for paramagnets in general, there exists a molecular field proportional to the intensity of magnetization acquired. So we can regard an effective field h_{eff} as the sum of the external field $h(\underline{r})$ and the internal field, written as an integral over the magnetization multiplied by the exchange interaction :

$$h_{eff}(\underline{r}) = h(\underline{r}) + \int I(\underline{r}-\underline{r}')\, m(\underline{r}')\, d\underline{r}'$$

$$= h(\underline{r}) + \bar{I}\, m(\underline{r}) \quad \ldots (4.10)$$

using the zero-range interaction defined in (4.5B). Take the limit $\omega = 0$ throughout. We can replace the terms $V_{\uparrow} - V_{\downarrow}$ in (4.9) by our $h_{eff}(r)$ in (4.10) to get

$$m(\underline{r}) = \int d\underline{r}'\, \chi^{\circ}(\underline{r},\underline{r}')\left\{h(\underline{r}') + \bar{I}\, m(\underline{r}')\right\}$$

$$\therefore \quad m(\underline{r}) = m^{\circ}(\underline{r}) + \bar{I}\int d\underline{r}'\, \chi^{\circ}(\underline{r},\underline{r}')\, m(\underline{r}')$$

which is the required equation (4.5).

This is the RPA integral equation we wished to derive. Despite the somewhat naive simplicity of the local molecular field method, it has led us to the correct result and so justifies its own use. Recourse to this method avoids many complications resulting from more rigorous methods. Equation (4.5) is the basic equation under scrutinisation in the following chapter which gives the results and discusses the solutions of our three-dimensional model.

FIG (4.1)

ILLUSTRATION OF THE VARIOUS REGIONS OF $A_{\varphi q_z q'_z}$ FOR DIFFERENT φ-VALUES (see Equ.(4.4E

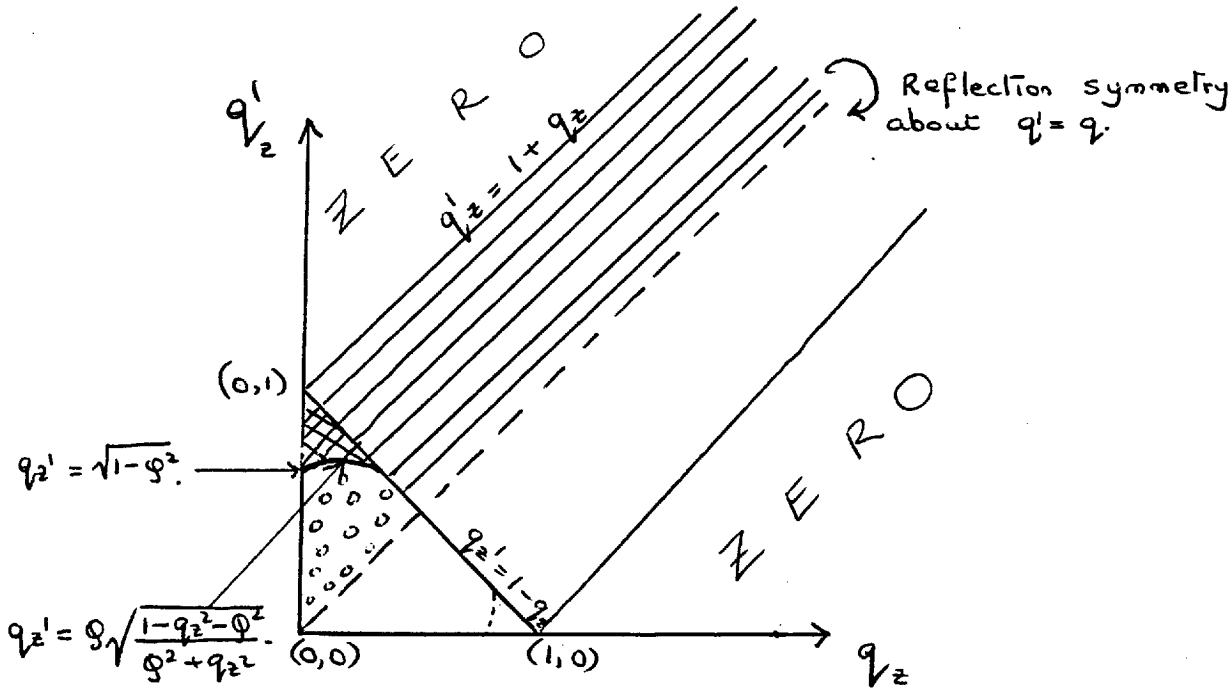

(A) $\varphi \leq 1/2$

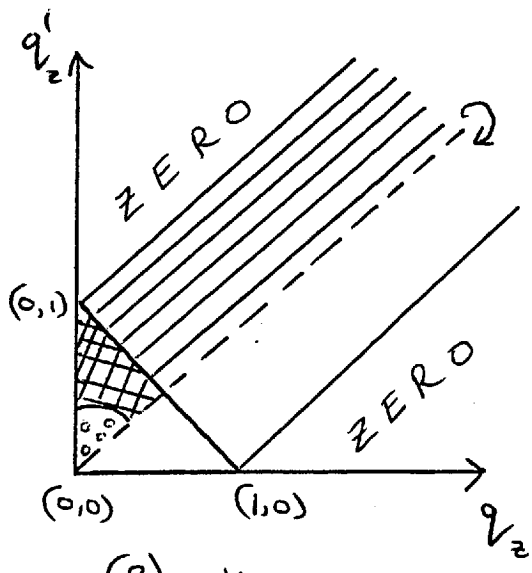

(B) $1/2 \leq \varphi < 1$

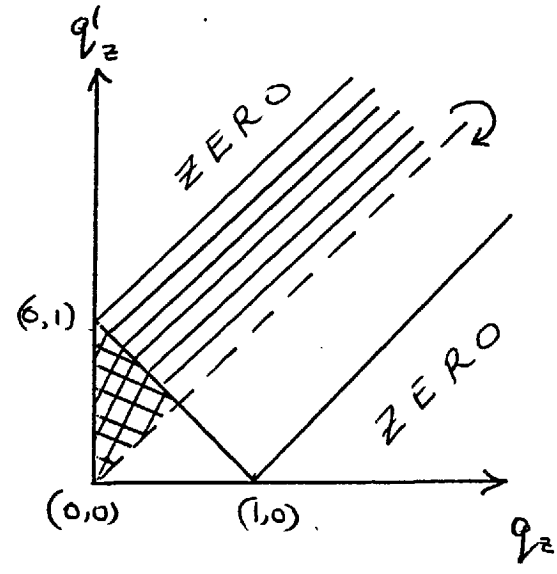

(C) $\varphi > 1$.

FIG (4.2)

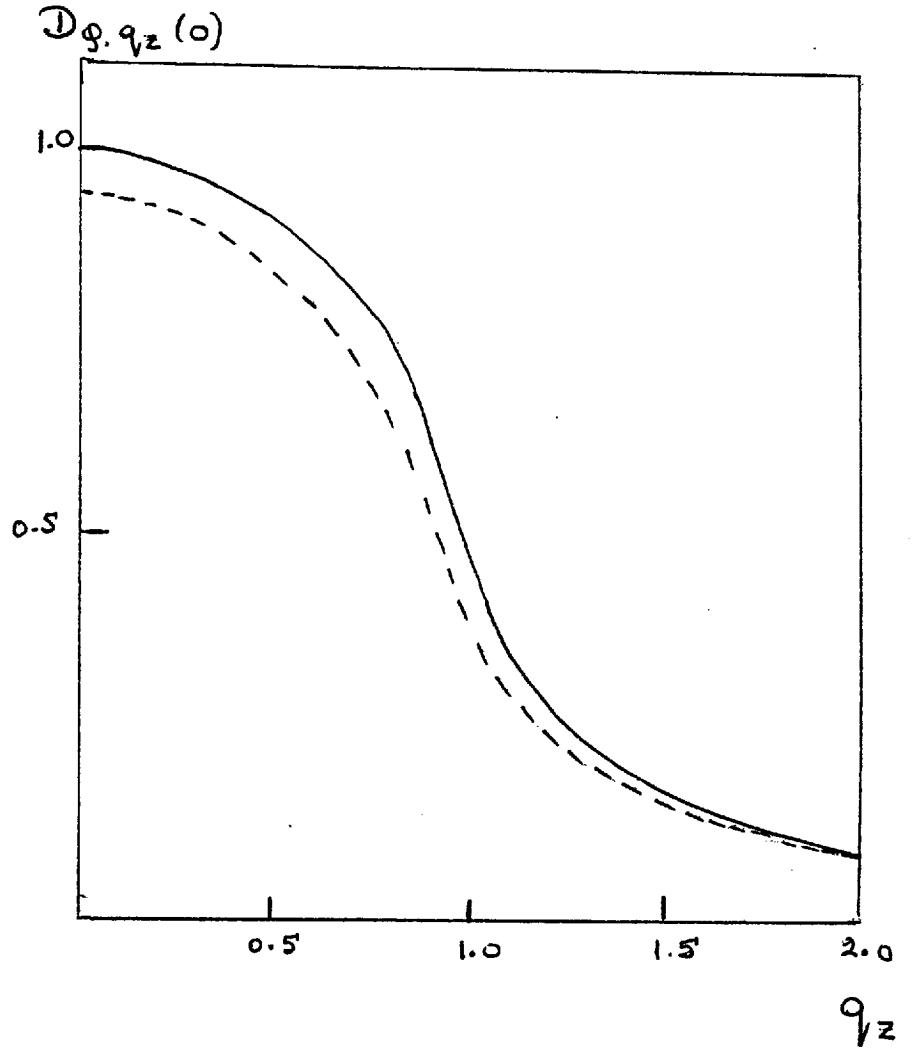

——— $\rho = 0.04$

- - - - $\rho = 0.4$

FIG (4.3).

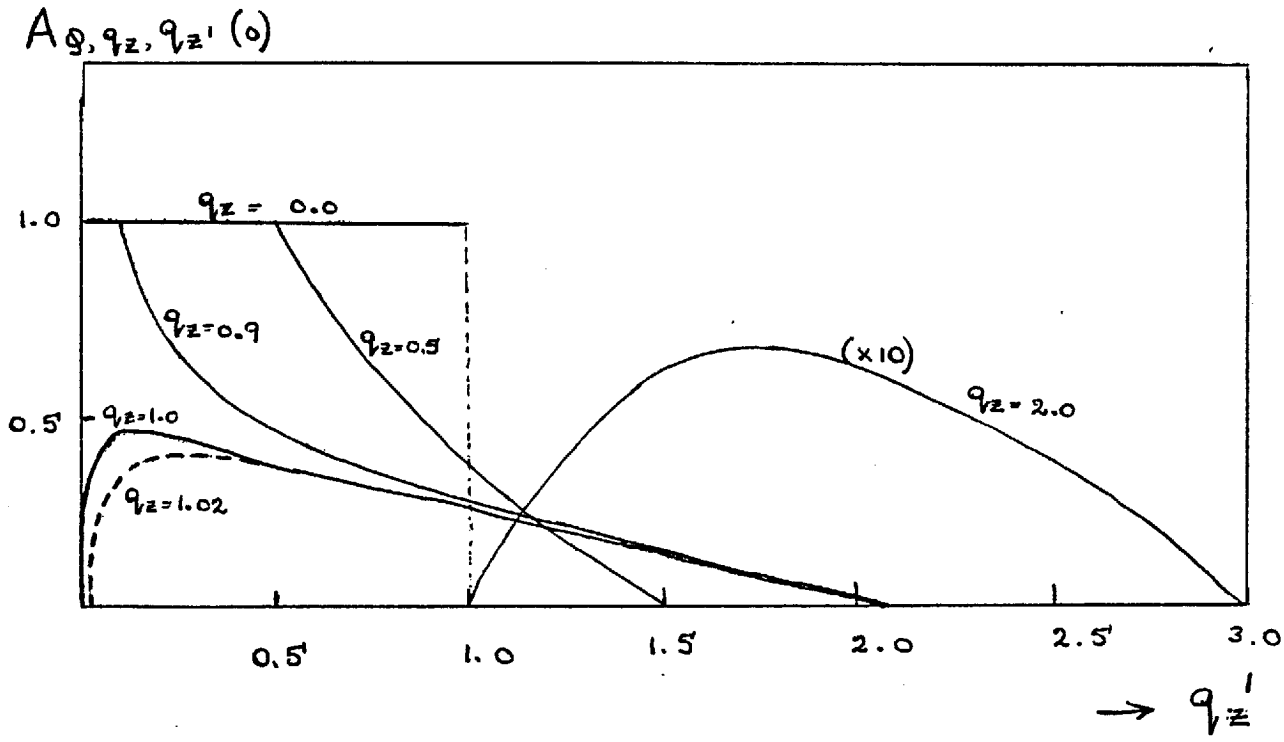

$\rho = 0.1$, q_z varied as indicated.

(FIG 4.4)

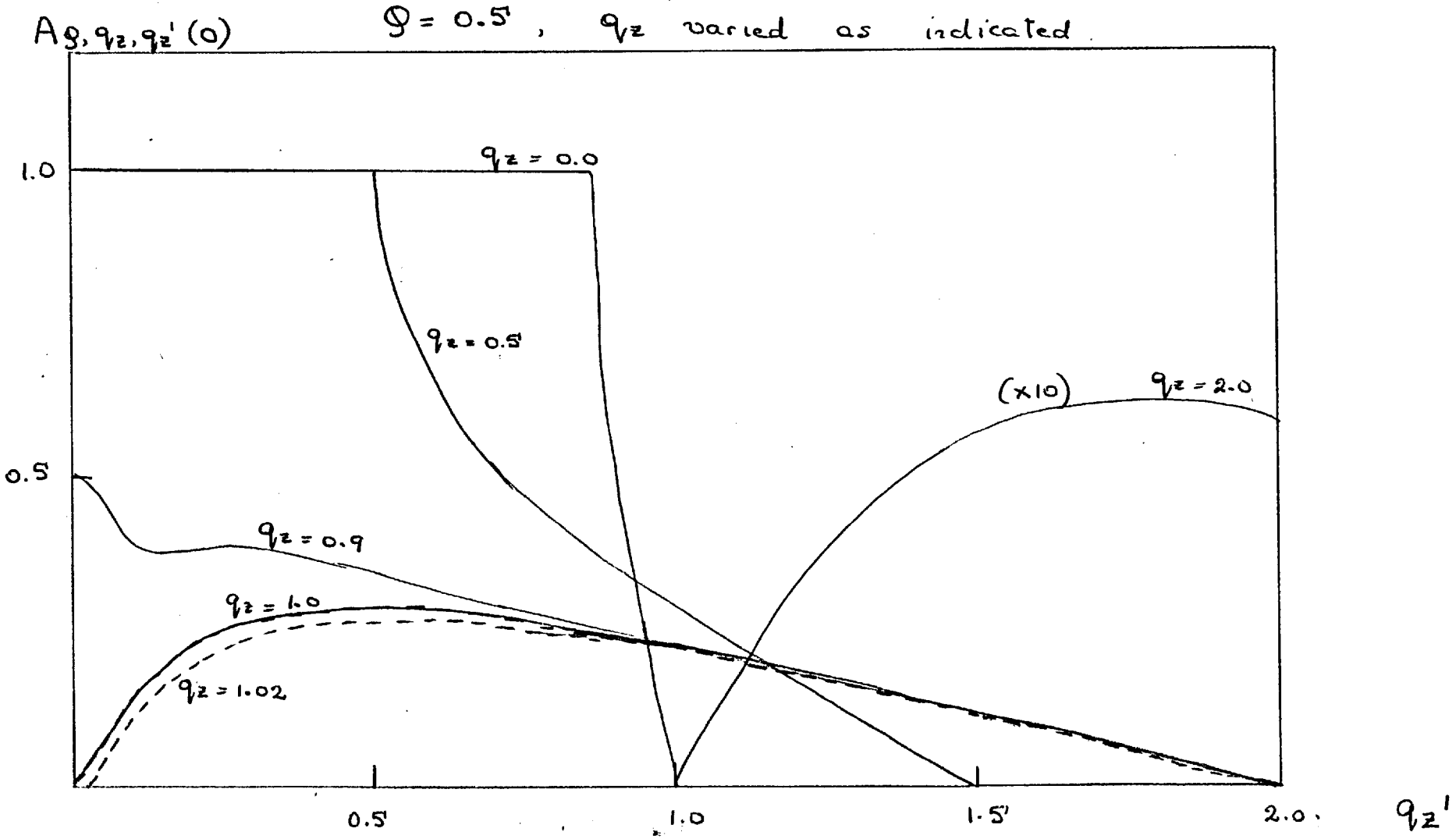
$A_{\rho, q_z, q_z'}(0)$
$\rho = 0.5$, q_z varied as indicated
1.0
0.5
$q_z = 0.0$
$q_z = 0.5$
(x10)
$q_z = 2.0$
$q_z = 0.9$
$q_z = 1.0$
$q_z = 1.02$
0.5
1.0
1.5
2.0
q_z'

FIG (4.5)

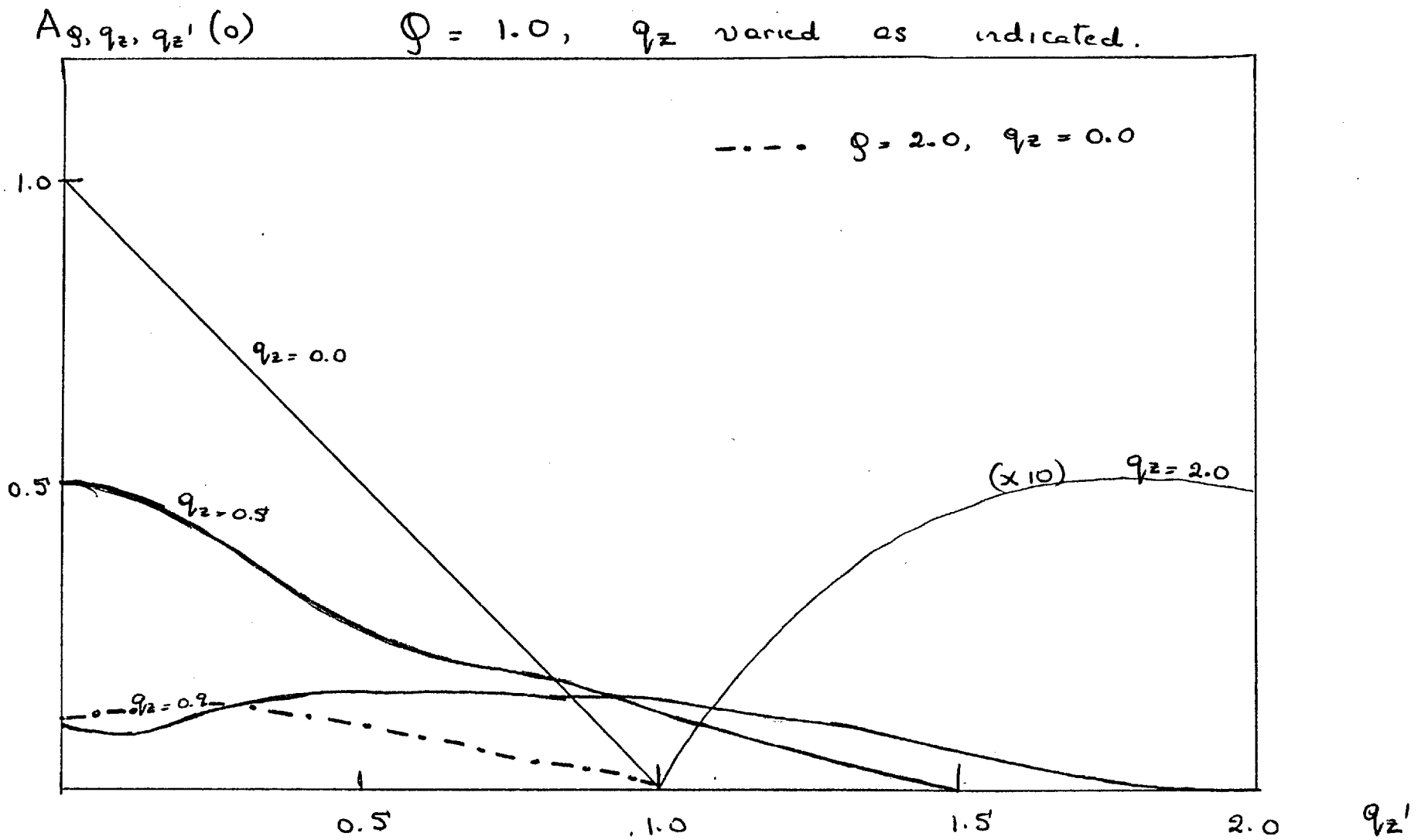
$A_{\rho, q_z, q_z'}(0)$
$\rho = 1.0$, q_z varied as indicated.
$\rho = 2.0$, $q_z = 0.0$
1.0
0.5
$q_z = 0.0$
$q_z = 0.5$
$q_z = 0.9$
(x 10)
$q_z = 2.0$
0.5
1.0
1.5
2.0
q_z'

FIG (4.6)

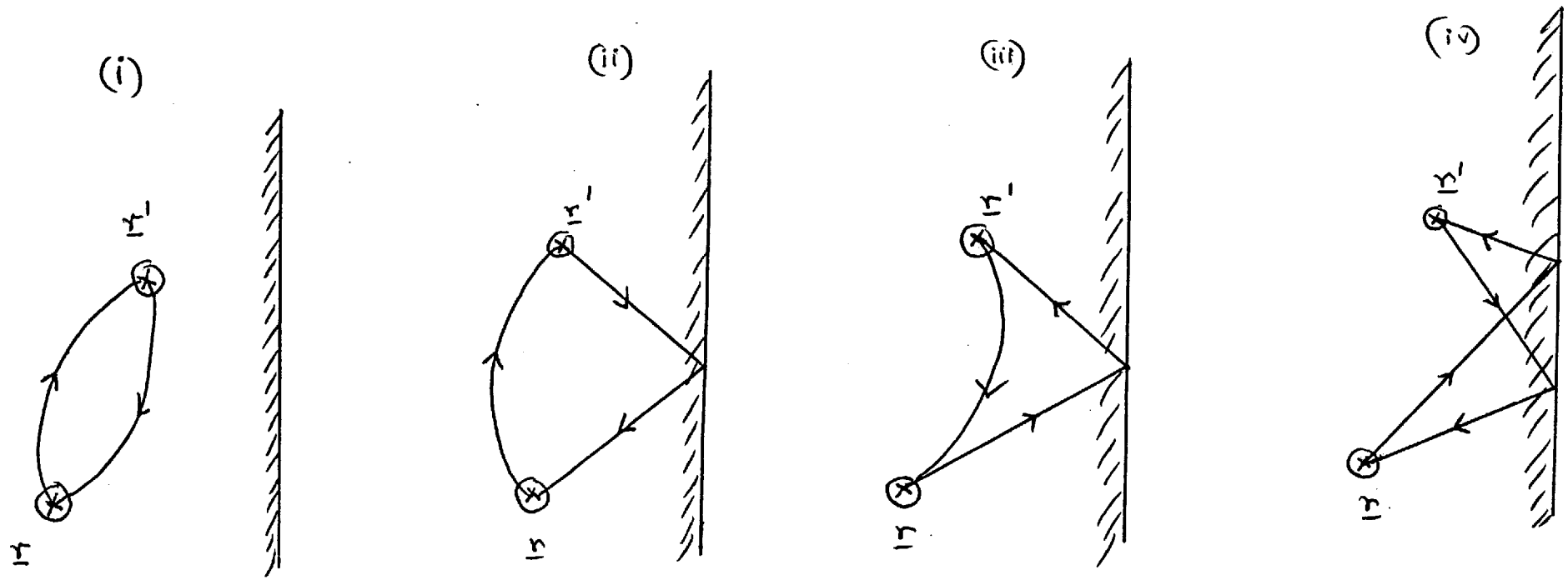

DIRECT PROPAGATION BETWEEN ELECTRON AND HOLE.

DIRECT PROPAGATION OF ELECTRON WHILE HOLE REFLECTS ON SURFACE

DIRECT PROPAGATION OF HOLE WHILE ELECTRON REFLECTS ON SURFACE.

BOTH ELECTRON AND HOLE REFLECT ON SURFACE.

A SCHEMATIC REPRESENTATION SHOWING THE PHYSICAL SIGNIFICANCE OF THE FREE PARTICLE SPIN SUSCEPTIBILITY.

CHAPTER V

SOLUTION OF THE RPA INTEGRAL EQUATION IN THE THREE DIMENSIONAL ISBM

In the previous chapter we have derived an RPA equation for the static surface spin magnetization which obeys the Bethe-Salpeter equation. In this chapter we shall be concerned with the variation of this surface magnetization in three-dimensional real space when there is an applied magnetic field $h(\underline{r})$ due to an atom adsorbed on the surface. We recall equation (4.5A) written in the non-dimensional form :

$$m(\underline{r}) = m^{\circ}(\underline{r}) + \bar{I} \int \chi^{\circ}(\underline{r}, \underline{s})\, m(\underline{s})\, d\underline{s} \quad \ldots (5.1)$$

This is an integral equation of the Fredholm type with a complicated kernel containing oscillatory terms due to the presence of the surface (given in Fourier transform by (4.4)).

Multiply (5.1) by $e^{i\underline{\rho}.\underline{x}} \cos(q_z z)$ and integrate over $\underline{r}$,

$$m(\underline{\rho}, q_z) = m^{\circ}(\underline{\rho}, q_z) + \bar{I} \int d\underline{r} \int d\underline{s}\; e^{i\underline{\rho}.\underline{x}} \cos(q_z z)\, \chi^{\circ}(\underline{r}, \underline{s})\, m(\underline{s})$$

$$= m^{\circ}(\underline{\rho}, q_z) + \bar{I} \int d\underline{s}\; \chi^{\circ}(\underline{\rho}, q_z, \underline{s})\, m(\underline{s}) \quad \ldots (5.2)$$

by interchanging the order of integration. Replace $m(\underline{s})$ by its Fourier cosine transform in (5.2) and use the property of translational invariance. This yields

$$m(\varrho, q_z) = m^\circ(\varrho, q_z) + \bar{I}\int dq_z' \, \chi^\circ(\varrho, q_z, q_z') m(\varrho, q_z') \quad \ldots\ldots (5.3)$$

where the response matrix $\chi^\circ(\varrho, q_z, q_z')$ has been given in terms of the diagonal and non-diagonal elements $D_{\varrho q_z}$ and $A_{\varrho q_z q_z'}$ respectively, for the ISBM in the last chapter- see equation (4.4).

Thus (5.3) is an integral equation for the magnetization in Fourier space with the kernel containing a 'non-uniform' part due to the surface. The only possible 'exact' way i.e. without resorting to any approximations, to solve the equation for the magnetization is by a numerical method which is given in a forthcoming section. We actually wish to convert (5.3) back to real space as follows:

$$m(\underline{r}) = m(\underline{X}, z) = \iiint d^2\varrho \, dq_z \, e^{-i\underline{\varrho}\cdot\underline{X}} \cos(q_z z) \, m(\varrho, q_z)$$

Convert to polar-coordinates and use $d^2\varrho = \varrho d\varrho d\theta$ to obtain

$$m(\underline{X}, z) = \int_0^\infty \int_{-\pi}^{\pi} \int_0^\infty e^{-i\varrho X \cos\theta} \cos(q_z z) \, m(\varrho, q_z) \, \varrho \, d\varrho \, d\theta \, dq_z$$

$$= \int_0^\infty \int_{-\pi}^{\pi} \int_0^\infty \varrho \cos(\varrho X \cos\theta) \cos(q_z z) \, m(\varrho, q_z) \, d\varrho \, d\theta \, dq_z$$

as the imaginary part of the integral is zero.

From Gradshtein and Ryshik's Integral Tables,

$$\int_{-\pi}^{\pi} \cos(\varrho X \cos\theta) \, d\theta = 2\pi J_0(\varrho X)$$

where J_0 is the zeroth order Bessel function. Hence,

$$m(X, z) = 2\pi \int_0^\infty d\varrho \, \varrho J_0(\varrho X) \int_0^\infty dq_z \, m(\varrho, q_z) \cos(q_z z) \quad \ldots\ldots (5.4)$$

The magnetic field h is taken to be of the mathematically convenient Yukawa form :

$$h(\underline{r}) = \frac{\kappa^2}{4\pi} \frac{e^{-\kappa|\underline{r}-\underline{r}_0|}}{|\underline{r}-\underline{r}_0|} \quad \ldots (5.5)$$

where $\underline{r}_0 = (0, 0, z_0)$, for simplicity; as $\kappa \to \infty$ this is of a δ -function form.

It can be shown by converting to polar co-ordinates that the Fourier cosine transform of (5.5) can be reduced to :

$$h(\rho, q_z) = \frac{\kappa^2}{\sqrt{\rho^2+\kappa^2}} \int_0^\infty e^{-\sqrt{\rho^2+\kappa^2}\,|z-z_0|} \cos(q_z z)\, dz$$

$$= \frac{\kappa^2}{\sqrt{\rho^2+\kappa^2}} \int_0^{z_0} e^{-\sqrt{\rho^2+\kappa^2}(z_0-z)} \cos(q_z z)\, dz + \int_{z_0}^\infty e^{-\sqrt{\rho^2+\kappa^2}(z-z_0)} \cos(q_z z)\, dz.$$

$$\therefore \quad h(\rho, q_z) = \kappa^2 \left\{ \frac{2\cos(q_z z_0) - e^{-z_0\sqrt{\rho^2+\kappa^2}}}{\rho^2 + q_z^2 + \kappa^2} \right\} \quad \ldots (5.6)$$

When $z_0 = 0$, this reduces to the well-known form $\dfrac{\kappa^2 e^{-z_0\sqrt{\rho^2+\kappa^2}}}{2(\rho^2+q_z^2+\kappa^2)}$

Surface Phase Transition

The problem here deals with a localised situation near the surface and the aim is to examine the surface phase transition in the three-dimensional situation.

This corresponds to whether or not there exists a solution to the equation :

$$m(Q, q_z) = \bar{I} \int_0^\infty \chi^\circ (Q, q_z, q_z') \, m(Q, q_z') \, dq_z' \quad \ldots (5.7)$$

when $\bar{I}$ equals $\bar{I}_s < 1$.

For the one-dimensional Q = 0 case, (5.7) can be easily solved numerically by using a suitable cut-off and replacing the integral by a summation over q_z'. By using the same number, n, of corresponding values for q_z and taking all the terms over on to one side we can build up a system of nxn simultaneous equations which will have a unique solution provided the determinant formed by the co-efficients of $m(Q, q_z)$ is equal to zero. We do this and find $\bar{I}_s = 0.985$ thus verifying the result by Muscat et al (1975) through this different method. For the three-dimensional case $Q \neq 0$ the situation is more complicated and we resort to another method described in the next section to determine $\bar{I}_s$ (which in principle should be the same, although the type of singularity occurring at the phase transition may differ).

Let us now consider an analytic approach to the problem using an operator and eigenvalue technique. In standard Dirac notation using bras and kets we can rewrite (5.7) as

$$\bar{I} \chi^\circ |m\rangle = |m\rangle \quad \ldots (5.8A)$$

where the kernel χ° is regarded as an operator which can be expanded in terms of a complete set of normalised eigenfunctions $|n\rangle$ with corresponding eigenvalues $\bar{I}_n^{-1}$ belonging to the homogeneous equation (5.8A) i.e.

$$\chi^{o} = \sum_{n}' \frac{|n\rangle\langle n|}{\bar{I}_n} \quad . \quad . \quad . \quad (5.8B)$$

From (4.6) and (5.8B) with some algebraic manipulation we can easily show that

$$\chi = \sum_{n}' \frac{|n\rangle\langle n|}{\bar{I}_n - \bar{I}} \quad . \quad . \quad . \quad (5.8C)$$

and hence

$$|m\rangle = \sum_{n}' \frac{|n\rangle\langle n|h\rangle}{\bar{I}_n - \bar{I}} \quad . \quad . \quad . \quad . \quad (5.8D)$$

which is evident from equation (4.1).

But if h is a magnetic field localised near the surface and $\bar{I}$ is very close to $\bar{I}_s$ we have

$$|m\rangle \simeq \frac{|s\rangle\langle s|h\rangle}{\bar{I}_s - \bar{I}} \quad , \quad \text{as} \quad \bar{I} \to \bar{I}_s$$

For the one-dimensional case, put $m_s(z) = \langle s|z\rangle$ and we obtain

$$m(z) = \frac{m_s(z)}{\bar{I}_s - \bar{I}} \int m_s(z)\, h(z)\, dz \quad . \quad . \quad . \quad . \quad (5.9)$$

as in Muscat et al (1975). We make use of equation (5.9) as a check on our numerical calculations in three dimensions as $Q \to 0$.

Numerical Procedure

The method of attack used is to transform the integral equation given by (5.3) to a matrix equation, thus :

$$\sum_{q'} \left[\left(1 - \bar{I} D_{qq'}\right) \delta_{qq'} + \bar{I} A_{qqq'} \right] m(q,q') = m^{\circ}(q,q) \quad \ldots (5.10)$$

where for convenience we write q, q′ instead of q_z, q'_z, and sum q′ from 1 to n, say. Now take a further step and let q run over these same values from 1 to n. A suitable cut-off used for the upper limit of the integral in (5.3) was $q'_{max} = 3.0$, which corresponds to a value of $6p_F$, where

$$q'_{max} = \frac{(2n+1)\pi}{l} \quad \ldots (5.11)$$

if we regard the process of summation over a film of length l.

Equation (5.10) may be written in matrix notation as

$$BM = M^{\circ} \quad \ldots (5.12A)$$

where $B = (b_{ij})$ for i, j = 1,.... n,

M, M° are column vectors of size n,

$$\left.\begin{aligned} \text{and } b_{ij} &= \bar{I} A_{qqq'} \qquad i \neq j \\ b_{ii} &= (1 - \bar{I} D_{qq}) + \bar{I} A_{qqq} \end{aligned}\right\} \quad \ldots (5.12B)$$

Hence $M = B^{-1} M^{\circ}$

and the solution of the integral equation (5.3) reduces to the evaluation of the inverse of the matrix B.

Writing the matrix equation (5.12A) in full to see the structure more clearly, we have

$$\begin{bmatrix} 1-\bar{I}D_1+\bar{I}A_{11} & \bar{I}A_{12} & \cdots & \bar{I}A_{1n} \\ \bar{I}A_{21} & 1-\bar{I}D_2+\bar{I}A_{22} & \cdots & \bar{I}A_{2n} \\ \vdots & & \ddots & \vdots \\ \bar{I}A_{n1} & \bar{I}A_{n2} & \cdots & 1-\bar{I}D_n+\bar{I}A_{nn} \end{bmatrix} \begin{bmatrix} m_1 \\ m_2 \\ \vdots \\ m_n \end{bmatrix} = \begin{bmatrix} m_1^\circ \\ m_2^\circ \\ \vdots \\ m_n^\circ \end{bmatrix} \quad \ldots \quad (5.12c)$$

Instead of taking the bulk Lindhard's logarithmic function for D_{qq}, we use the discrete sum

$$D_{qq} = \sum_{q'} A_{qqq'}$$

cutting off at $q' = 3.0$ and of course multiplying by the step length in q' considered for computer calculations.

The following three checks were made to ensure our programme was working correctly:

(1) Initially we took $\bar{I} \to 0$ and found m in close agreement with the computed non-interacting magnetization m°.

(2) We use the Muscat et al (1975) version for the magnetic field viz. $h(z) = \sin z/z$ and examine the magnetization as a function of z for $Q = 0.0001$ and $\bar{I} = 0.95$, 0.98 and 0.983. The graphs are displayed in Fig(5.0A) and are in very good agreement with their $Q = 0$ results.

However we notice that the magnetization should actually be negative for this choice of the magnetic field, a fact unnoticed in their paper, but can be verified analytically if we consider the variational function for the magnetization, given by

$$m_v(z) = e^{-\beta z} - \frac{\sin z}{z} \quad \ldots \quad (5.13A)$$

where β is a constant (usually small).

Substitute (5.13A) for $m_s(z)$ in (5.9) yields

$$(\bar{I}_s - \bar{I})m(z) = -\left(e^{-\beta z} - \frac{\sin z}{z}\right)\left(\tan^{-1}\beta + \frac{\pi}{2}\right) \quad \ldots \quad (5.13B)$$

Since $\bar{I}_s > \bar{I}$, the above equation clearly shows the negative behaviour of the magnetization for a localised field of the form sinz/z.

(3) Thus encouraged by our previous two checks, we returned to our Yukawa form for h given by (5.5) and computed the magnetization curves for Q = 0.0001, $\bar{I}$ = 0.95, 0.98, 0.983 ; χ = 1.0, z = 0.0. These graphs are given in Fig. (5.0B). The behaviour of the curves are similar to those discussed above with the highest peaks occurring at z = 4.5. The ratios of the peak heights are tabulated in Table (5.1) and compared with the corresponding ones obtained from Fig. (5.0A). These are in good agreement showing that the ratio of the enhancement being independant of the type of magnetic field applied.

In Fig. (5.0C) and (5.0D) we plot the inverse of the magnetization peaks obtained in checks (2) and (3) at $z = 4.5$ as a function of $\bar{I}$ and note the linear behaviour. Extending the lines to cut the $\bar{I}$-axis gives an intercept $\bar{I}_s$ in both cases such that $0.985 < \bar{I}_s < 0.986$. This is the point of divergence of the magnetization in good agreement with results by Zaremba (Thesis 1974) and Muscat et al (1975) who obtained a value of 0.985 for $\bar{I}_s$ in the case $Q = 0$. Our slightly higher value is due to the finiteness of Q.

Now the aim is to proceed ahead with calculations for the magnetization for further finite Q-values upto an appropriate range, sum over these values and finally examine the variation of the magnetization in three-dimensional space.

Results For Our Model in Three Dimensions.

The resultant graphs computed for the local magnetization as a function of z are given in Figs. (5.1A, 5.2A, 5.3 and 5.4) for the following values of X, $\varkappa$, z :

Fig. (5.1A) : $X = 0.0$, $\varkappa = 1.0$, $z = 0.0$.

Fig. (5.2A) : $X = 0.1$, $\varkappa = 1.0$, $z = 3.0$.

Fig. (5.3) : $X = 5.0$, $\varkappa = 1.0$, $z = 1.0$.

Fig. (5.4) : $X = 5.0$, $\varkappa = 0.5$, $z = 1.0$.

In each figure the four curves displayed correspond to the values of $\bar{I}$ between 0.95 and 0.988. For values of $\bar{I} < 0.985$ we obtained excellent convergence to within 1% by inverting a 20 x 20 B-matrix (see equation 5.12c) and performing a summation over 10 Q - steps. A maximum upper limit of 3.0 for q and 1.0 for Q (corresponding to 6_{pF}, 2_{pF} respectively) were found to be sufficient since negligible contributions arose by increasing these values. However for $\bar{I} \geqslant 0.985$, most steps are required to obtain good convergence viz. 80q x 10Q was applied.

The value X = 0.0 was chosen to examine the variation of the magnetization in the plane through the point $(0,0,z_0)$ about which the magnetic field is localised, and it is expected that in this plane lies the highest intensity of the variation. We note the constant uniformity of shape of the magnetization curves, with the highest peaks occurring at z = 4.5, the second smaller peak occurring at z = 10.5 and the third even smaller peak at z = 17.5, in agreement with the work by Beal - Monod et al (1972), Zaremba (thesis 1974) and Muscat et al (1975). The largest effect of the magnetization is therefore felt nearest to the surface, with oscillations gradually diminishing in height and tending towards zero further away from the boundary. This oscillatory behaviour is essentially due to the inclusion in our calculations of the surface correction terms $A_{qq'}$ defined in (4.4E) i.e.

due to use of the ISBM as opposed to the previous SCISBM which neglected these terms and dealt with the bulk term D_{qq} alone. Recall the behaviour of the electron-density profiles plotted in Fig.(2.1) for both the models (but note that $z < 0$ is taken to be the metal region there, as opposed to $z > 0$ which we are now considering). This same argument is reflected there, with the maximum peak in the Friedel oscillations occurring nearest to the plane $z = 0$ in the ISBM.

Fig. (5.1A, 5.2A, 5.3) show the effect of varying z_0 upon the magnitude of the oscillations. This is significant e.g. the difference in the heights of the curves for $z_0 = 0.0$, 3.0 is by a factor of about ten.

Fig. (5.3, 5.4) reflect the effect of the range $\eta = 1/\kappa$ which appears in magnetic field. Increasing the range from $\eta = 1.0$ to $\eta = 2.0$ gives an increase in magnitude of the curves for different values of $\bar{I}$.

We examine the lateral behaviour of the magnetization in Figs. (5.1B, 5.2B) by fixing a value of z (equals 4.5) and plotting $m(X) \sim X$. Due to transitional invariance assumed throughout in the problem, this varies as a function of mod$\underline{X}$ i.e. the points on the graph represent values of the magnetization on concentric circles, centre (0,0,z) and radius X. As expected, the graphs show a smooth fall-off of the magnetization with increasing X. It indicates the long range behaviour as $\bar{I}$ increases

in value upto 0.988. However for smaller values of $\bar{I}$ (= 0.0, 0.5) indicated by the dashed curves show the short-range behaviour for these values.

The next step is to examine at what value of $\bar{I}$ a surface phase transition occurs and as in the one-dimensional treatment (see equation (5.9)) we plot the inverse of the magnetization height at $z = 4.5$ as a function of $\bar{I}$ in Figs. (5.1C), (5.2C). In contrast to the one-dimensional cases (Figs. 5.0C, 5.0D), these curves are now non-linear and extrapolate to zero for a value $\bar{I}_s \simeq 0.989$. Although only two graphs showing this $\bar{I}_s$ are displayed at the end of this chapter, further calculations were carried out to consistently give this same value for $\bar{I}_s$. Our numerical calculations confirmed this conclusion as they were non-convergent for $\bar{I} \geqslant 0.99$. Thus we conclude that for $\bar{I}_s$=0.989 the surface region has a distinct tendency of becoming ferromagnetic. The discrepancy between the values obtained for $\bar{I}_s$ in the cases Q=0 and Q≠0 is most likely to be numerical.

It is only at $z = 0$, where the magnetization vanishes for all values of $\bar{I}$, where no enhancement is felt. This is consistent with the theory : multiply each side of (5.3) by cos(qz) and integrate over dq,

$$m(\rho, z) = m^{o}(\rho, z) + \bar{I}\int dq \int dq' \left(D_{\rho q}\delta_{qq'} - A_{\rho qq'}\right) m(\rho, q') \times \cos(qz)$$

Interchanging the order of the integrals and putting z =0,

$$m(q,0) = m^{\circ}(q,0) + \bar{I}\int dq' \left\{ D_{qq} - \int dq\, A_{qqq'} \right\} \times m(q,q')$$

$$\Rightarrow \quad m(q,0) = m^{\circ}(q,0)$$

since $\{\ \} = 0$ from the sum rule given by (4.4B).

We conclude this chapter with a comment and calculation of the binding energy ΔE for an adatom pertinent to our system.

THE BINDING ENERGY

Schiach (1976) has examined the second order contribution to the binding energy of an ad-spin i.e. he calculates to the lowest non-vanishing order the energy change in the system due to the extra coupling from a fixed local spin $\underline{S}$ at $\underline{R}$. In his model he considers a finite range electron-electron interaction of the Yukawa type (similar to Zaremba and Griffin, 1973, 1975) to avoid the possibility of a surface phase transition and a similar type of exchange interaction $V(\underline{R}-\underline{r})$ with $\underline{S}$, with the same range parameter (for simplicity), but a different strength of interaction. The extra binding energy E is given by

$$\Delta E \propto \int d\underline{r} \int d\underline{r}'\, V(\underline{R}-\underline{r})\, \chi(\underline{r},\underline{r}')\, V(\underline{r}-\underline{R}) \qquad \ldots (5.14)$$

where the constant of proportionality is of the form $-\frac{1}{2}\alpha^2 S(S+1)$ where α is the ratio of the strengths of the two exchange-interactions. In his calculations he uses two approximations :

(1) by ignoring the $A_{\rho}qq'$ terms in χ^{o} and approximating $D_{\rho}q$. This is identical to the approximation used by Zaremba and Griffin, 1975, and physically corresponds to treating the surface scattering as specular and classical.

(2) by including the effects of $A_{\rho}qq'$ through a separable symmetric approximation.

His results for ΔE, normalized with respect to its bulk value, are plotted in Fig. (5.5A) for $\bar{I}$ = 0.9, 0.99. The dashed curves are due to approximation (1) while the solid lines come from use of approximation (2).

This is the quantity we wish to calculate in our model, avoiding any approximation and using the exact expression for χ^{o}. For simplicity let us assume that our extra coupling due to an adatom at $\underline{r}_o = (0,0,z_o)$ and the substrate metal electrons comes from a finite range exchange interaction of the form

$$V(\underline{r} - \underline{r}_o) = \frac{\chi^2}{4\pi} \frac{e^{-\kappa|\underline{r}-\underline{r}_o|}}{|\underline{r}-\underline{r}_o|} \quad . \quad . \quad . \quad (5.15)$$

i.e. same as the magnetic field $h(\underline{r})$ given by equation

(5.5). Translating this into equation (5.14) and absorbing all constants into $h(\underline{r})$ we have

$$\Delta E(x, z_0) = \int d\underline{r}\; m(\underline{r})\, h(\underline{r}) \quad \ldots (5.16A)$$

i.e. ΔE is a function of x, z_0 alone.

Now Parseval's theorem states that if $f(x)$, $g(x)$ are two functions with corresponding Fourier Transforms $F(q)$, $G(q)$ then

$$\int F(q)\, G(-q)\, dq = \int f(x)\, g(x)\, dx$$

Using this theorem in three dimensions with the fact that $h(q) = h(-q)$ (see 5.6), we get

$$\Delta E(x, z_0) = 2\pi \int \rho\; m(\rho, q_z)\, h(\rho, q_z)\, d\rho\, dq_z \quad \ldots (5.16B)$$

For calculation purposes, we choose $x = 1.0$ and compute ΔE as a function of z_0. The graphs are plotted in Fig. (5.5B) for $\bar{I} = 0.0$, 0.5, 0.95, 0.98, 0.983

After an initial rise at $z = 4.5$, the oscillatory behaviour smooths out relatively quickly compared with the magnetization profiles, approaching steady constant values for different $\bar{I}$ values as we go deeper into the

bulk. The behaviour is reminiscent of the electron density profile for the ISBM in Fig. (2.1).

As expected, our $\Delta E \sim z_o$ curves using the exact expression for χ^o differs with respect to Schiach's approximate versions. In contrast ours is oscillatory in character, but similarly it tends to a constant levelling-off value far away from the surface. At the boundary our curves go exactly to zero (as expected from the form of our magnetization curves using the exact expression for χ^o) whereas his ΔE extends slightly into the negative region for z_o - outside the surface.

From the form of our ΔE function (equation 5.16A) a plot of $\Delta E \sim \log(\bar{I}_s - \bar{I})$ for a fixed value of z_o seems suggestive of a linear behaviour (Newns & Edwards, 1977). Taking $\bar{I}_s = 0.989$, this was done for $z_o = 4.5$ corresponding to the maximum peak in ΔE. The results are illustrated in Fig. 5.5C and show an excellent tendency towards a straight line. Further checks were made by varying z_o and confirming this conclusion. This is an encouraging result although it might be unwise at this stage to read too much meaning into it.

A word should be said at this stage on the experimental situation. Experiments have been performed with the high density fluid of liquid helium^3 and the evidence does suggest that it behaves as an itinerant ferromagnet near the surface (Ahonen et al, 1976). They examine the low temperature magnetic susceptibility of normal and superfluid helium^3 bounded in a narrow slab geometry and obtain a field dependant enhancement of the pure helium^3 magnetic susceptibility over the bulk Fermi liquid value. The excess susceptibility follows a Curie-Weiss law which is consistent with the assumptions that there exists a quasi-two-dimensional sheet of itinerant ferromagnetic high density liquid helium between the first few layers of solid helium^3 and the bulk paramagnetic liquid, as pointed out by Beal-Monod and Doniach, 1977. However further future experiments with nearly ferromagnetic materials in confined geometries would be welcome.

In conclusion, let us recall that our free electron model with an infinite square surface barrier is a highly idealised one, which would in effect be unrealistic in describing properties of strongly paramagnetic transition metals such as palladium and platinum. However, even our simple model cannot be discarded as it does contain interesting information on phenomena like magnetic phase transitions at surfaces which have been predicted by a more appropriate tight-binding model (Weiner, 1973).

Simple as the model is, the formula for the magnetization involving $\chi^{0}(\phi, q_z, q_z')$ given by equation (4.4) is far from easy to deal with. Thus there seems to be little hope that one can solve the integral equation for the magnetization for a realistic model without an extensive programme of numerical studies.

Our calculations have involved use of the RPA and based on the molecular field approximation. But the bounded surface problem presents a dimensionality d somewhere between $2 < d < 3$ and therefore imposes the questionability of such an approximation in handling surface problems in a meaningful way. The RPA is valid for low momentum transfers (Pines, 1964), but in our surface problem where high momentum transfers become appreciable one should perhaps go over and beyond the RPA to calculate the system properties.

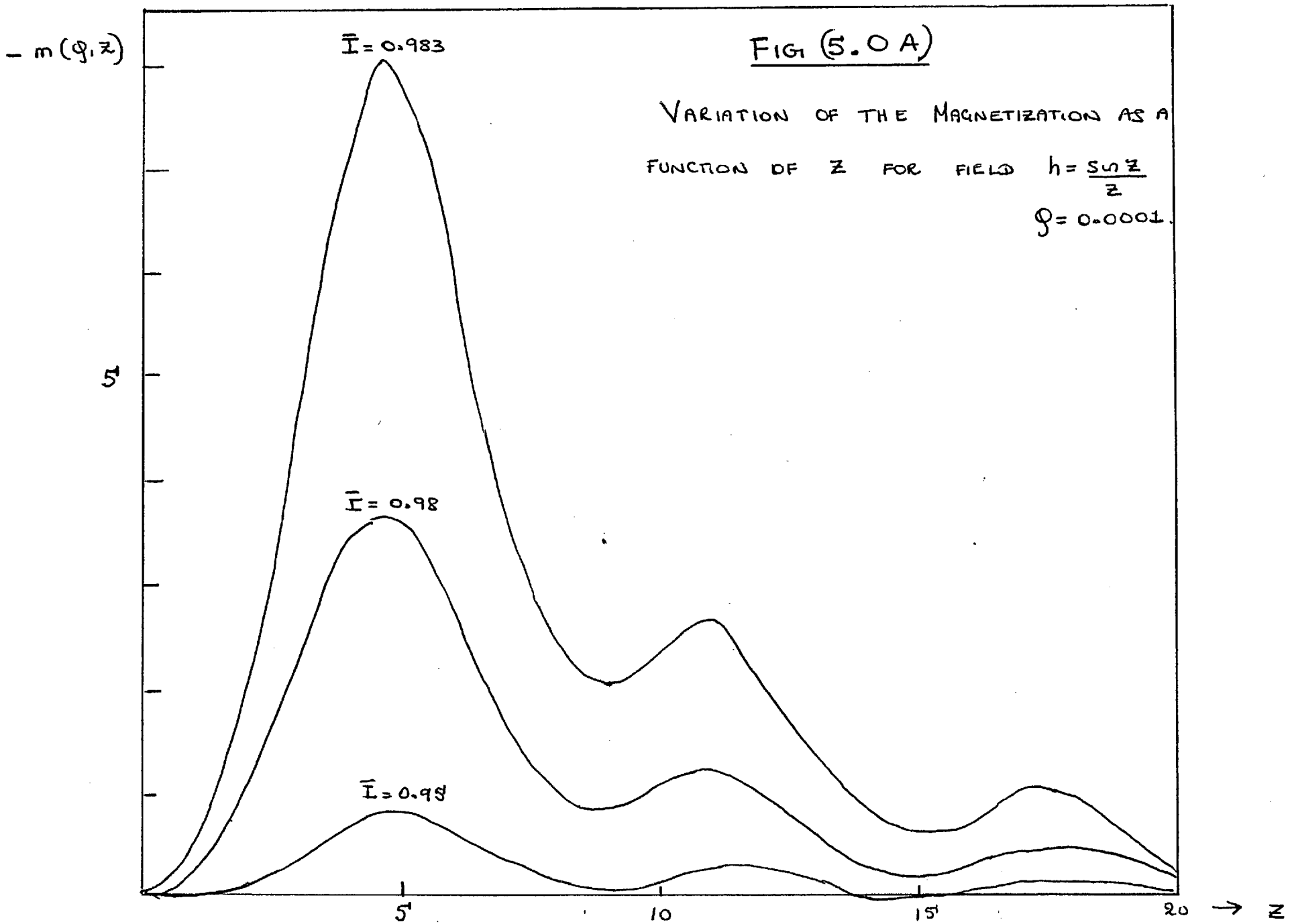

FIG (5.0 A)

VARIATION OF THE MAGNETIZATION AS A FUNCTION OF Z FOR FIELD $h = \frac{\sin z}{z}$

$\rho = 0.0001$.

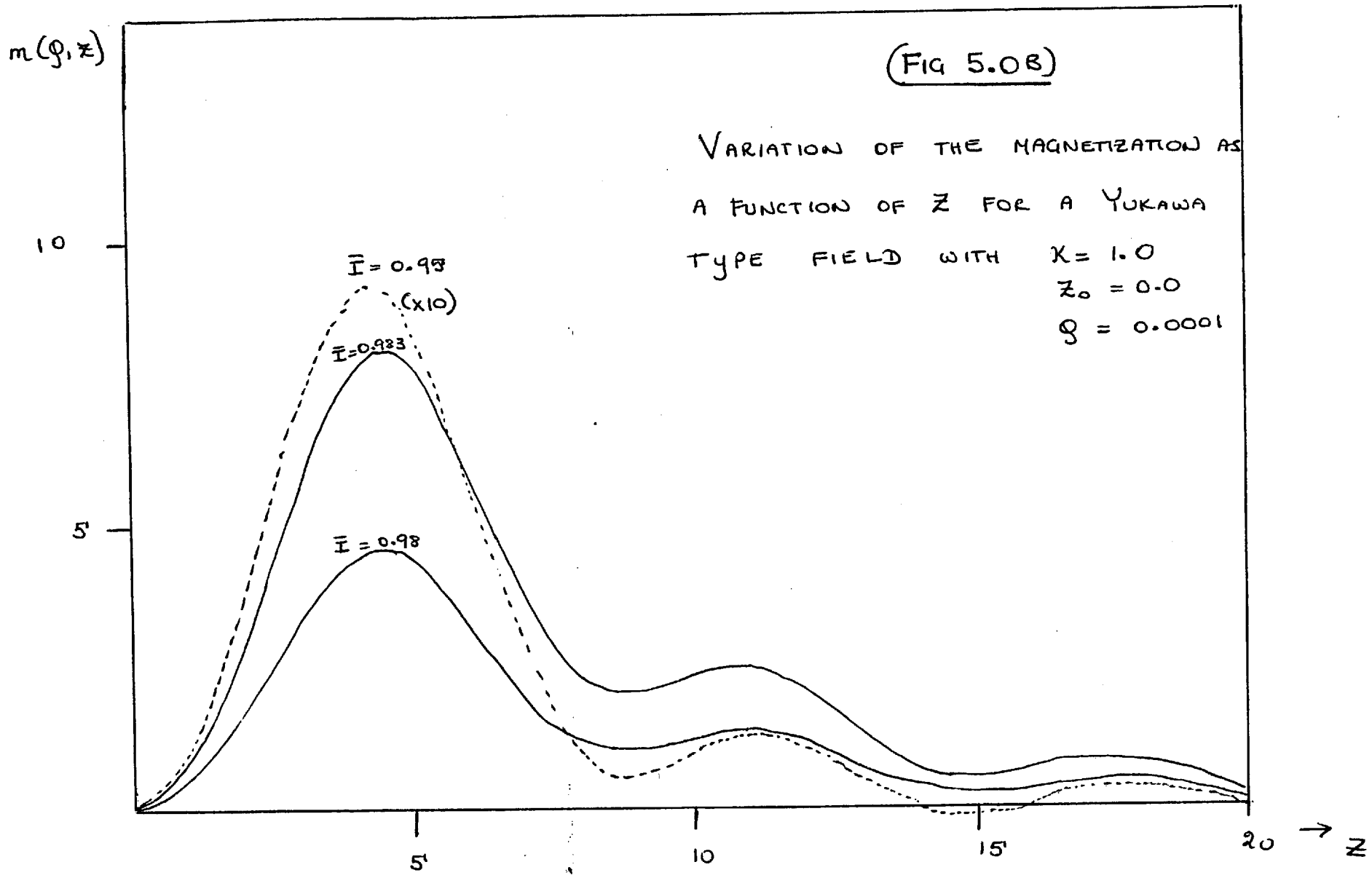

(FIG 5.0B)

VARIATION OF THE MAGNETIZATION AS A FUNCTION OF Z FOR A YUKAWA TYPE FIELD WITH $K = 1.0$, $z_0 = 0.0$, $\rho = 0.0001$

FIG (5.0C)

A PLOT OF THE HEIGHT OF THE INVERSE MAGNETIZATION AT $Z = 4.5'$ AS A FUNCTION OF $\bar{I}$ FOR FIELD $\frac{\sin Z}{Z}$ ($\rho = 0.0001$)

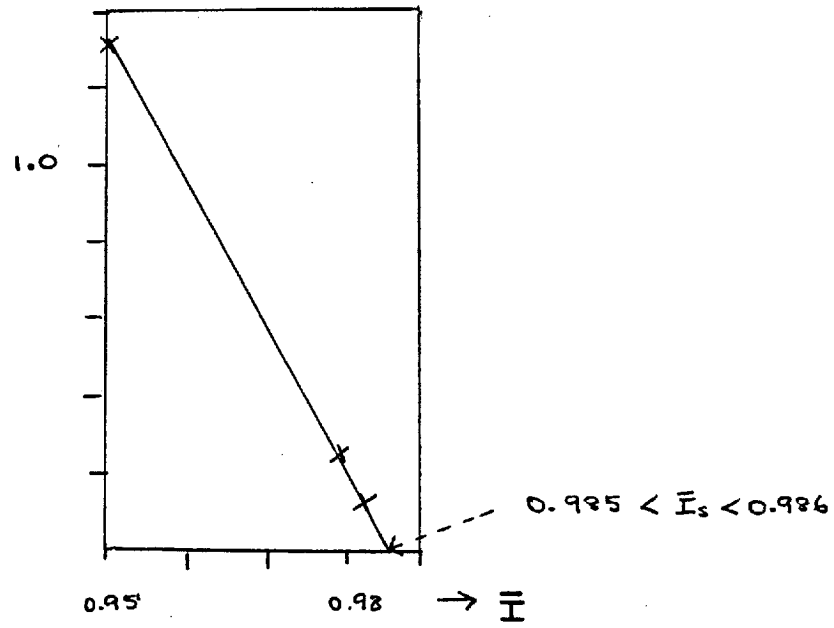

FIG (5.0D)

A PLOT OF THE HEIGHT OF THE INVERSE MAGNETIZATION AT $Z = 4.5'$ AS A FUNCTION OF $\bar{I}$ FOR A YUKAWA MAGNETIC FIELD; $K = 1.0$
$Z_0 = 0.0$
$\rho = 0.0001$

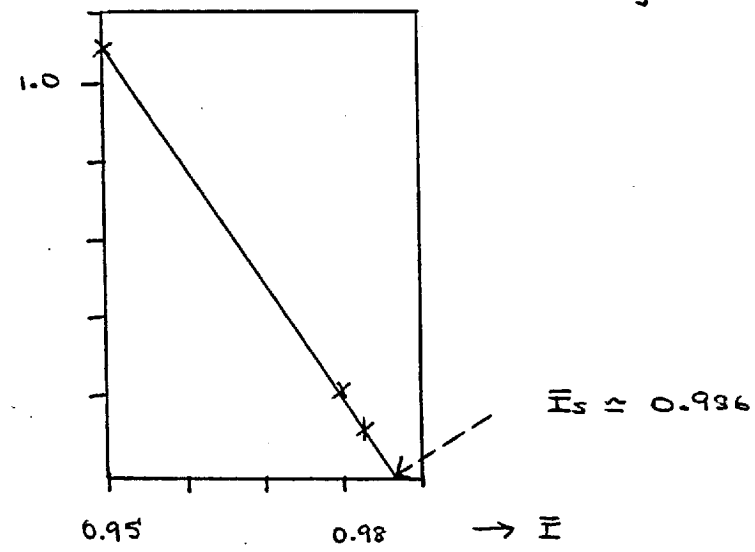

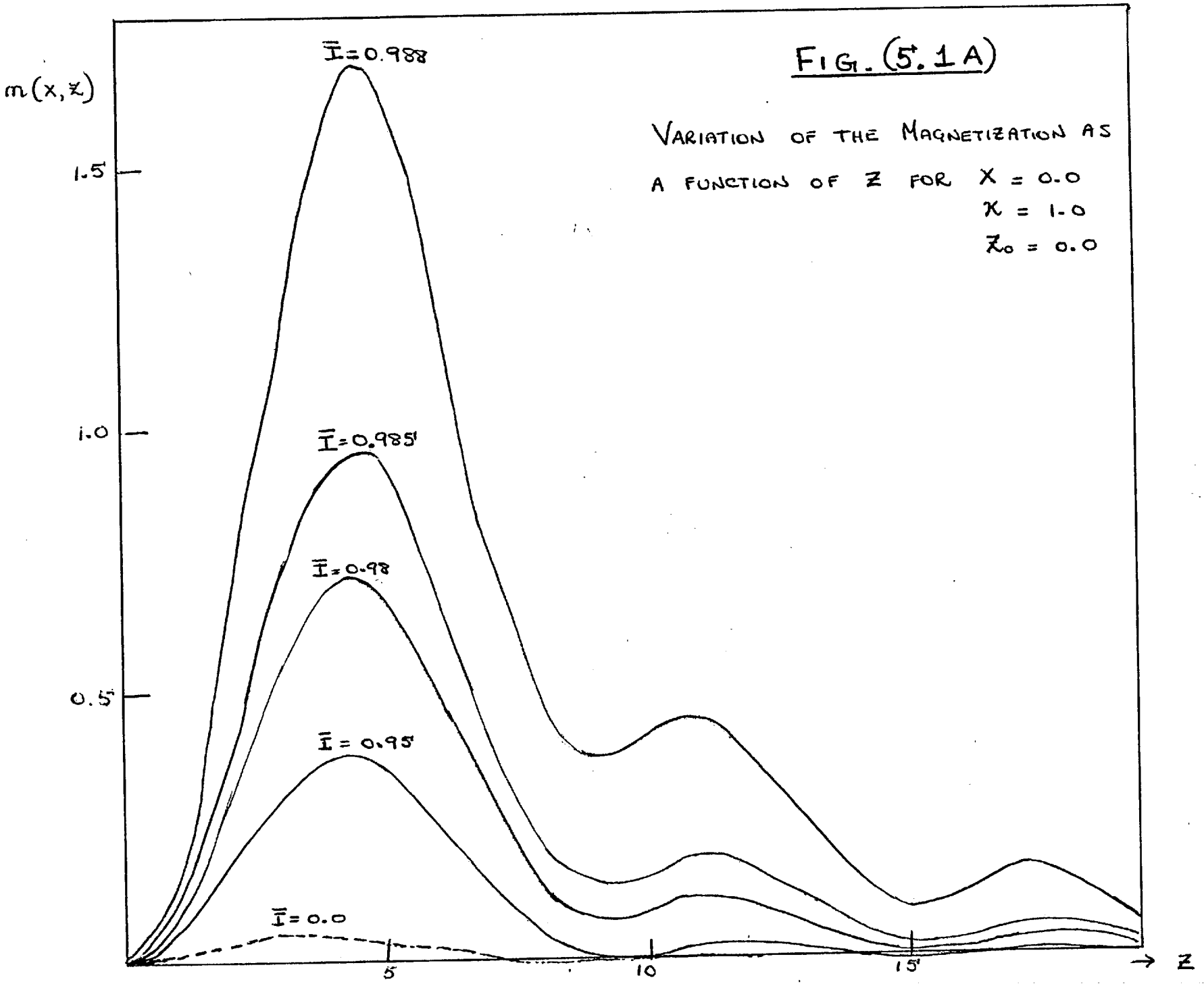

FIG. (5.1A)

VARIATION OF THE MAGNETIZATION AS A FUNCTION OF Z FOR $X = 0.0$, $\mathcal{K} = 1.0$, $Z_0 = 0.0$

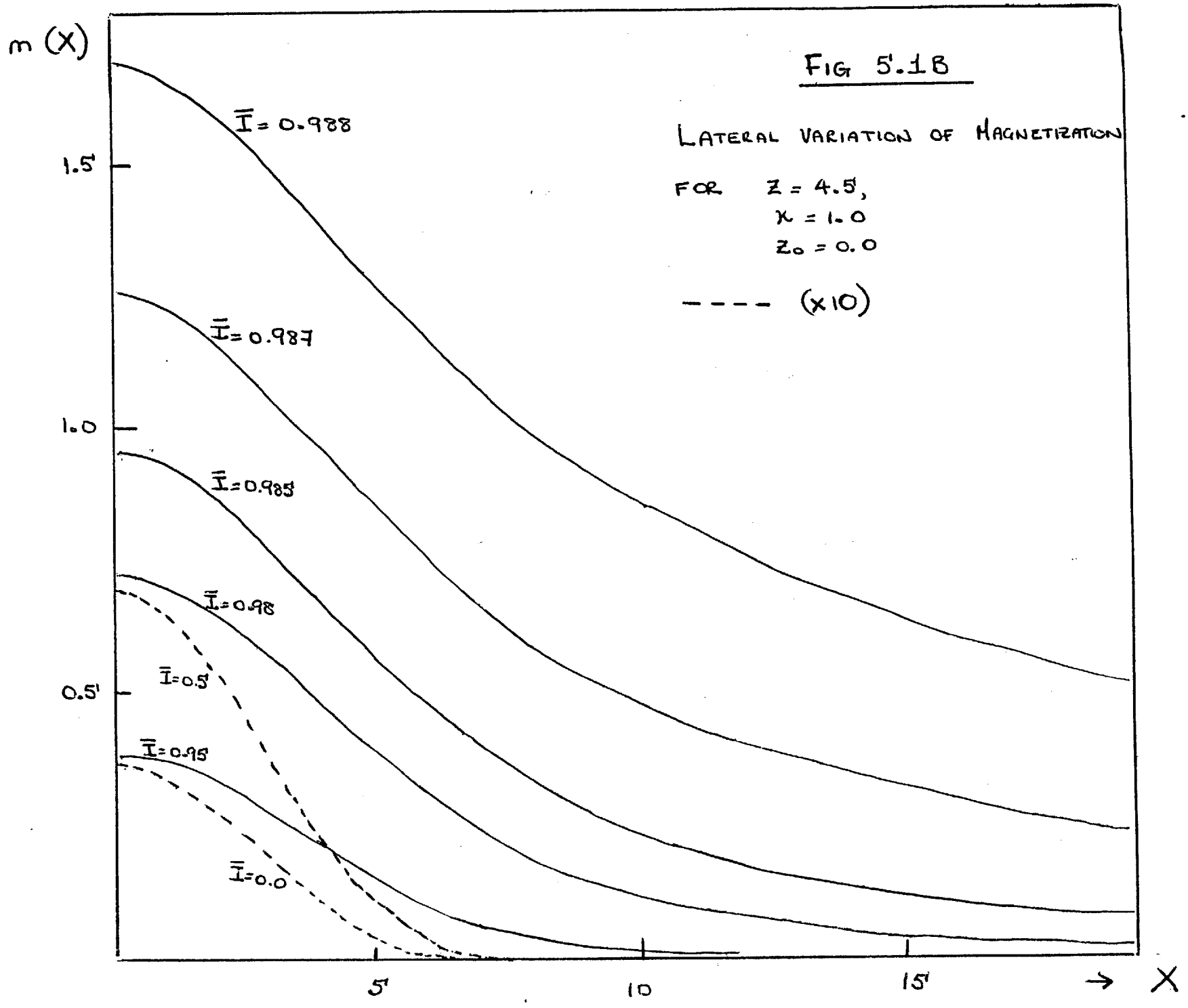
m (X)
1.5
1.0
0.5
5
10
15
→ X
$\bar{I}$ = 0.988
$\bar{I}$ = 0.987
$\bar{I}$ = 0.985
$\bar{I}$ = 0.98
$\bar{I}$ = 0.5
$\bar{I}$ = 0.95
$\bar{I}$ = 0.0
FIG 5.1B
LATERAL VARIATION OF MAGNETIZATION
FOR Z = 4.5,
x = 1.0
Z_0 = 0.0
---- (x10)

FIG (5.1C)

A PLOT OF THE HEIGHT OF THE INVERSE MAGNETIZATION AT $Z = 4.5$ AS A FUNCTION OF $\bar{I}$ FOR A YUKAWA MAGNETIC FIELD: $X = 0.0$, $K = 1.0$, $Z_0 = 0.0$.

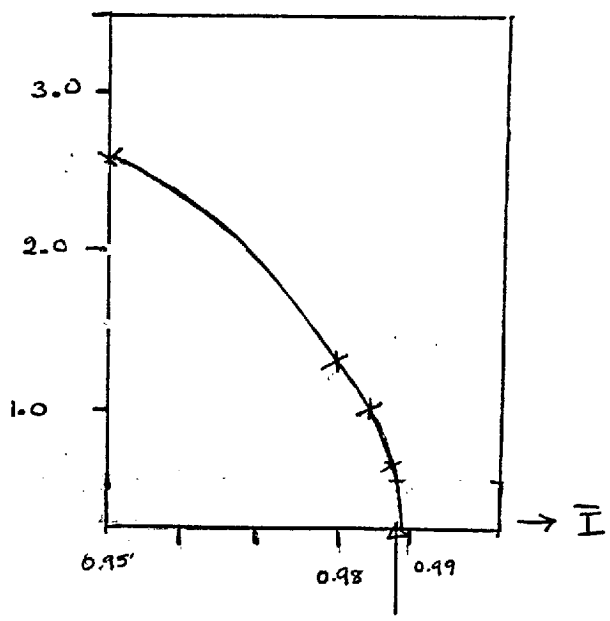

Intercept at $\bar{I} = \bar{I}_s \simeq 0.989$.

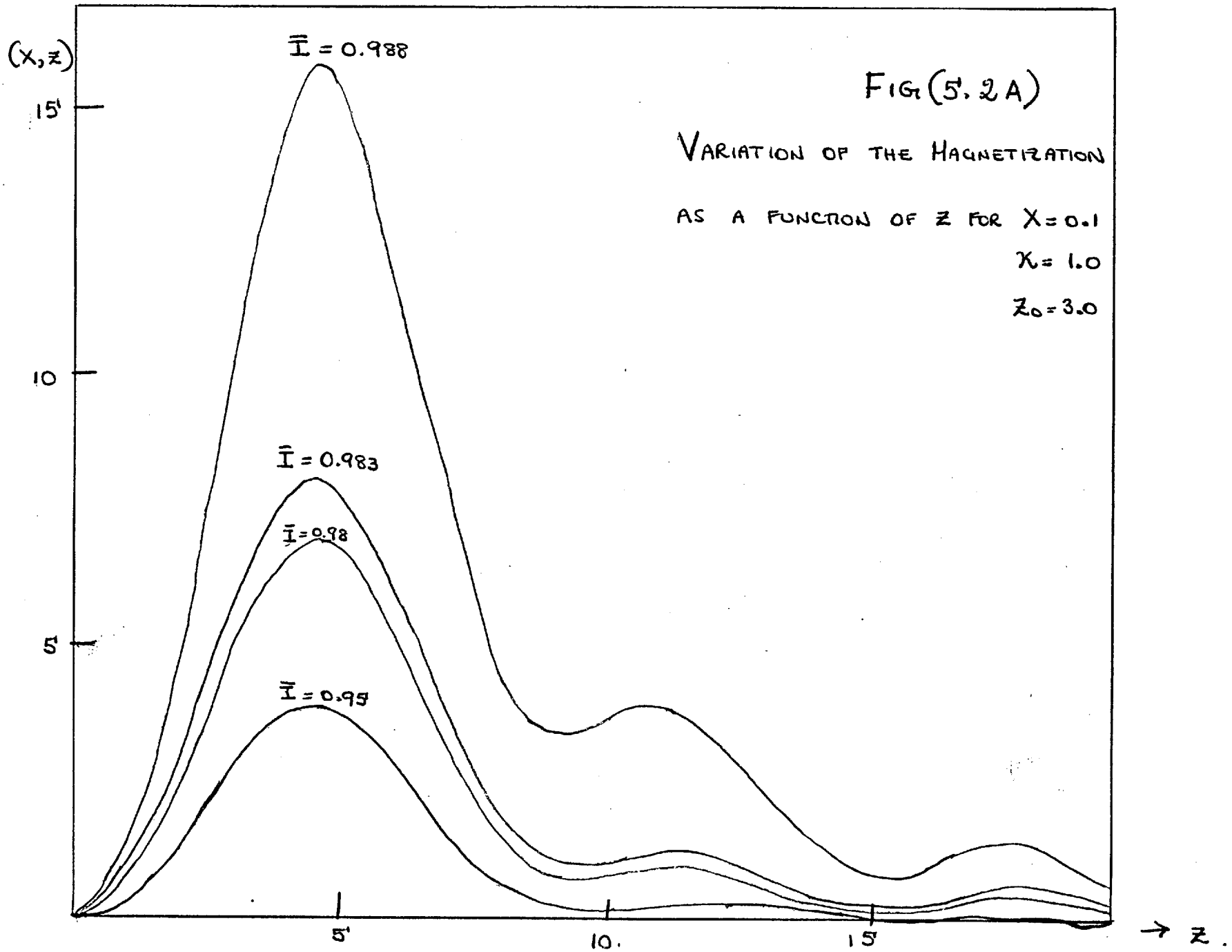

FIG (5.2A)

VARIATION OF THE MAGNETIZATION AS A FUNCTION OF Z FOR $X = 0.1$

$\kappa = 1.0$

$Z_0 = 3.0$

FIG (5.2B)

LATERAL VARIATION OF MAGNETIZATION FOR $z = 4.5$, $x = 1.0$, $z_0 = 3.0$

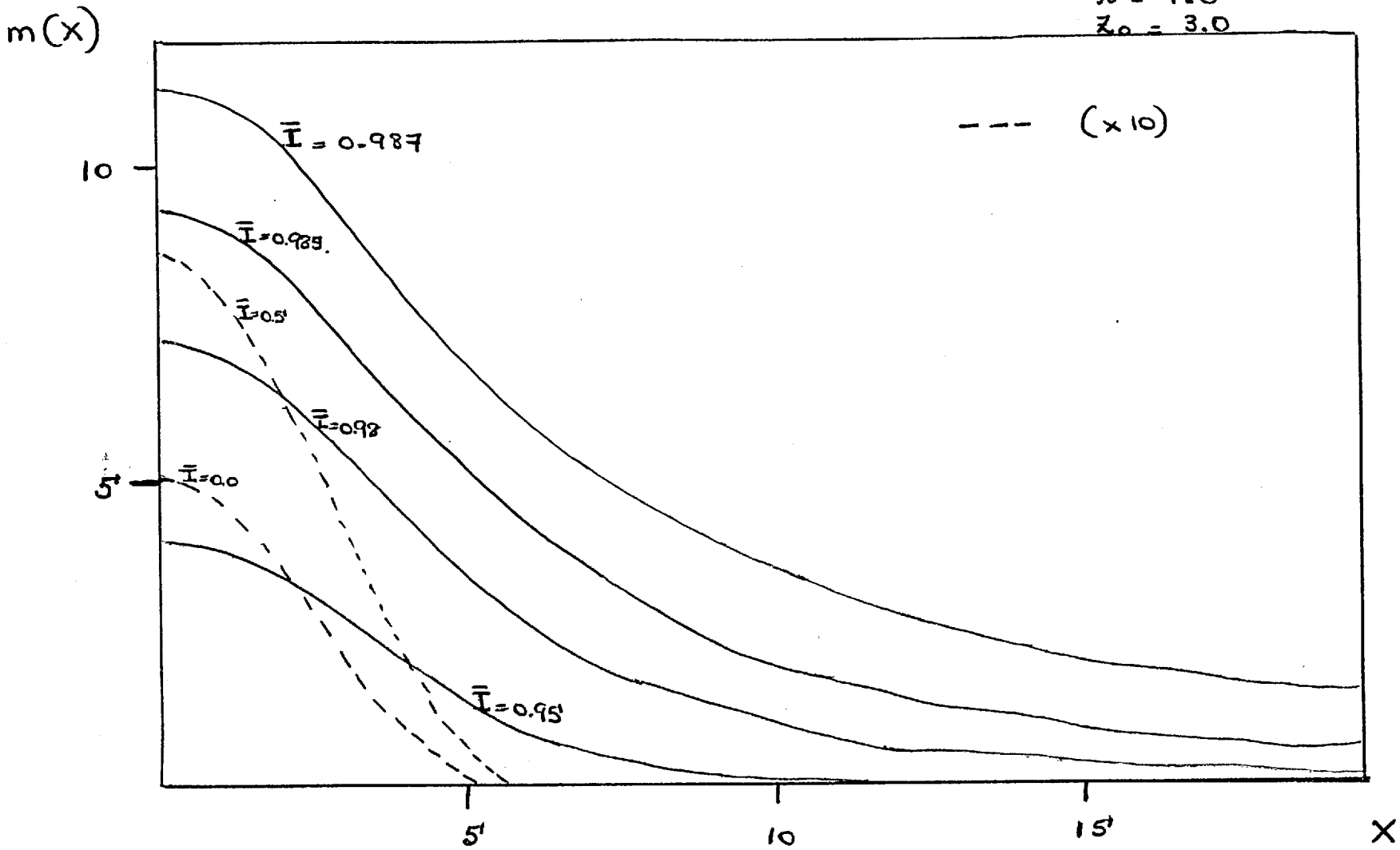

FIG (5.2c)

A PLOT OF THE HEIGHT OF THE INVERSE MAGNETIZATION AT $z = 4.5$ AS A FUNCTION OF $\bar{I}$ FOR A YUKAWA MAGNETIC FIELD : $X = 0.1$
$\kappa = 1.0$
$z_0 = 3.0$

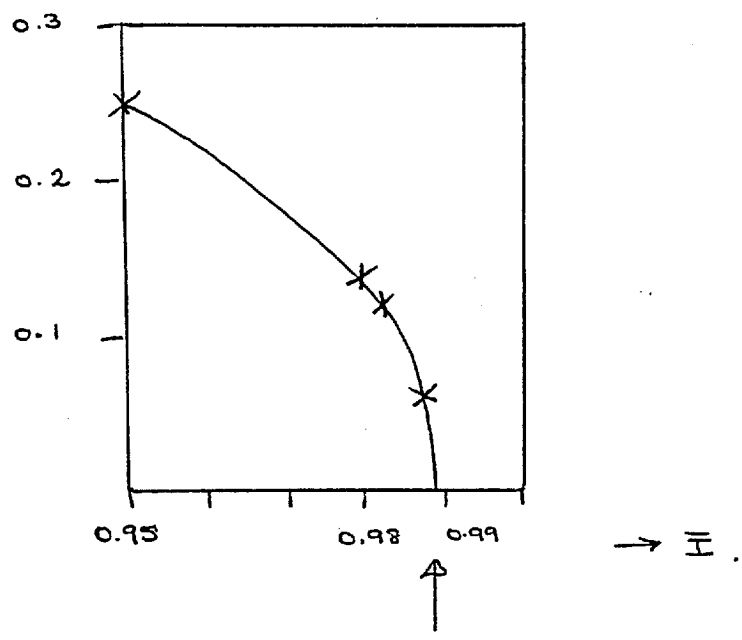

Intercept at $\bar{I} = \bar{I}_s \simeq 0.989$.

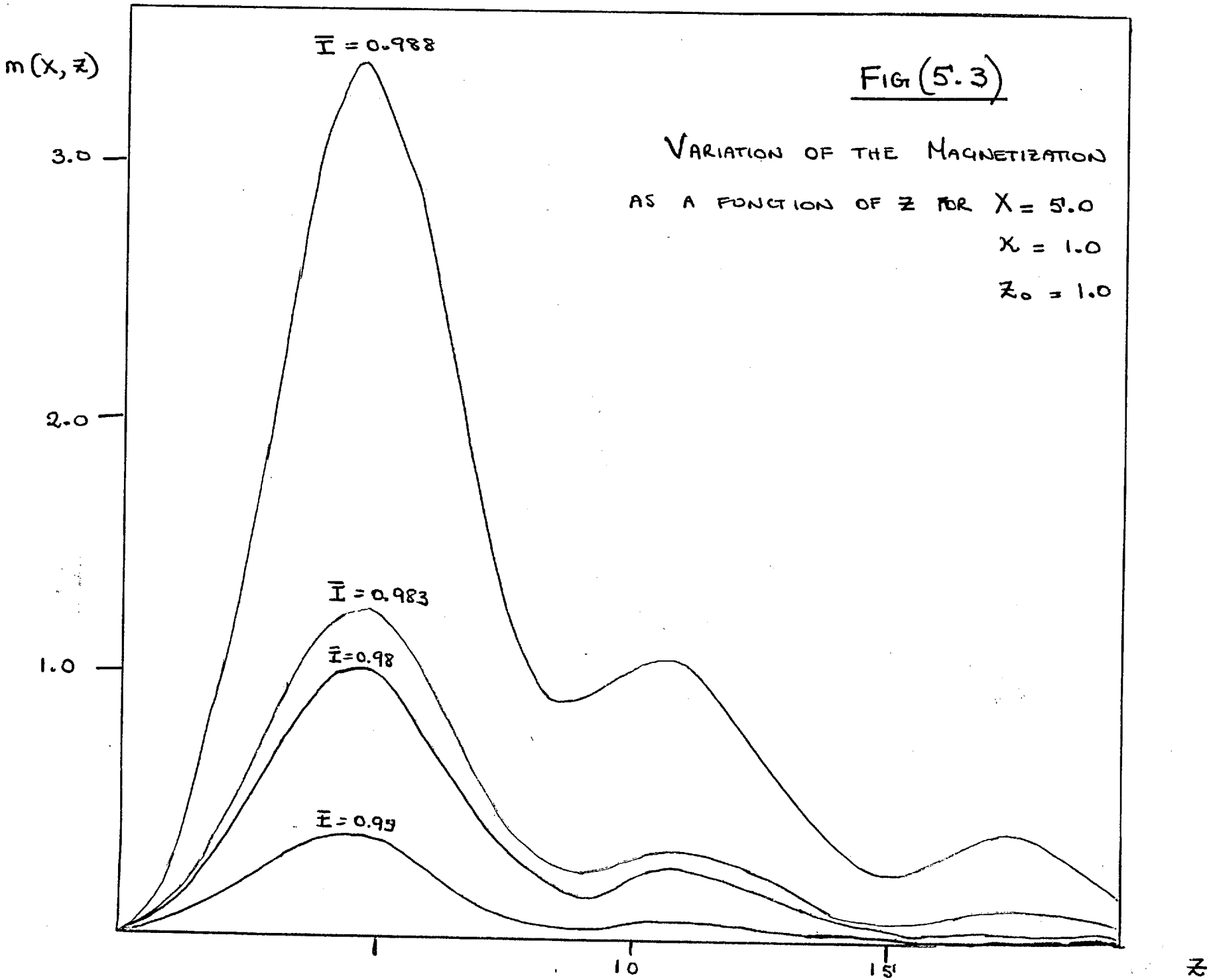

FIG (5.3)

VARIATION OF THE MAGNETIZATION AS A FUNCTION OF Z FOR X = 5.0

$\kappa = 1.0$

$Z_0 = 1.0$

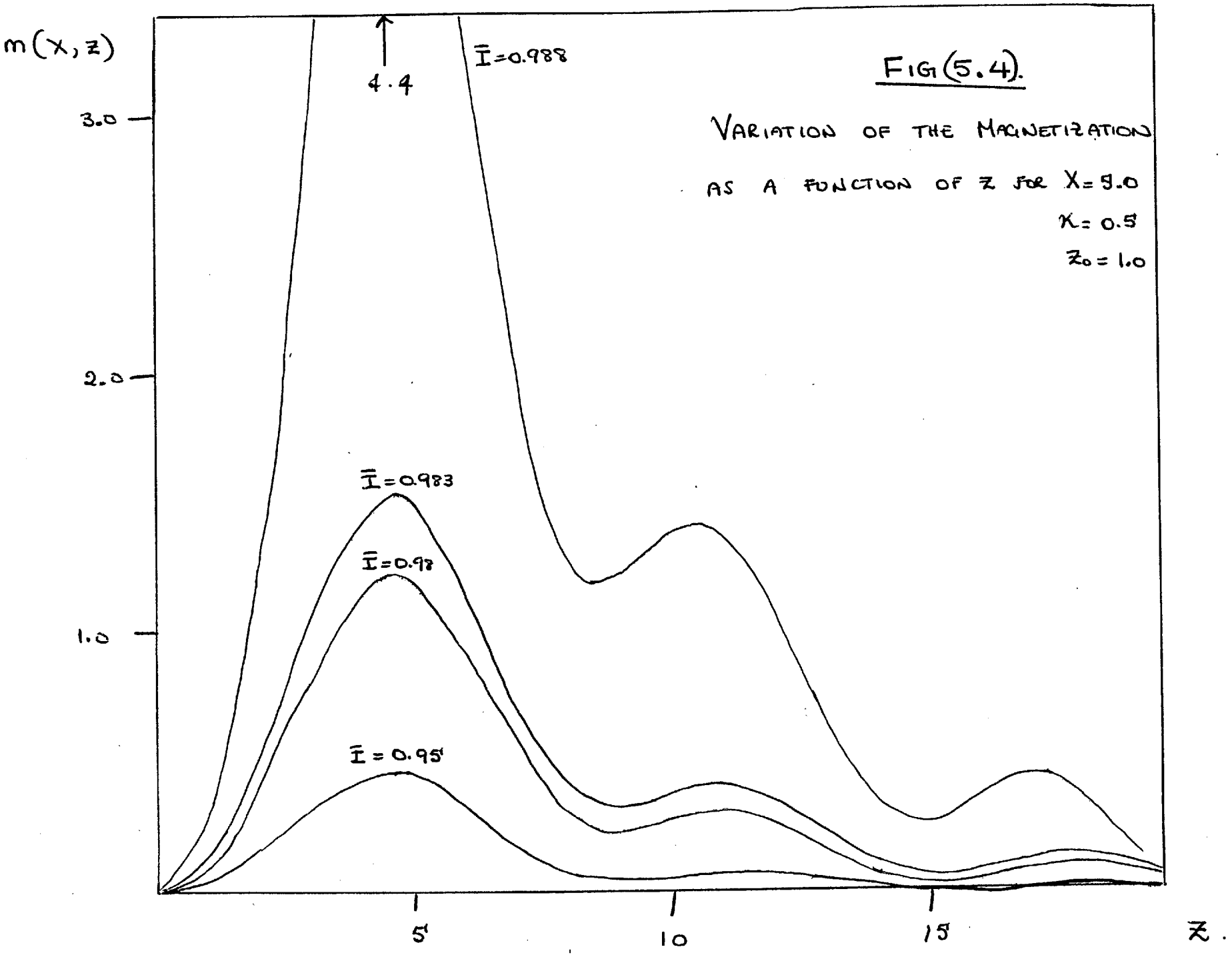

FIG (5.4).

VARIATION OF THE MAGNETIZATION AS A FUNCTION OF Z FOR X = 5.0

$\kappa = 0.5$

$z_0 = 1.0$

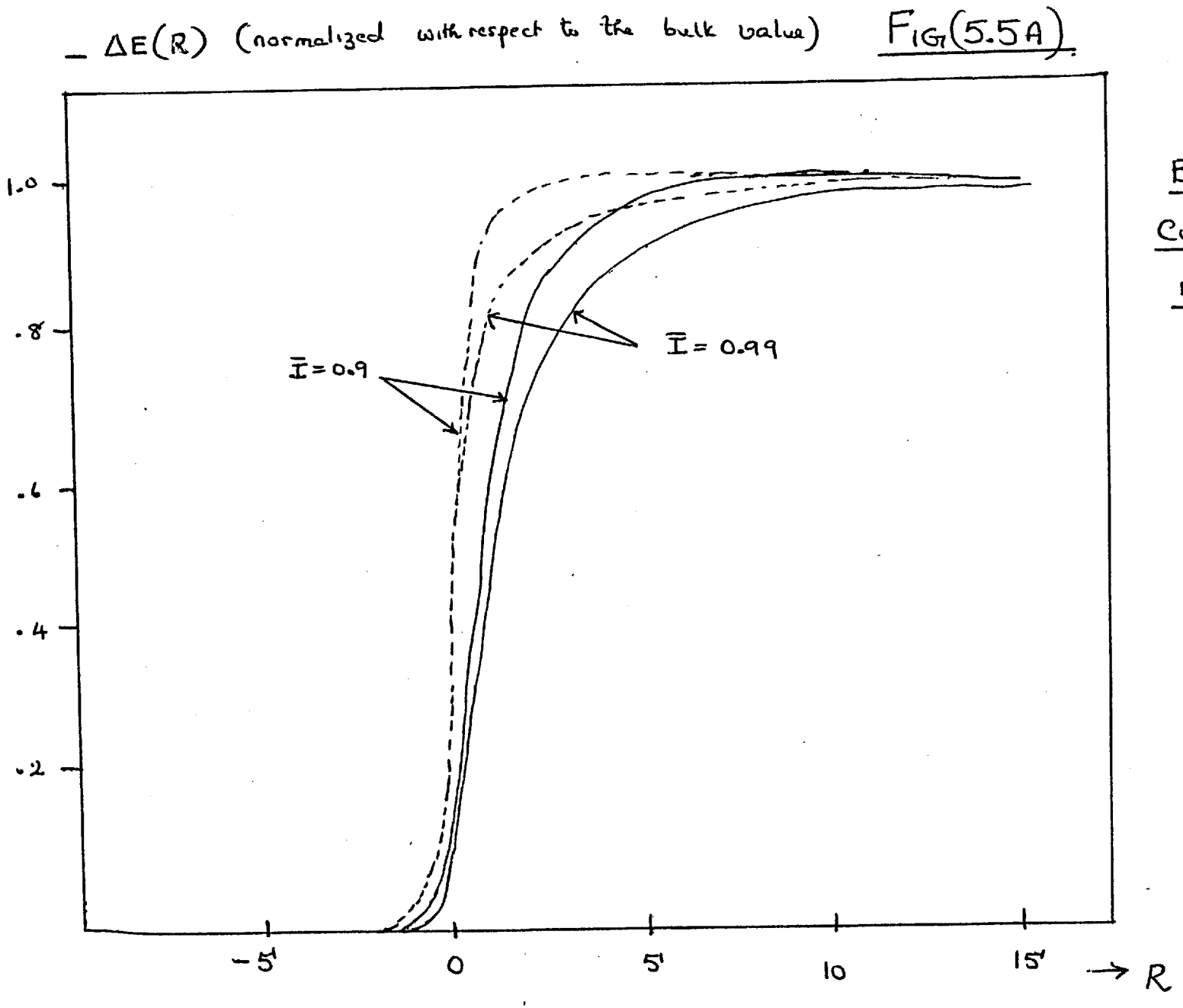

FIG (5.5A)

BINDING ENERGY CURVES COMPUTED BY SCHIACH (1976)

FIG (5.5 B)

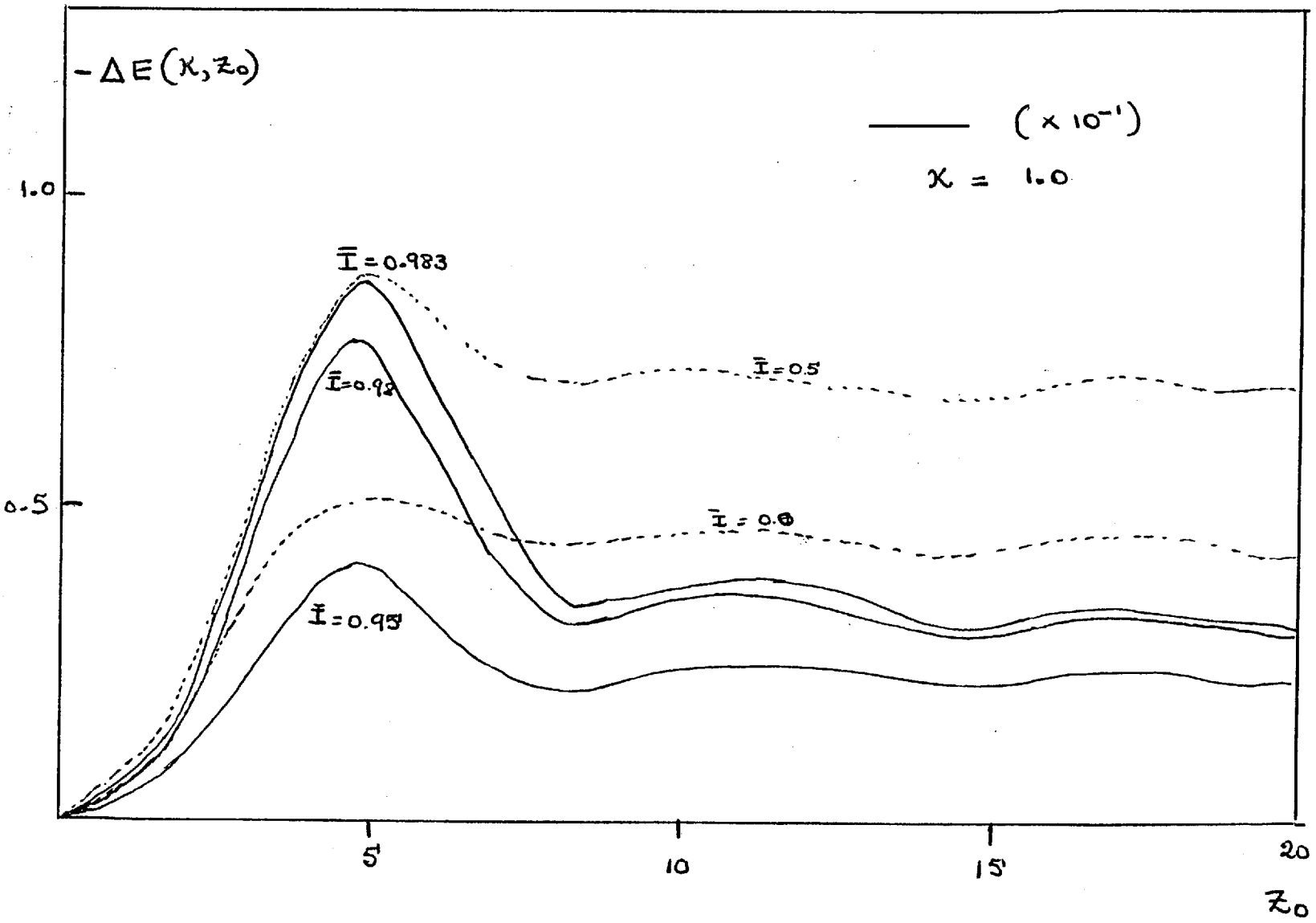

BINDING ENERGY CURVES COMPUTED IN THIS WORK.

FIG (5.5C)

POINTS OBTAINED FROM FIG (5.5B)

AT $z_0 = 4.5$. $\bar{I}_s = 0.989$, $\kappa = 1.0$

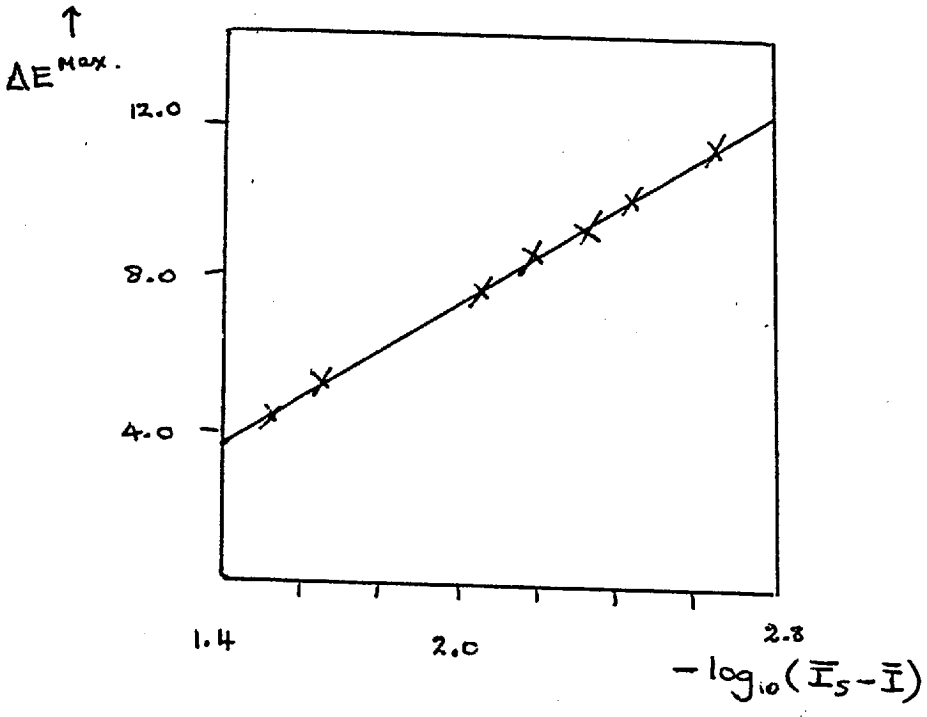

TABLE (5.1)

THIS SHOWS A COMPARISON OF THE RATIO OF THE HEIGHTS OF THE MAGNETIZATION CURVES $m(\varrho, z) \sim z$, $\varrho = 0.0001$, $\bar{I} = 0.95, 0.98, 0.983$ FOR THE TWO FIELDS $h = \sin z / z$ and Yukawa type

TYPE OF MAGNETIC FIELD	$m_{0.95}$	$m_{0.98}$	$m_{0.983}$	$m_{0.983}/m_{0.95}$	$m_{0.983}/m_{0.98}$	$m_{0.98}/m_{0.95}$
$h = \sin z / z$	0.8	4.3	8.4	10.5	1.95	5.3
$h' =$ Yukawa $x = 1.0$, $z_0 = 0.0$	0.92	4.5	8.6	9.4	1.91	4.9

REFERENCES

1. Abrikosov et al, 'Methods of Quantum Field Theory in Statistical Physics'; Prentice-Hall Inc, 1963.
2. Acton : 'Numerical Methods that Work'.
3. Ahonen et al : J. Phys C, 9, 1665, 1976.
4. Anderson : Phys Rev Lett, 24, 1049, 1967.
5. Ballu, Lecante & Newns : private communication, 1976.
6. Barton : private communication, 1976.
7. Beal-Monod et al : Solid St Comm, 11, 855, 1972.
8. Beal-Monod & Doniach, J. of Low Temp Phys, 28, 175, 1977.
9. Beck & Celli : Phys Rev B2, 2955, 1970.
10. Beck : Phys Rev B, 4(2), 1555, 1971.
11. Beck & Celli : Phys Rev Lett, 28, 1124, 1972.
12. Bennett : Phys Rev B1, 203, 1970.
13. Bradshaw et al : Proceedings of an International Symposium on Photoemission, No-ordwijk, Netherlands,1976.
14. Bueckner & Sawada : Phys Rev 112, 328, 1958.
15. Clogston et al : Phys Rev 134, A 650, 1964.
16. Datta & Newns : Proceedings of an International Symposium on Photoemission, No-ordwijk, Netherlands, 1976.
17. Datta & Newns : Phys Lett 59A, 326, 1976.
18. Doniach & Sunjic : J. Phys C, 3, 285, 1970.
19. Doniach & Sunjic : Phys Rev B2, 3898, 1970.
20. Economou : Phys Rev B, 182, 539, 1969.

21. Ehrenreich & Phillip : Phys Rev 128, 1622, 1962.

22. Equiluz et al : Phys Rev B 11, 2118, 1975.

23. Equiluz et al : Phys Rev B 14, 1347, 1976.

24. Feibelmann : Phys Rev B 3, 220, 1971.

25. Feibelmann : Phys Rev Lett, 30, 975, 1973.

26. Fuggle et al : Surf Sci, 52, 521, 1975.

27. Gadzuk : 'Electron Spectroscopy of Surfaces via Field & Photoemission', Nato Advanced Study Institute Series, Namur, 1975.

28. Gadzuk : Phys Rev B 14, 4, 5458, 1976.

29. Gadzuk : Proc. 7th Intern. Vac. Congr. & 3rd Intern. Conf. Solid Surfaces, Vienna, 1977.

30. Gradshtein & Ryshik : 'Table of Integral Series & Products', Academic Press, 1965.

31. Griffin & Zaremba : Phys Rev A, 8(1), 486, 1973.

32. Grimley : Nato Advanced Study Institute Series, Namur, Belgium, 1975.

33. Gumhalter & Newns : Phys Lett 53A, 137, 1975.

34. Gumhalter : Thesis, (Imperial College), 1976.

35. Gumhalter : J Phys C, 10, L219, 1977.

36. Harris : Solid St Comm, 16, 671, 1975.

37. Heisenberg : Z. Physik, 49, 619, 1928.

38. Herring : 'Magnetism', edited by Rado & Suhl, Academic Press, 1966.

39. Hubbard : Proc. Roy. Soc, A276, 238, 1963.

40. Ichimaru :'Basic Principles of Plasma Physics - A Statistical Approach', Frontiers in Physics, 197
41. Inglesfield : Solid St Comm, 15, 1727, 1974.
42. Inglesfield & Wikborg : Solid St Comm, 16, 335, 1975.
43. Izuyama et al : J Phys Soc, Jap 18, 1025, 1963.
44. Jackson :'Classical Electrodynamics'; John Wiley & Sons Inc, 1962.
45. Kloos & Raether : Phys Lett A44, 157, 1973.
46. Krane & Raether : Phys Rev Lett, 37, 1355, 1976.
47. Kubo et al : J Phys Soc, Jap 11, 549, 1956.
48. Kubo : J Phys Soc, Jap 12, 570, 1957.
49. Lang : 'Solid State Physics', edited by Ehrenreich et al, 28, 225, 1973.
50. Langreth : Phys Rev B 1, 471, 1970.
51. Lynch et al : Private Communication.
52. Mahan : Phys Rev, 163, 612, 1967.
53. Mills, Beal-Monod & Weiner (MBW) : Phys Rev B 5, 4637, 1972.
54. Muscat : J Phys F 5, L119, 1975.
55. Muscat et al : Phys Rev B, 1437, 1975.
56. Muscat : J Phys F 6, L231, 1976.
57. Muscat : Surf Sci 58, 557, 1976.
58. Merzbacher : 'Quantum Mechanics', John Wiley & Sons Inc, 2nd Edition, 1970.
59. Messiah : 'Quantum Mechanics', Vols. 1, 2, North Holland, 1961.

60. Newns : Phys Rev B, 11(8), 3304, 1970.

61. Newns : 'Theory of Surface Plasmons and Inelastic Electron Scattering', Electron Spectroscopy Summer School, York, 1975.

62. Newns : Lecture Notes on 'Surface Physics', delivered in Aarhus, Denmark, 1975 (unpublished).

63. Newns : Phys Lett 38A, 341, 1972.

64. Newns : Private Communication, 1977.

65. Newns & Edwards : Private Communication, 1977.

66. Pardee et al : Phys Rev B 11, 3614, 1975.

67. Pearson : Tables of Incomplete Gamma Functions.

68. Perdew : Pre-print, 1977.

69. Peuckert : Z Physik, 241, 191, 1971.

70. Pines : 'Elementary Excitations in Solids', p.156, W.A. Benjamin Inc, 1964.

71. Powell & Swan : Phys Rev 118, 640, 1960.

72. Raether : Proc. of 4th Int. Mat. Sym, 'The Structure & Chemistry of Solid Surfaces', Univ. California, Berkeley ; 10 - 1, 1968.

73. Raimes : 'Many Electron Theory', North Holland, 1972.

74. Ritchie : Phys Rev 106(5), 874, 1957.

75. Ritchie : Prog. Theor. Phys. (Kyoto), 29, 607, 1963.

76. Ritchie & Marusak : Surf. Sci. 4, 234, 1966.

77. Ritchie : Surf. Sci. 34, 1, 1973.

78. Schiach : Phys Rev B 14(2), 1488, 1976.

79. Schrieffer : J App. Phys. 39, 642, 1968.

80. Schrieffer & Gomer : Surf. Sci. 25, 315, 1971.

81. Weaver et al : Phys Rev B 10, 1974.

82. Weiner : AIP, Conf. Proc. 18, Pt. 2, 'Magnetism & Magnetic Materials', 19th, Boston 1973.

83. Weiner, Beal-Monod & Mills (WBM) : Phys Rev B 7, 3399, 1973.

84. Weiss : J de Phys (4), 6, 661, 1907.

85. White : 'Quantum Theory of Magnetism'; McGraw Hill Book Co. 1970.

86. Wohlfarth : Lecture Notes on ' Ferromagnetism', delivered at Imperial College, 1976.

87. Woolley : Adv. in Phys. 25, 27, 1976.

88. Yates & Erikson : Surf. Sci. 44, 489, 1974.

89. Ying et al : Solid St Comm 18, 359, 1976.

90. Zaremba : Ph.D Thesis (Univ. of Toronto), 1974.

91. Zaremba & Griffin : Solid St Comm 13, 1697, 1973.

92. Zaremba & Griffin : Can. J. Phys. 53, 891,1975.

NB. Explicit mention may not have been made to each of the above individually, but each reference has helped in the formation of this thesis.

Additional References

1. Butkov : 'Mathematical Physics'.

2. Brenig, Z Physik B 20, 55, 1975.

3. Cullity : 'Introduction to Magnetic Materials', Addison - Wesley Publishing Co., 1972.

4. Gadzuk : Surf Sci, Oct. '77.

5. Gomer : Solid States Physics (Ed. Ehrenreich, Turnbull & Seitz), 30, 94, 1975.

6. Grimley : Prog. in Surf. & Memb. Sci. , 9, 71, 1975.

7 . Heck : 'Magnetic Materials and their Applications', (Trans. German), Crane Russack & Co., N. Y. 1974.

8. Lang & Williams : Phys. Rev. Lett. , 34, 531, 1975.

9. Muscat & Newns : To be Published, 1977.

10. Nozieres & Pines : 'Quantum Theory of Liquids', Vol. 1; Normal Fermi Liquids, W.A. Benjamin Inc., 1966.

11. Nozieres & Dominicis : Phys. Rev. 178, 3, 1072, 1969.

12. Paulson & Schrieffer : Surf. Sci., 48, 329, 1975.

13. Suhl, Smith & Kumar : Phys. Rev. Lett., 25, 1442, 1970.

14. Ying, Smith & Kohn : Phys. Rev. B 11, 1483, 1975.

15. Ying & Kohn : Surf. Sci. Oct. '77.

XPS SATELLITE SPECTRA FOR ADSORBED ATOMS

A. DATTA and D.M. NEWNS
Department of Mathematics, Imperial College, London SW7, England

Received 28 October 1976

The surface plasmon and electron-hole satellite spectra in core-level XPS of a large adsorbed atom are calculated for an idealised model of a metal surface.

In XPS spectra of core levels of adsorbed atoms, satellite structure on the low kinetic energy side of the core line is expected. For a sufficiently fast outgoing election [1], this satellite structure should be dominantly intrinsic, i.e. due to the sudden appearance of the localised core hole. Methods of separating out the intrinsic and extrinsic effects have been considered by Bradshaw et al. [2] for the case of O and Al. For a large radius physisorbed atom such as Xe, the intrinsic core CPS satellite spectrum should approximate that for a point charge just outside the surface. Its interest lies in its action as a probe of the surface excitation spectrum at moderately large wavevectors.

The sudden approximation for switching on of the core hole, appropriate for intrinsic satellites, gives the "zero-work" sum rule that the first moment of the core XPS spectrum lies at the gas-phase position of the core level [3]. The elastic threshold of the adsorbate core XPS spectrum is however shifted towards the high kinetic energy side by the "relaxation shift" v. In our approximation v is the static interaction energy of a point charge at the adatom with the surface. For an adatom of radius d the classical image theorem would give $v \sim e^2/4d$ for a metal. If the satellite spectrum is dominated by a single peak at the surface plasmon frequency ω_s (taking elastic threshold as energy zero), then the "zero work" sum rule gives $p = v/\omega_s$ for the strength p of the satellite peak relative to elastic peak in Born approximation.

Our aim here is to calculate the intrinsic satellite spectrum $N_+(\omega)$ taking into account within a simple model microscopic properties of the electron gas such as finite screening length, surface plasmon dispersion and damping and electron-hole excitations. In Born approximation $N_+(\omega)$ is given by

$$N_+(\omega) = \frac{e^2}{\omega^2} \int_0^\infty e^{-2Qd} S_Q(\omega)\, dQ\,. \qquad (1)$$

Here ω, taken as >0, is frequency measured away from elastic threshold, Q is wavevector parallel to surface, and d = distance of core from surface. $S_Q(\omega)$ is the surface spectral density, defined as $S_Q(\omega) = -(1/\pi) \times \mathrm{Im}\, R_Q(\omega)$, where the image response function $R_Q(\omega)$ may be defined by

$$R_Q(\omega) = q_Q^{\mathrm{im}}(\omega)/q_Q(\omega)\,. \qquad (2)$$

In eq. (2), $g_Q(\omega)$ is the (Q, ω) Fourier transform of a charge outside the surface, q^{im} being the image of

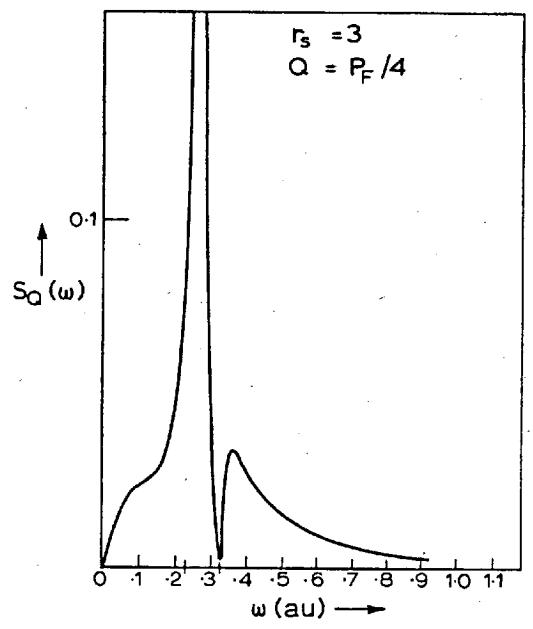

Fig. 1. Surface spectral density $S_Q(\omega)$ for $r_s = 3$, $Q = p_F/4$.

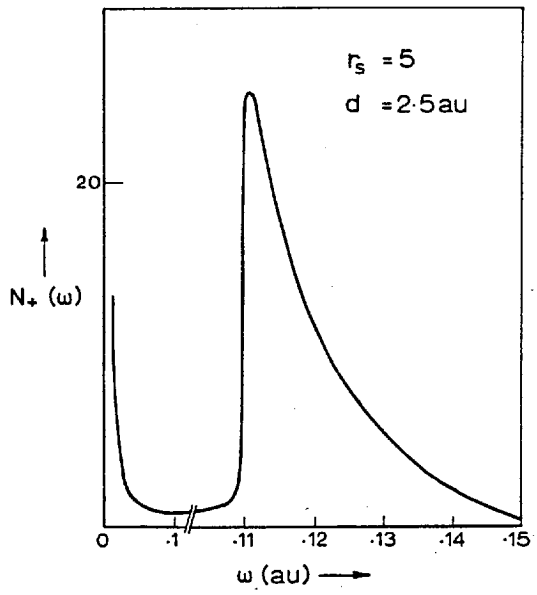

Fig. 2. Intrinsic satellite intensity $N_+(\omega)$ at energy ω below elastic threshold [note scale change].

q in the surface from which d is measured. The classical image theorem gives $\lim_{Q\to 0} R_Q(0) = -1$.

The solid is here treated as an electrongas, and the surface approximated by the "Semi-Classical Infinite Barrier Model" (SCIBM), which unrealistically has a step-function electron density at the surface but reasonable dynamical properties [4]. In this model [4] $R_Q(\omega) = [1-\epsilon_Q(\omega)]/[1+\epsilon_Q(\omega)]$, where

$$\frac{1}{\epsilon_Q(\omega)} = \frac{2Q}{\pi}\int_0^\infty \frac{dq_z}{q^2\epsilon(q,\omega)} . \tag{3}$$

Here $q = \sqrt{q_z^2 + Q^2}$ and $\epsilon(q,\omega)$ is the Lindhard dielectric function. An approximation to (3) is

$$\frac{1}{\epsilon_Q(\omega)} \approx a_0(\omega) + 2Q(\alpha_1(\omega) + i\beta_1(\omega)) , \tag{4}$$

leading to

$$S_Q(\omega) \approx \frac{-\pi^{-1}\beta_1 Q(\omega^2-\omega_p^2)^2}{[\omega^2-\omega_s^2+Q\alpha_1(\omega^2-\omega_p^2)]^2+[Q\beta_1(\omega^2-\omega_p^2)]^2} \tag{5}$$

From eq. (5), we see that $S_Q(\omega)$ should have a peak at $\omega \approx \omega_s(1+\frac{1}{2}Q\alpha_1)$ of width $\sim Q\beta_1\,\omega_s/2$, and minimum at $\omega = \omega_p = \sqrt{2}\omega_s$, the bulk plasma frequency.

Table 1
Relaxation shifts, satellite intensities and asymmetry parameters.

r_s	ω_s(au)	d [a](au)	υ [b](au)	υ/ω_s	$p^c_{calc.}$	γ
3	0.24	4.0	0.049	0.21	0.125	0.03
		2.5	0.069	0.29	0.16	0.06
5	0.11	4.0	0.045	0.41	0.30	0.08
		2.5	0.062	0.54	0.35	0.14

a) d measured from edge of substrate electron density.
b) υ is calculated from $\upsilon = -\frac{1}{2}e^2\int_0^\infty R_Q(0)\,e^{-2Qd}dQ$.
c) Relative area under surface plasmon satellite – see text.

In fig. 1 we illustrate the spectral density $S_Q(\omega)$ for an electron density of $r_s = 3$ and with Q at one quarter the Fermi wavevector. Calculations using (3) directly or the approximation (5) agree quite well. Both the peak at ω_s and the bulk plasmon "antiresonance" are in evidence; the latter feature also appears in a recent work of Barton [5]. Also visible in fig. 1 is the electron-hole structure, approximately linear in ω at small ω. This is responsible for the "infra-red divergence" in the XPS spectrum at small ω [6].

In fig. 2 is illustrated the XPS satellite spectrum calculated from eq. (1). Results calculated using (3) with numerical integration or (5) are found to agree rather well. Of course the total spectrum also contains an elastic peak given by a delta function at the origin. Note that d may be roughly estimated as the adatom atomic radius, the values for Ne and Xe being about 3 and 4 au respectively. The case chosen ($r_s = 5$, $d = 2.5$ au) for illustration involves small d and low electron density in order to maximise the non-classical effects under discussion here. The surface plasmon peak is seen in fig. 2 to be asymmetric, due to the positive surface plasmon dispersion in this model, so that the surface plasmon resonance lies in $\omega > \omega_s$. The resultant approximately exponential form was predicted by Harris [1], though our result contains also the damping and intensity fall-off effects. Perhaps most remarkable is the narrowness of the satellite, whose width is only $\sim 0.1\,\omega_s$. Effectively, for the relatively large d concerning us here, the Q-values brought in via (1) appear to be small enough to approach the classical behaviour $S_Q(\omega) = \frac{1}{2}\omega_s\,\delta(\omega-\omega_s)$. The area under the surface plasmon satellite, from threshold to about $0.9\,\omega_p$, is compared

in table 1 with the classical result $p = v/\omega_s$. It is found that only about 55–70% of the classical intensity v/ω_s is found in the calculated satellite, though the upper cut-off of the latter is rather subjective.

A non-classical phenomenon appearing in fig. 2 is the divergence at $\omega \to 0$. This is basically the infra-red divergence discussed for this problem by Gumhalter and Newns [6]. Eq. (5) of ref. [6] goes over, as the asymmetry parameter γ becomes small, to $N_+(\omega) = \gamma/\omega$ for small ω. This is the Born approximation limit, and fig. 2 shows this ω^{-1} divergence at small ω. In fact for small ω and $r_s = 3$ our present result agrees quite well with eq. (5) of ref. [6], perhaps justifying the Q-independent cut-off taken in ref. [6]. In practice one cannot see the small-ω divergence, due to finite lifetime of the core hole, but only an asymmetry in the otherwise symmetrical lineshape of the "elastic peak" [7]. In experimental work on XPS from substrate core levels attempts have been made to extract the γ-parameters [8]. Accordingly estimates of γ from the formula of ref. [6] are included in table 1. The results show that γ is significant only for low electron density substrates.

In conclusion, we have carried out a simple theoretical treatment of the intrinsic XPS satellite structure for a large physisorbed atom on a free-electron like substrate. The surface plasmon satellite is the dominant feature and is quite well described by the simple classical picture based on a single non-dispersing mode. Bulk plasmons contribute negligibly to the spectrum provided the atom lies outside the surface. The electron-hole excitations contribute divergent small-ω behaviour which, in the presence of a finite core lifetime, gives an asymmetry to the core peak characterised by the quantity γ. The asymmetry seems likely to be measurable only for low electron density substrates and perhaps non-free-electron type substrates.

References

[1] J. Harris, Solid State Commun. 16 (1975) 671.
[2] A.F. Bradshaw, L.S. Cedarbaum and W. Domcke, Proc. of ESA Conf. on Photoemission from surfaces, Noordwijk 1976.
[3] L. Hedin, B.I. Lundqvist and S. Lundqvist, Solid State Commun. 5 (1967) 237;
D.C. Langreth in Nobel Symposium, Collective properties of physical systems (Academic, 1974).
[4] R.H. Ritchie and A.L. Marusak, Surface Science 4 (1966) 234;
J. Harris and R.O. Jones, J. Phys. C7 (1974) 3751;
D.M. Newns, Phys. Rev. B1 (1970) 3304.
[5] G. Barton, private communication.
[6] B. Gumhalter and D.M. Newns, Phys. Lett. 53A (1975) 137.
[7] S. Doniach and M. Sunjic, J. Phys. C3 (1970) 285.
[8] G.K. Wertheim and S. Hufner, Phys. Rev. Lett. 35 (1975) 53.